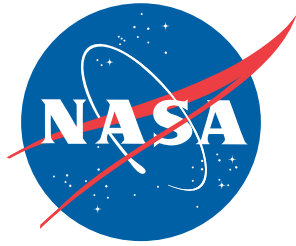


NASA/TM-2011-217182/Volume II
NESC-RP-09-00596



Comparison of the Booster Interface Temperature in Stainless Steel (SS) V-Channel versus the Aluminum (Al) Y-Channel Primer Chamber Assemblies (PCAs)

Appendices

*Roberto Garcia/NESC
Langley Research Center, Hampton, Virginia*

*Regor L. Saulsberry
White Sands Test Facility, Las Cruces, New Mexico*

NASA STI Program . . . in Profile

Since its founding, NASA has been dedicated to the advancement of aeronautics and space science. The NASA scientific and technical information (STI) program plays a key part in helping NASA maintain this important role.

The NASA STI program operates under the auspices of the Agency Chief Information Officer. It collects, organizes, provides for archiving, and disseminates NASA's STI. The NASA STI program provides access to the NASA Aeronautics and Space Database and its public interface, the NASA Technical Report Server, thus providing one of the largest collections of aeronautical and space science STI in the world. Results are published in both non-NASA channels and by NASA in the NASA STI Report Series, which includes the following report types:

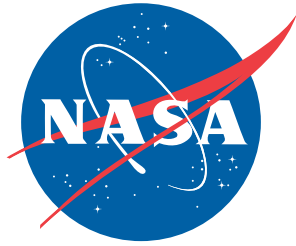
- **TECHNICAL PUBLICATION.** Reports of completed research or a major significant phase of research that present the results of NASA programs and include extensive data or theoretical analysis. Includes compilations of significant scientific and technical data and information deemed to be of continuing reference value. NASA counterpart of peer-reviewed formal professional papers, but having less stringent limitations on manuscript length and extent of graphic presentations.
- **TECHNICAL MEMORANDUM.** Scientific and technical findings that are preliminary or of specialized interest, e.g., quick release reports, working papers, and bibliographies that contain minimal annotation. Does not contain extensive analysis.
- **CONTRACTOR REPORT.** Scientific and technical findings by NASA-sponsored contractors and grantees.
- **CONFERENCE PUBLICATION.** Collected papers from scientific and technical conferences, symposia, seminars, or other meetings sponsored or co-sponsored by NASA.
- **SPECIAL PUBLICATION.** Scientific, technical, or historical information from NASA programs, projects, and missions, often concerned with subjects having substantial public interest.
- **TECHNICAL TRANSLATION.** English-language translations of foreign scientific and technical material pertinent to NASA's mission.

Specialized services also include creating custom thesauri, building customized databases, and organizing and publishing research results.

For more information about the NASA STI program, see the following:

- Access the NASA STI program home page at <http://www.sti.nasa.gov>
- E-mail your question via the Internet to help@sti.nasa.gov
- Fax your question to the NASA STI Help Desk at 443-757-5803
- Phone the NASA STI Help Desk at 443-757-5802
- Write to:
NASA STI Help Desk
NASA Center for AeroSpace Information
7115 Standard Drive
Hanover, MD 21076-1320

NASA/TM-2011-217182/Volume II
NESC-RP-09-00596



Comparison of the Booster Interface Temperature in Stainless Steel (SS) V-Channel versus the Aluminum (Al) Y-Channel Primer Chamber Assemblies (PCAs)

Appendices

*Roberto Garcia/NESC
Langley Research Center, Hampton, Virginia*

*Regor L. Saulsberry
White Sands Test Facility, Las Cruces, New Mexico*

National Aeronautics and
Space Administration


Langley Research Center
Hampton, Virginia 23681-2199

October 2011

The use of trademarks or names of manufacturers in the report is for accurate reporting and does not constitute an official endorsement, either expressed or implied, of such products or manufacturers by the National Aeronautics and Space Administration.

Available from:

NASA Center for AeroSpace Information
7115 Standard Drive
Hanover, MD 21076-1320
443-757-5802

	NASA Engineering and Safety Center Technical Assessment Report	Document #: NESC-RP- 09-00596	Version: 1.0
Title: Pyrovalve Booster Interface Temperature Measurement			Page #: 1 of 92

Volume II: Appendices

Comparison of the Booster Interface Temperature in Stainless Steel (SS) V-Channel versus the Aluminum (Al) Y-Channel Primer Chamber Assemblies (PCAs)

July 21, 2011



	NASA Engineering and Safety Center Technical Assessment Report	Document #: NESC-RP- 09-00596	Version: 1.0
Title: Pyrovalve Booster Interface Temperature Measurement			Page #: 2 of 92

Table of Contents

Appendix A.	Pyrometer Measurements with a Hole Pre-Cut in the Booster Cover Simulator ...	3
Appendix B.	Pyrometer Noise.....	9
Appendix C.	Pressure Transducer Drop Test.....	11
Appendix D.	Assessment of Area versus Temperature Indication.....	16
Appendix E.	PCA Thermal Analysis	18
Appendix F.	Phase I Statistical Analysis and Results.....	37
Appendix G.	Phase IIB Statistical Analysis and Results.....	57
Appendix H.	Numerical Simulations of Single and Simultaneous Dual Firing Initiators in the SS V-PCA Design.....	82

	NASA Engineering and Safety Center Technical Assessment Report	Document #: NESC-RP- 09-00596	Version: 1.0
Title: Pyrovalve Booster Interface Temperature Measurement			Page #: 3 of 92

Appendix A. Pyrometer Measurements with a Hole Pre-Cut in the Booster Cover Simulator

To more accurately assess the response of the high-speed video and the infrared pyrometer to test conditions, especially when the test produces a hole through the booster cover simulator (often referred to as the diaphragm), a special test was performed.

In this test, a hole with a diameter of 0.115-inch was cut in the center of the booster cover simulator. The booster cover simulator is a 304 SS disk 0.003inches thick. The pre-cut hole diameter was chosen as a reasonable approximation of some of the holes produced in single NASA Standard Initiators (NSI) tests with the stainless steel (SS) V-Primer Chamber Assembly (PCA). Note that area visible through the sapphire window is 0.250 inches in diameter. Thus, the pre-cut represented about 46 percent of the visible diameter and about 21 percent of the total visible area.

The sapphire window and perforated diaphragm were assembled in a SS V-PCA. The V-PCA has flow paths with the nominal 0.060-inch diameter. Assembly was performed according to the standard procedure used for all the tests. A single NSI was fired in the SS V-PCA to see if the pyrometer and high-speed video would give reasonable results.

Figure A-1 shows a graph of the temperature of the underside of the booster cover simulator as seen by the infrared pyrometer. Note that the first visible video indication occurs at 123 μ s (microseconds) after the first application of current to the NSI. Other data indicated that the NSI end closure opened at 112 μ s, which would make the first picture 11 μ s after the end closure opened. The camera takes 20,000 frames per second, so frames are 50 μ s apart. Also note that the upper detection limit for the pyrometer is 2,000 °C or 3,632 °F.

The sequence of pictures shown in Figures A-2 to A-6 show light and then hot gases arriving first at the booster interface followed by what appear to be burning particles of zirconium potassium perchlorate (ZPP). The white circle in Figure A-2 is one of the 0.060-inch-diameter flow paths from one of the NSI chambers in the top of the V-PCA. Part of a circular arc can be seen along the left-hand side of the picture. This is part of the edge of the pre-cut hole in the booster cover simulator.

SS melts at about 2,550 °F. The metal changes color from a darker red-brown to yellow or white as it approaches that temperature. The last picture is after all the ZPP has burned and the only light is coming from the cooling, white-hot SS.

In the picture taken at 973 μ s, the larger, irregular circle with some areas still glowing is the melted edge of the pre-cut hole in the diaphragm (see Figure A-6). To the left and down, a portion of a still larger circle can be seen. That is the bottom or outer edge of the sapphire window and the “booster” cavity. The smaller circle with the glowing edge is the flow passage.


	NASA Engineering and Safety Center Technical Assessment Report	Document #: NESC-RP- 09-00596	Version: 1.0
Title: Pyrovalve Booster Interface Temperature Measurement			Page #: 4 of 92

Figure A-7 shows a graph of the NSI current and cavity pressures versus time for SS V-PCA with 0.115-inch-diameter pre-cut hole in the diaphragm.

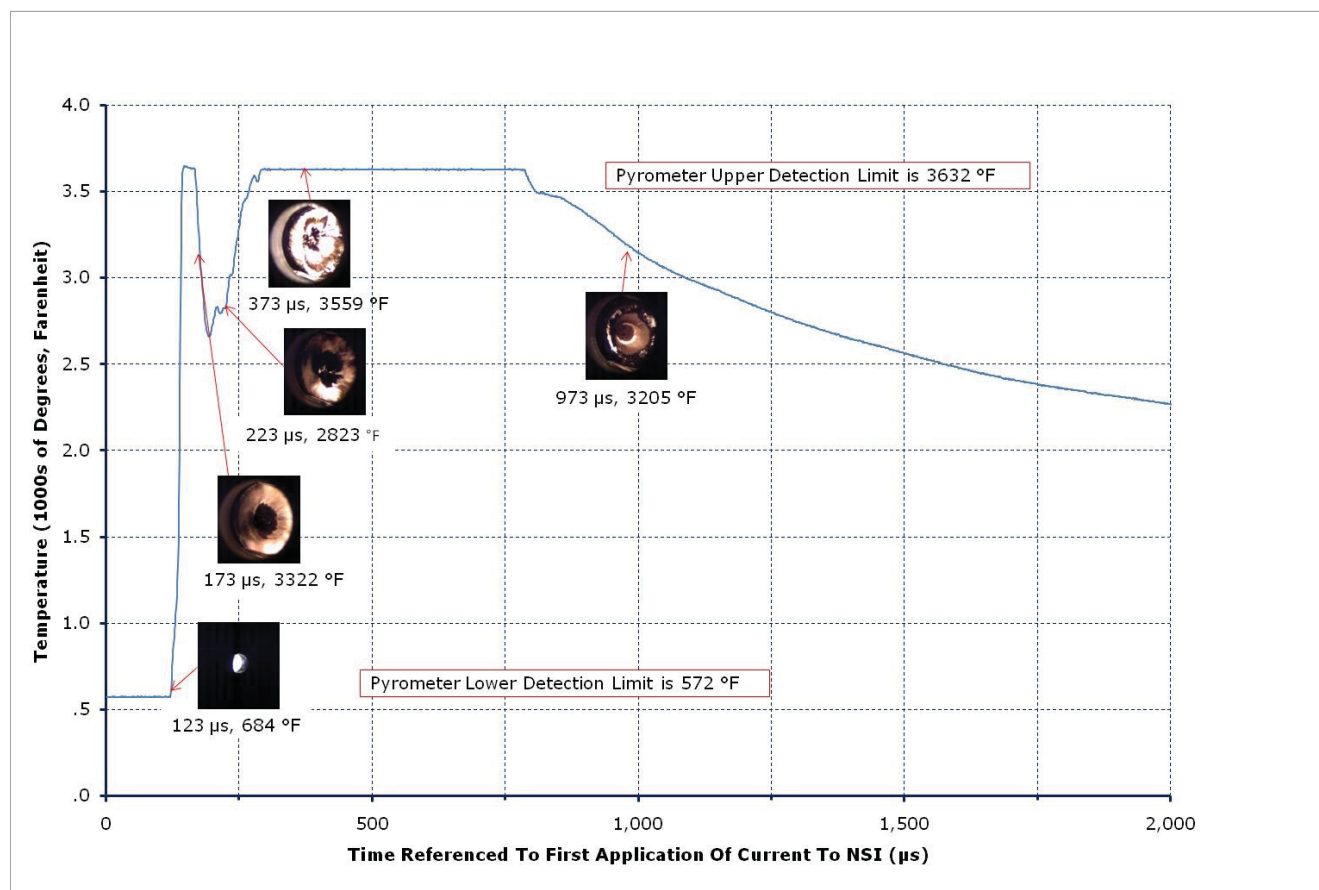



Figure A-1. Booster Interface Temperature versus Time, SS V-PCA with 0.115-Inch-Diameter Pre-Cut Hole in Diaphragm

	NASA Engineering and Safety Center Technical Assessment Report	Document #: NESC-RP- 09-00596	Version: 1.0
Title: Pyrovalve Booster Interface Temperature Measurement			Page #: 5 of 92

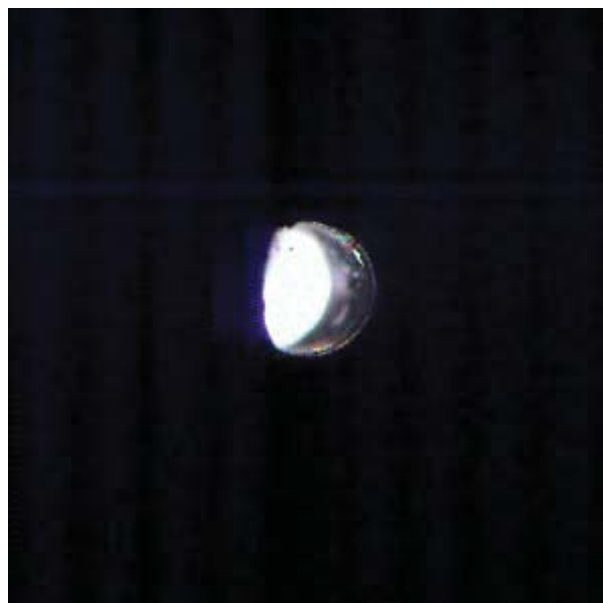


Figure A-2. At 123 μ s, One of the 0.060 NSI Flame Channels can be seen Illuminated. The Pyrometer is just Starting to Indicate Temperature with a Reading of 684 $^{\circ}$ F

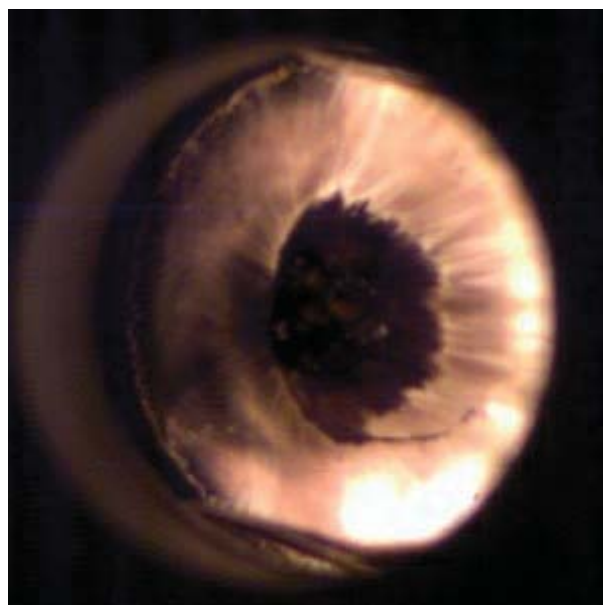



Figure A-3. At 173 μ s, the Pre-Cut Hole in the Booster Cover Simulator Can Be Seen

	NASA Engineering and Safety Center Technical Assessment Report	Document #: NESC-RP- 09-00596	Version: 1.0
Title: Pyrovalve Booster Interface Temperature Measurement			Page #: 6 of 92

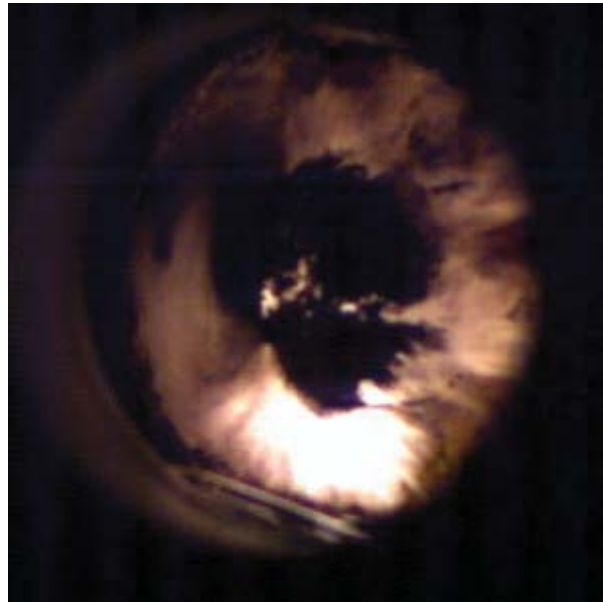


Figure A-4. At 223 μ s

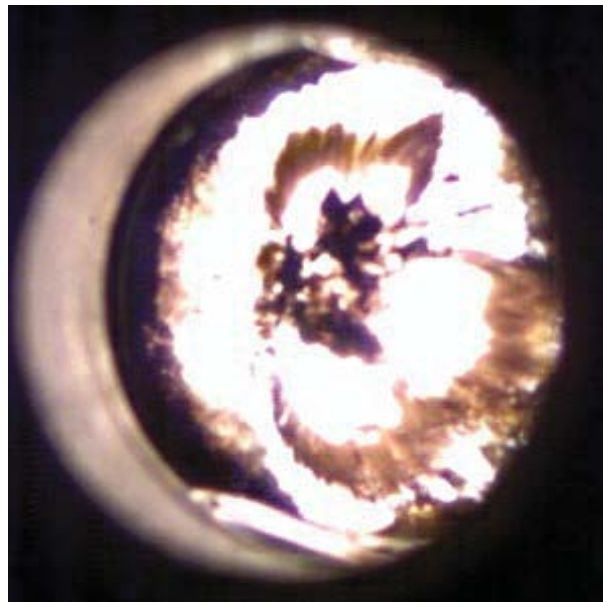


Figure A-5. At 373 μ s


	NASA Engineering and Safety Center Technical Assessment Report	Document #: NESC-RP- 09-00596	Version: 1.0
Title: Pyrovalve Booster Interface Temperature Measurement			Page #: 7 of 92



Figure A-6. At 973 μ s, the Edge of the Now Partially Melted Pre-Cut Hole can be seen AND the Still Glowing Edge of One of the Flame Channels. A Larger Arc at the lower left-hand corner is Part of the Hole through the Retainer Nut that Holds the Sapphire Window Assembly onto the V-PCA.



**NASA Engineering and Safety Center
Technical Assessment Report**

Document #:
**NESC-RP-
09-00596**

Version:
1.0

Title:
Pyrovalve Booster Interface Temperature Measurement

Page #:
8 of 92

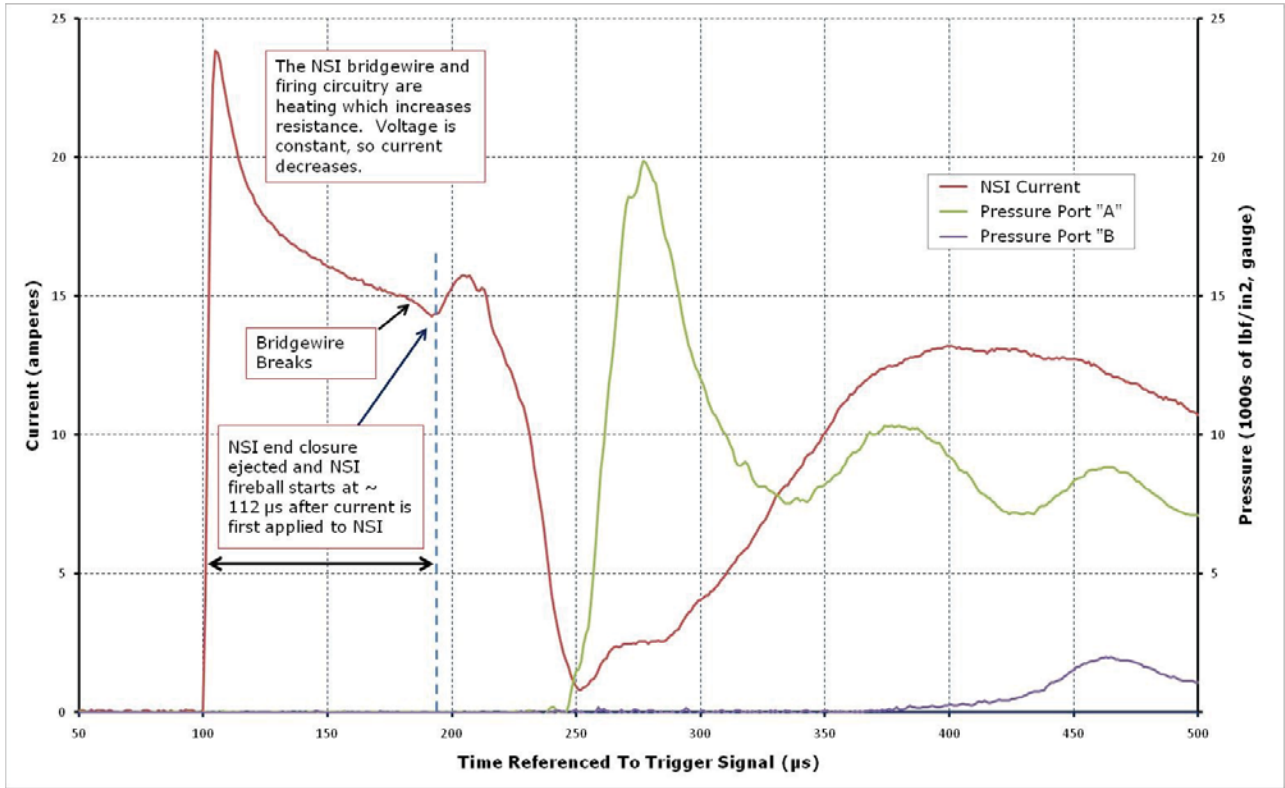


Figure A-7. NSI Current and NSI Cavity Pressures Versus Time, SS V-PCA with 0.115-Inch-Diameter Pre-Cut Hole in Diaphragm

	NASA Engineering and Safety Center Technical Assessment Report	Document #: NESC-RP- 09-00596	Version: 1.0
Title: Pyrovalve Booster Interface Temperature Measurement			Page #: 9 of 92

Appendix B. Pyrometer Noise

During testing, a question arose as to whether interference from the firing circuitry or some other source might be affecting the booster interface temperature readings from the infrared pyrometer.

Therefore, a special test was performed. In this test, two NSIs were fired with a 250- μ s skew. These NSIs were from a different lot than those used for the actual temperature measurement tests. This was because it was desired to perform all the temperature tests from one lot of NSIs and the team wanted to conserve that particular lot. For this checkout test, whichever lot was used would not make any difference.

The main difference in this test was that the pyrometer lens was completely blocked. The pyrometer would not be able to sense any energy from the booster interface at all. If any disturbance was seen in the pyrometer readings, it would have to be from some other effect.

As seen in Figures B-1 and B-2, the amperages and pressures produced during the test were normal. However, there was no effect on the pyrometer readings.

Therefore, it was concluded that the pyrometer readings seen during the actual test series were unaffected by other test conditions.

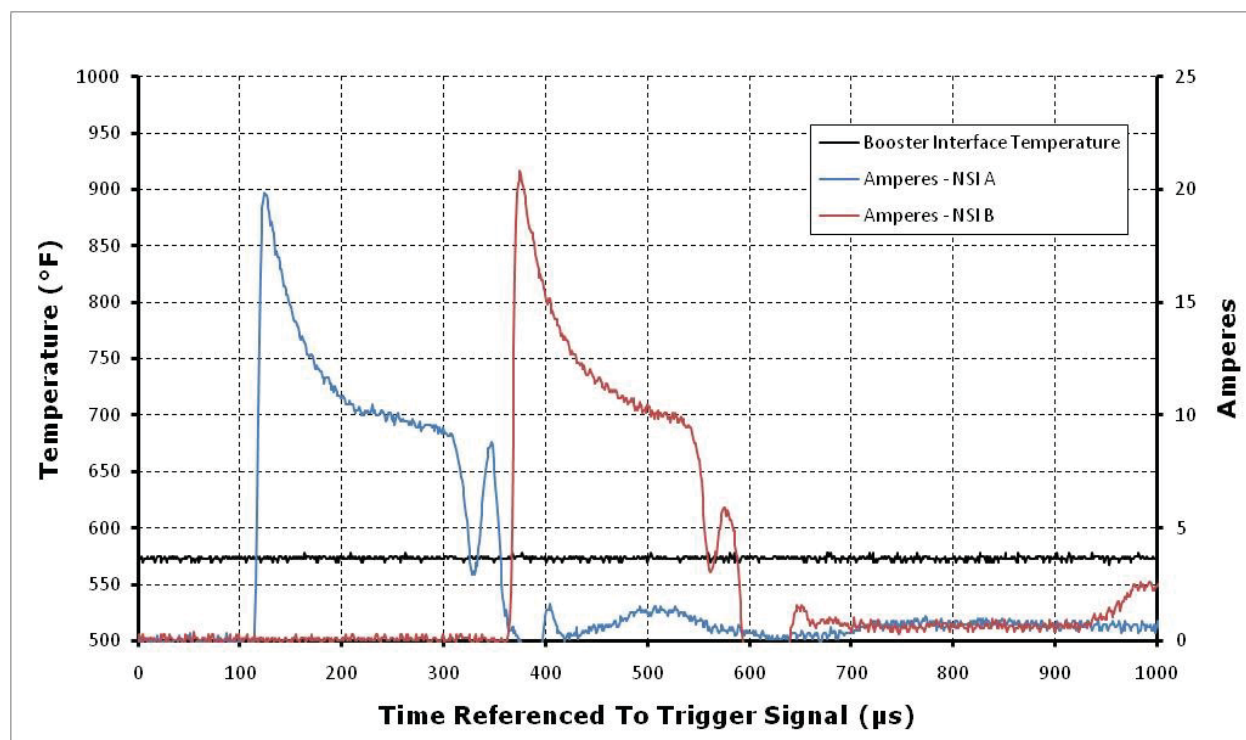


Figure B-1. Pyrometer Readings Hold Steady at Minimum when Two NSIs Were Fired with a 250- μ s Skew and when the Pyrometer Lens is Blocked



**NASA Engineering and Safety Center
Technical Assessment Report**

Document #:
**NESC-RP-
09-00596**

Version:
1.0

Title:

Pyrovalve Booster Interface Temperature Measurement

Page #:

10 of 92

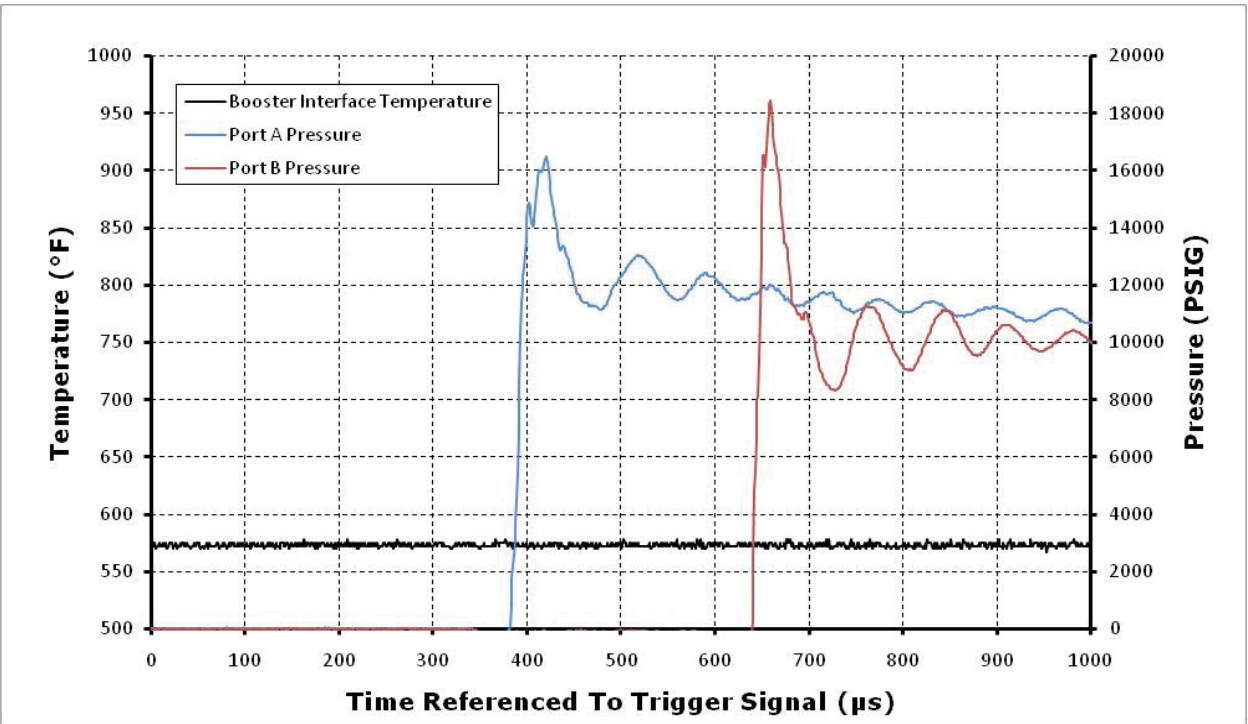



Figure B-2. Pyrometer Readings Hold Steady at Minimum when Two NSIs were Fired with a 250- μs Skew and when the Pyrometer Lens is Blocked

	NASA Engineering and Safety Center Technical Assessment Report	Document #: NESC-RP- 09-00596	Version: 1.0
Title: Pyrovalve Booster Interface Temperature Measurement			Page #: 11 of 92

Appendix C. Pressure Transducer Drop Test

During Run 6 of Phase IIB, one of the pressure transducers failed to register any pressure readings at all. Troubleshooting revealed this to be a failure of the pressure transducer itself.

As a result of this failure, a new pre-test checkout procedure for the pressure transducers was initiated.

Each pressure transducer was installed in an oil-filled reservoir. A tube or pipe was installed in the top of the reservoir such that a weight could be positioned at a certain height and held in place with a mechanical pin. When the pin was removed, the weight would fall down inside the tube and make contact with a rod that would then push into the oil reservoir. The pressure transducer would then sense this pressure shock.

Figures C-1 and C-2 show typical pressure traces that are obtained from the drop test. Data were collected once every microsecond. The data are not suitable for calibrating the pressure transducers. However, the test was valuable to ensure that the pressure transducers work and the cable connections are good.

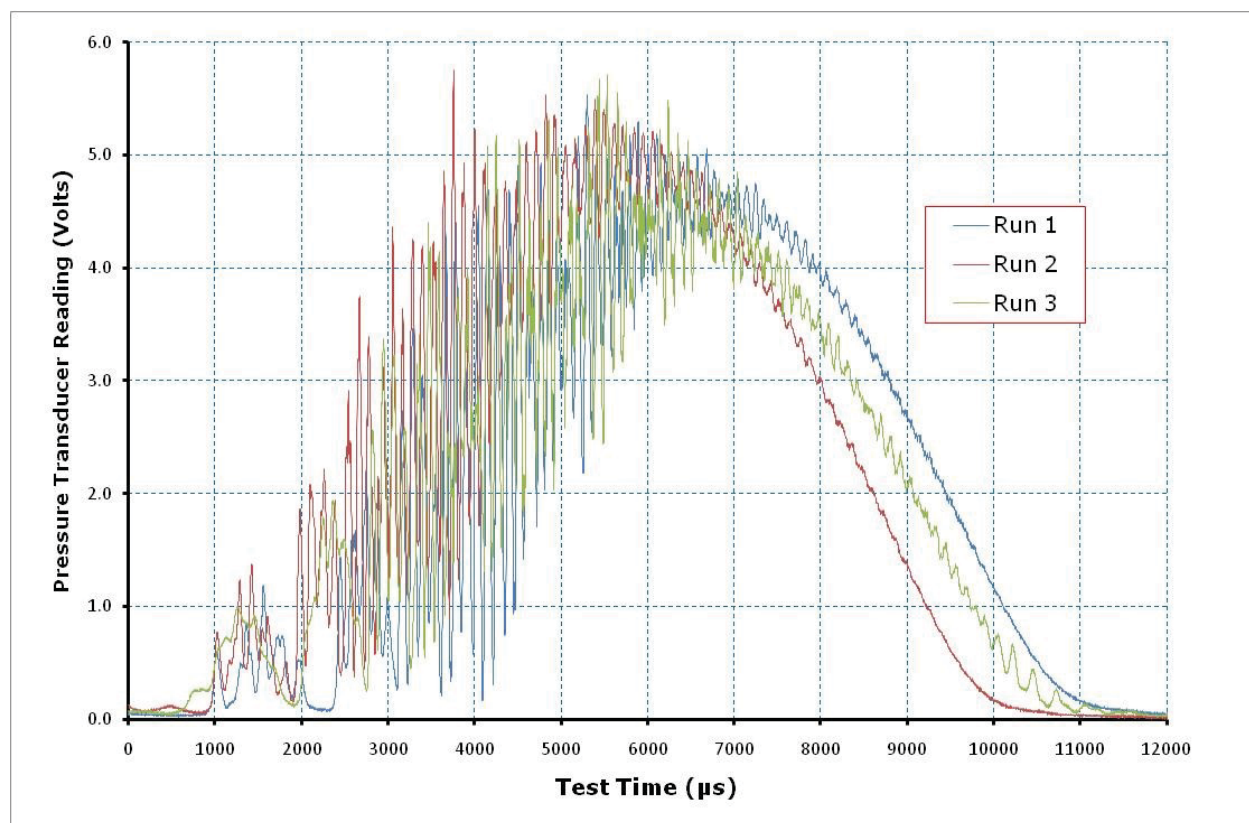


Figure C-1. Typical Drop Test Results Showing Pressure Transducer Output in Volts versus Test Time


	NASA Engineering and Safety Center Technical Assessment Report	Document #: NESC-RP- 09-00596	Version: 1.0
Title: Pyrovalve Booster Interface Temperature Measurement			Page #: 12 of 92

Figure C-2 shows the same data except that the 100 data point moving average is plotted.

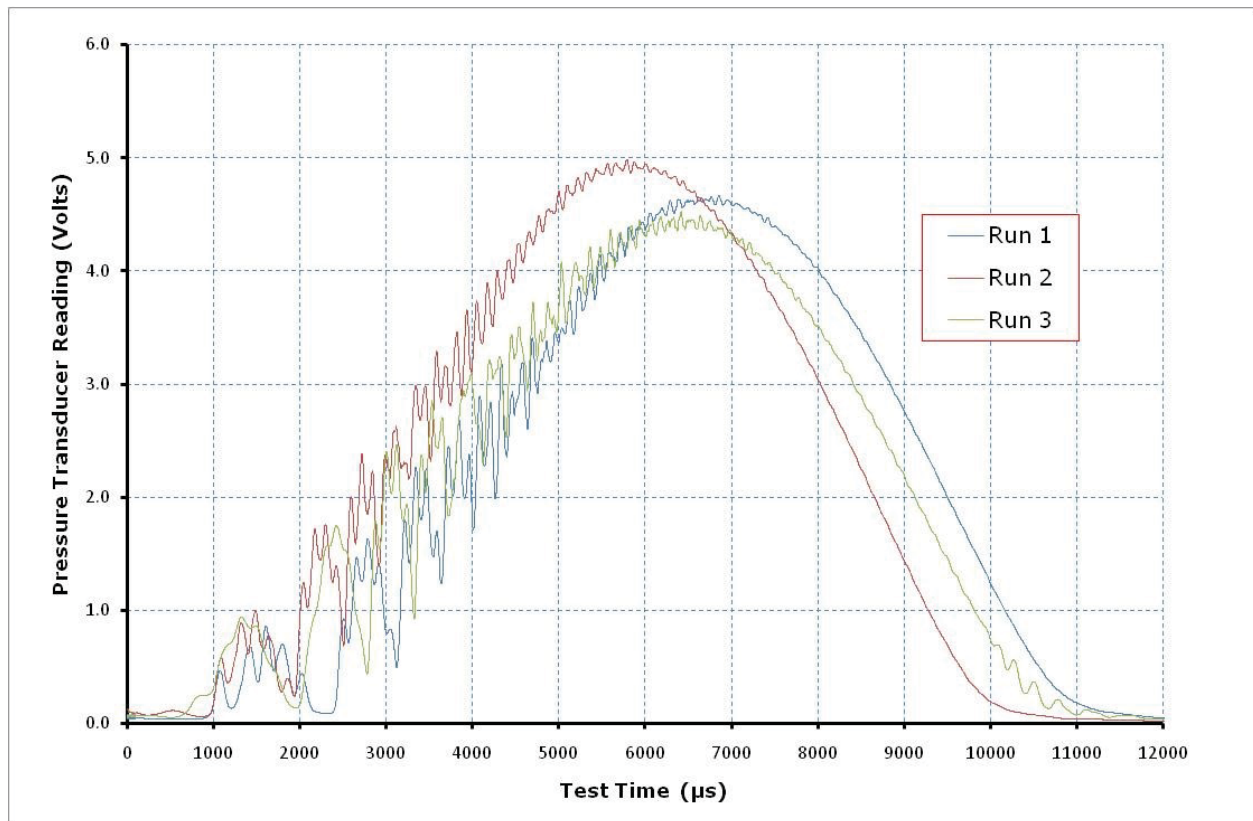


Figure C-2. Typical Drop Test Results Showing Pressure Transducer Output in Volts Versus Test Time. 100 Data Point Moving Average.

Figures C-3 through C-5 shows the drop tester.


	NASA Engineering and Safety Center Technical Assessment Report	Document #: NESC-RP- 09-00596	Version: 1.0
Title: Pyrovalve Booster Interface Temperature Measurement			Page #: 13 of 92



Figure C-3. The Assembled Drop Tester. A Pressure Transducer is Installed into the Oil Reservoir at the Bottom. The Drop Weight is Alongside. Holes Are Drilled in the Guide Tube at Various Heights so that the Drop Weight can be Positioned to get the Desired Effect.


	NASA Engineering and Safety Center Technical Assessment Report	Document #: NESC-RP- 09-00596	Version: 1.0
Title: Pyrovalve Booster Interface Temperature Measurement			Page #: 14 of 92



Figure C-4. The Drop Tester with the Guide Tube Removed to Show the Rod that Transmits the Impact of the Weight to the Oil Reservoir



	NASA Engineering and Safety Center Technical Assessment Report	Document #: NESC-RP- 09-00596	Version: 1.0
Title: Pyrovalve Booster Interface Temperature Measurement			Page #: 15 of 92



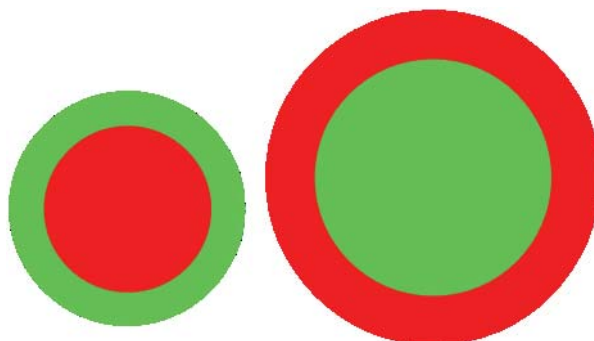
Figure C-5. In this Photograph of the Oil Reservoir, the Impact Rod has been Removed to Show the Installed O-Ring. This Photograph also provides a Closer View of the Pressure Transducer Installation.

	NASA Engineering and Safety Center Technical Assessment Report	Document #: NESC-RP- 09-00596	Version: 1.0
Title: Pyrovalve Booster Interface Temperature Measurement			Page #: 16 of 92

Appendix D. Assessment of Area versus Temperature Indication

During Phase IIB of the test program, a question arose over whether the larger flow passage diameters might be biasing the pyrometer readings by increasing the heated area within the pyrometer field of view (FOV).


In other words, consider the following situation where the green circle represents the pyrometer FOV and the red circle is the heated area of the diaphragm. In the illustration below, the green circle representing the FOV is the same size. However, the red circle on the right is twice the diameter of the one of the left to represent the case where the flow passage being tested had 4 times the nominal cross-sectional area. Could this “FOV effect” give a higher temperature reading even if the temperature is the same?



The manufacturer’s literature gave FOV information at various distances from the target and the pyrometer was located a specific distance from the sapphire window of the test article to give the desired FOV; but, to experimentally verify that a special test was performed.

A target heat source was positioned behind where the underside of the booster cover simulator in the test article would normally be. The temperature of the target was unimportant so long as it remained constant at a value above the minimum detectable by the pyrometer. A variable aperture was located in the exact plane where the underside of the test article booster cover simulator would be. The diameter of the aperture was incrementally reduced until the temperature indicated by the pyrometer started to drop off.

Figure D-1 shows the results of the four test runs that were made and how the determination of the FOV was determined.

	NASA Engineering and Safety Center Technical Assessment Report	Document #: NESC-RP- 09-00596	Version: 1.0
Title: Pyrovalve Booster Interface Temperature Measurement			Page #: 17 of 92

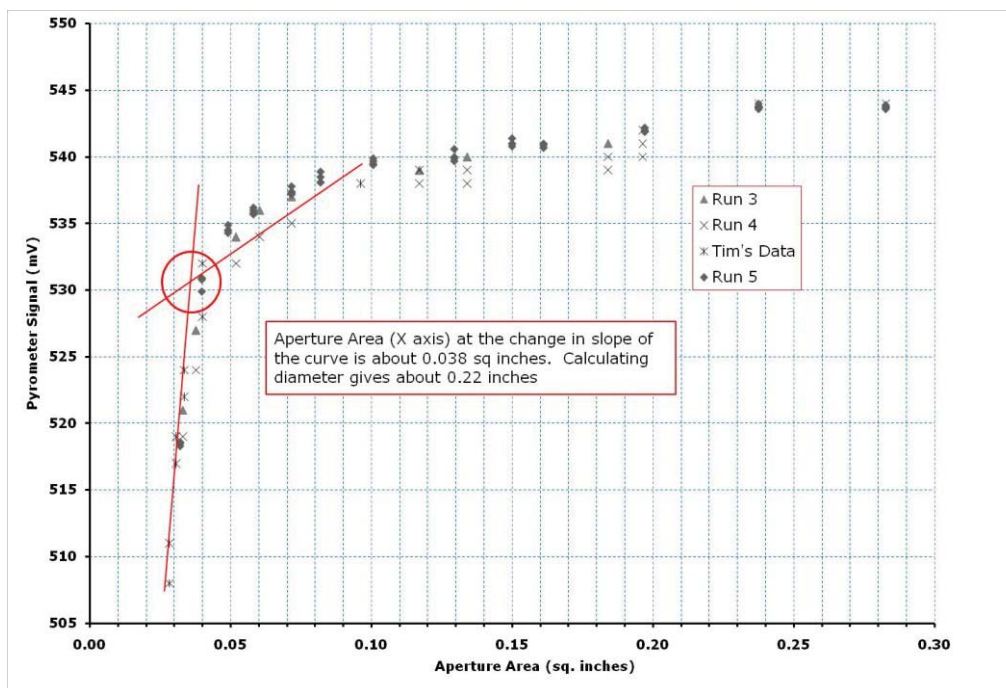



Figure D-1. Pyrometer Signal versus Aperture Area for a Constant Temperature Target

The diameter of the variable aperture was measured using calipers. The measured diameter was used to calculate the area of the aperture, which was then plotted against the pyrometer signal in millivolts. The objective was to look for a sharp change in slope of the curve to indicate at what point the aperture was starting to restrict the pyrometer's FOV.

The data were divided into two groups near where the change in slope occurred. A least-squares regression analysis was performed on both data groups to determine the best lines to represent the data. The intersection of those two lines gave the aperture area where the attenuation began to occur. From that area, the aperture diameter was calculated to be 0.22 inches. This then was the experimentally determined FOV.

The measured diameter of the underside of the booster cover simulator that is visible through the sapphire window is 0.25 inches. The NSI flame channel diameters ranged from 0.060 to 0.120 inches. Therefore, the pyrometer FOV was set appropriately to give the best possible indication of the actual temperature on the underside of the booster cover simulator. Another point worth noting is that the FOV was always the same from one test to another so that the measured temperatures would not be biased in any case.

	NASA Engineering and Safety Center Technical Assessment Report	Document #: NESC-RP- 09-00596	Version: 1.0
Title: Pyrovalve Booster Interface Temperature Measurement			Page #: 18 of 92

Appendix E. PCA Thermal Analysis

Heat transfer in the PCA may result from a variety of mechanisms described in detail in Reference 1. In this analysis, three heat transfer mechanisms to the booster cap surface were studied, individually:

1. Convective heat transfer from hot combustion gases;
2. Heat transfer via deposition and subsequent solidification of molten zirconia (ZrO_2) spray resulting from combustion; and
3. Deposition and subsequent combustion of ZPP.

Heat transfer in the PCA is complex and the analyses required simplifying assumptions to allow analytical study. These will be discussed further for each particular assumption.

All thermal network models developed for this analysis were created using Thermal Desktop[®] and solved using the Systems Improved Numerical Differencing Analyzer/Fluid Integrator (SINDA/FLUINT[®]). Both products were developed by Cullimore and Ring Technologies.

It is recognized that there are performance differences between the SS and Al PCA units. No attempt was made in this analysis to explain the differences. Rather, it is seen that both PCA designs require heating of the booster cap to actuate the device. The team's focus is on mechanisms that affect heating to the booster cap. Compression heating was not investigated in detail for this study and may have a significant contribution to the overall heat transfer to the booster cap. Such an analysis would require a flow analysis that was beyond the scope of this work.

E.1.1 Lumped-Mass Assessment of Convective Heat Transfer to the Booster Cap

A simplified closed-form thermal assessment of the SS booster cap response was performed considering only convective heat transfer to the cap and the effects of its thermal mass. The thermal analysis network schematic is depicted in Figure E.1-1.

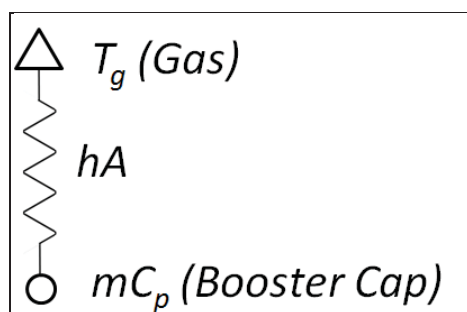



Figure E.1-1. Simplified Lumped-Mass Network Representation

	NASA Engineering and Safety Center Technical Assessment Report	Document #: NESC-RP- 09-00596	Version: 1.0
Title: Pyrovalve Booster Interface Temperature Measurement			Page #: 19 of 92

For this analysis, the booster cap was assumed to be a single lumped-mass heated only by convection. With this assumption, the overall heat transfer is given by:

$$mC_p \frac{\partial T}{\partial t} = hA(T_g - T(t)) \quad \text{EQ. 1}$$

where m is the booster cap mass, C_p is the booster cap specific heat, h is the convective heat transfer coefficient, A is the booster cap surface area exposed to the hot gas, $T(t)$ is the booster cap temperature at time, t , and T_g is the gas temperature. In this analysis, the specific heat, convective heat transfer coefficient and gas temperature are assumed to be constant. The constant gas temperature assumption results in a conservative analysis since the hot gas in the real configuration does not have infinite capacitance and would cool rapidly as heat is transferred to the PCA wall and booster cap.

$$\theta = \frac{T_g - T(t)}{T_g - T_0} \quad \text{EQ. 2}$$

where T_0 is the initial booster cap temperature. Then:

$$\frac{d\theta}{dt} = -\frac{1}{\tau} \theta \quad \text{EQ. 3}$$

where τ is the time constant given by:

$$\tau = \frac{mC_p}{hA} \quad \text{EQ. 4}$$

Furthermore, if the top of the booster cap is represented as a disk of radius, r , and thickness, d , the expression for the mass becomes:

$$m = \rho V = \rho \pi r^2 d \quad \text{EQ. 5}$$

where the surface area exposed to the hot combustion gases is given by:


$$A = \pi r^2 \quad \text{EQ. 6}$$

The expression for the time constant, τ , simplifies to:

$$\tau = \frac{mC_p}{hA} = \frac{\rho \pi r^2 d C_p}{h \pi r^2} = \frac{\rho d C_p}{h} \quad \text{EQ. 7}$$

Rearranging EQ. 3 yields:

$$\frac{d\theta}{\theta} = -\frac{1}{\tau} dt \quad \text{EQ. 8}$$

	NASA Engineering and Safety Center Technical Assessment Report	Document #: NESC-RP- 09-00596	Version: 1.0
Title: Pyrovalve Booster Interface Temperature Measurement			Page #: 20 of 92

and integration leads to:

$$\ln \theta = -\frac{1}{\tau}t + C \quad \text{EQ. 9}$$

where C is a constant of integration. But at $t = 0$, $T = T_0$ and $\theta = 1$. This implies $C = 0$. EQ. 9 becomes:

$$\ln \left(\frac{T_g - T(t)}{T_g - T_0} \right) = -\frac{th}{\rho d c_p} \quad \text{EQ. 10}$$

Simplifying and solving for h :

$$h = \frac{\rho d c_p}{t} \ln \left(\frac{T_g - T_0}{T_g - T(t)} \right) \quad \text{EQ. 11}$$

EQ. 11 allows exploration of the convective heat transfer coefficient required to produce temperatures seen on the booster cap. By specifying a constant gas temperature, T_g , and a time, t , at which a booster cap temperature $T(t)$ is observed, the required h value may be determined. By comparing the magnitude of h required to produce the observed temperature rise with published literature, an assessment of the contribution of convective heating to the overall booster cap temperature rise may be performed.

The h value required to produce a booster cap temperature of 866 K (1,100 °F) at a time of 500 μ s for various constant gas temperatures is presented in Figure E.1-2.

	NASA Engineering and Safety Center Technical Assessment Report	Document #: NESC-RP- 09-00596	Version: 1.0
Title: Pyrovalve Booster Interface Temperature Measurement			Page #: 21 of 92

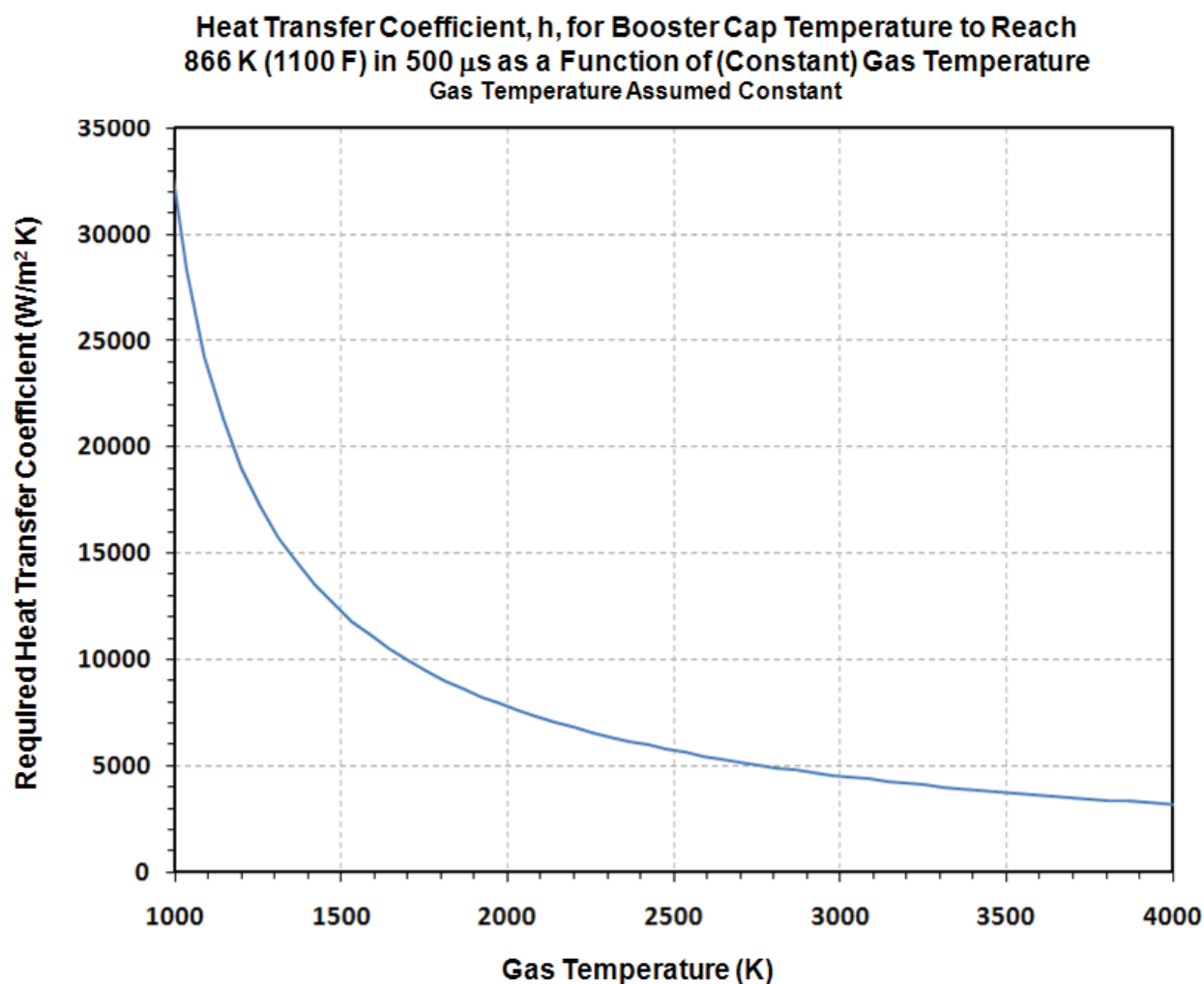



Figure E.1-2. Convective Heat Transfer Coefficient and Gas Temperature Parametric Analysis Results

Figure E.1-2 shows the required heat transfer coefficient is far beyond that found in the published literature [ref. 2] for lower gas temperatures (< 2,500 K), which suggests heat transfer coefficients on the order of:

1,000 W/m² K to 6,000 W/m² K (176 Btu/hr ft² °F to 1,056 Btu/hr ft² °F)

However, for gas temperatures above 2,500 K, the range of required heat transfer coefficients is within the range specified in Reference 2.

	NASA Engineering and Safety Center Technical Assessment Report	Document #: NESC-RP- 09-00596	Version: 1.0
Title: Pyrovalve Booster Interface Temperature Measurement			Page #: 22 of 92

This intuitively large range required convective heat transfer coefficients in concert with the assumption of constant gas temperature for this simplified analysis suggests that the observed booster cap transient temperature response may not be explained by convective heat transfer alone. Therefore, additional heat transfer mechanisms are investigated.

E.1.2 Zirconia (ZrO₂) Deposition


It was concluded in the previous section that high convective heat transfer coefficients are required to account for the rapid temperature rise observed in the booster cap. Another possible energy transfer mechanism is the exchange of heat through the deposition and solidification of molten ZrO₂ onto the PCA internal surfaces including the booster cap.

The NSI contains 114 mg (2.51×10^{-4} lbm) of ZPP. An estimated 71 percent [ref. 1, Section 7.4.1.2.2.2] of this material after combustion exists in the form of ZrO₂ and is expected to condense on surfaces cooler than 3,000 K (4,940 °F). The effect of ZrO₂ deposition and solidification and the associated heat transfer was simulated in the thermal model by assuming the following:

- 71 percent of 114 mg (80.94 mg) (1.78×10^{-4} lbm) of molten ZrO₂ is deposited uniformly onto the PCA internal walls and the top of the booster cap;
- The ZrO₂ deposition is present at the initiation time of the thermal model ($t = 0 \mu\text{s}$) and is in perfect contact with the Al walls and SS booster cap top;
- The assumed initial temperature for the PCA is 293 K (68 °F) and 2950.3 K (4851 °F) for the ZrO₂ which is just above the ZrO₂ melting temperature of 2,950 K (4,850 °F) [ref. 3];
- The heat of fusion for ZrO₂ is 707 J/g (304 Btu/lbm) [ref. 4];
- The internal exposed surface area of the A PCA was calculated to be 8.4 cm² (1.302 in²) based on the computer-aided design (CAD) representation derived from Reference 5. Subsequently, a 0.762-cm (0.3-inch) diameter booster cap was added to close out the volume; and
- The assumed density of the ZrO₂ was 5.68 g/cm³ (0.205 lbm/in³) [ref. 3].

Assumptions (e) and (f) may be used to determine a ZrO₂ deposition thickness, assuming uniform coating of all interior surfaces, of 0.017 mm (6.657×10^{-4} inches).

A one-dimensional thermal network model was developed to study the effect of ZrO₂ spray onto the booster cap and is depicted in Figure E.1-3.

	NASA Engineering and Safety Center Technical Assessment Report	Document #: NESC-RP- 09-00596	Version: 1.0
Title: Pyrovalve Booster Interface Temperature Measurement			Page #: 23 of 92

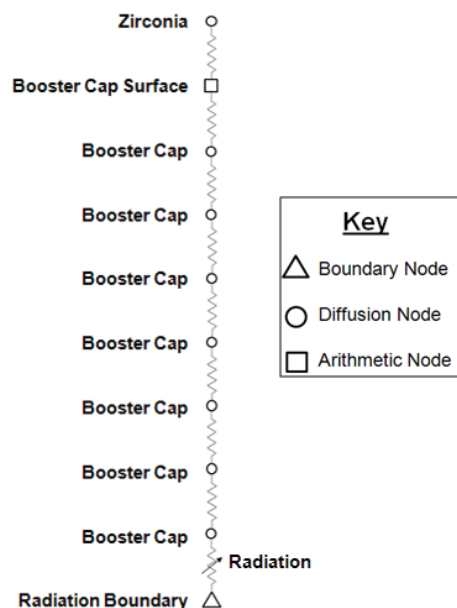



Figure E.1-3. Zirconia Spray Thermal Network Model

The predicted temperature response is depicted in Figure E.1-4.

	NASA Engineering and Safety Center Technical Assessment Report	Document #: NESC-RP- 09-00596	Version: 1.0
Title: Pyrovalve Booster Interface Temperature Measurement			Page #: 24 of 92

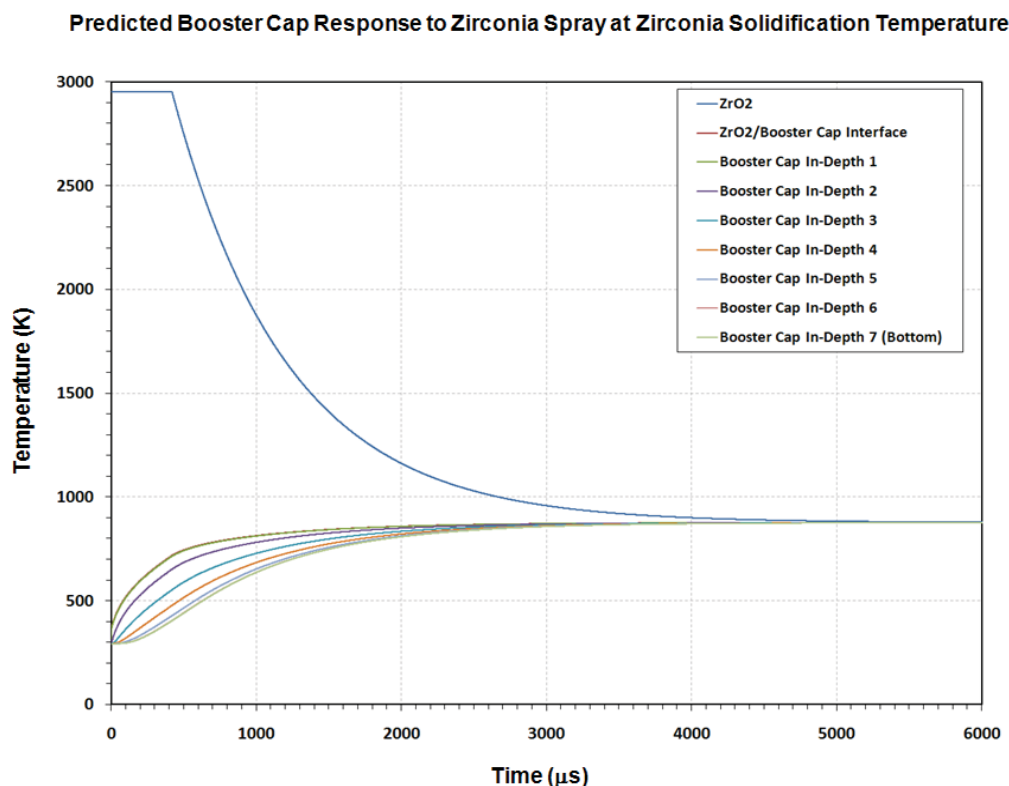



Figure E.1-4. Zirconia Spray Thermal Analysis Results

The effect of zirconia solidification is seen in Figure E.1-4. Latent heat stored in the melted zirconia conducts into the booster cap causing temperatures to rise. When the zirconia has solidified, conduction to the booster cap continues and a temperature drop is observed as the flow of sensible heat. While a zirconia deposit of uniform thickness can raise the temperature of the bottom of the booster cap to temperatures greater than that required for booster propellant ignition, the timeframe required for this is well beyond what has been observed in PCA firing tests. Additionally, with the assumption of constant thickness deposition, there is insufficient energy stored in the deposited zirconia to raise the temperature of the booster cap above its melt temperature. Melting of a portion of the booster cap has been seen in many of the PCA firing tests.

A sensitivity analysis was performed by assuming double zirconia deposition thickness. The same thermal model was used except that the mass of the zirconia was doubled and the conductance from the double-thickness zirconia node was halved to account for the increased thickness; no additional nodal subdivision was added. The results of the analysis are presented in Figure E.1-5.

	NASA Engineering and Safety Center Technical Assessment Report	Document #: NESC-RP- 09-00596	Version: 1.0
Title: Pyrovalve Booster Interface Temperature Measurement			Page #: 25 of 92

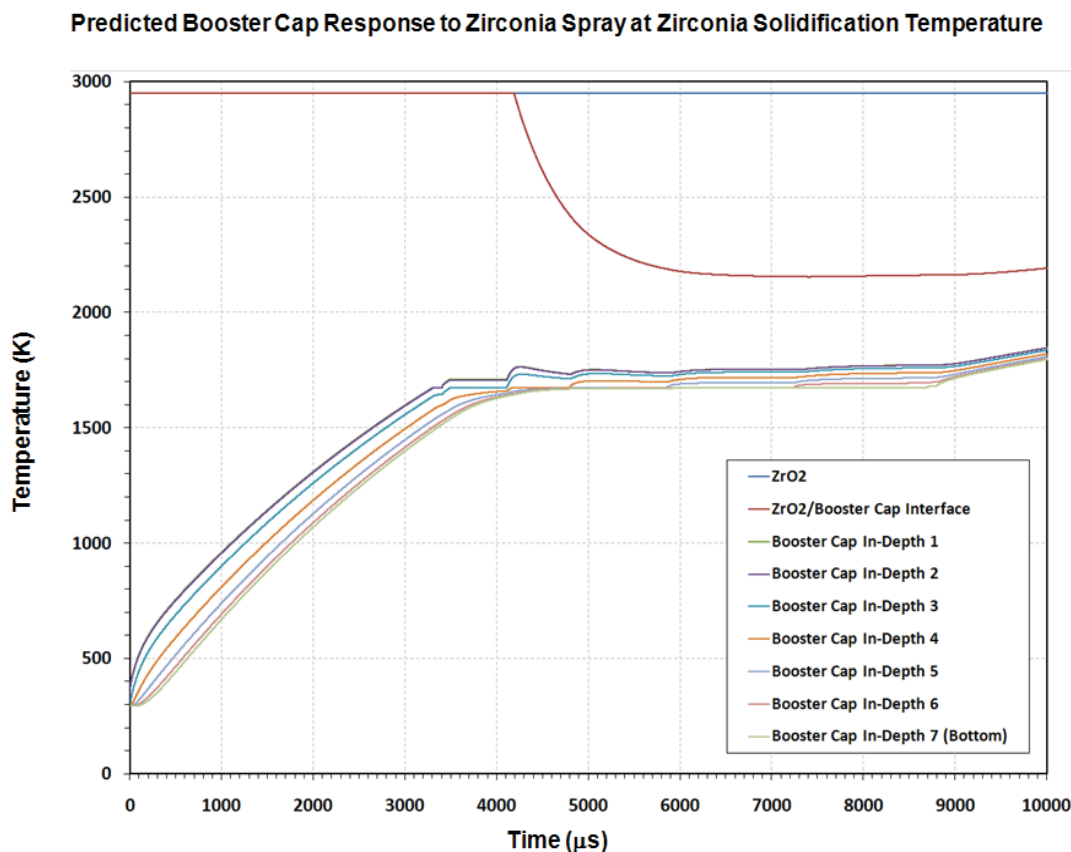



Figure E.1-5. Zirconia Spray Thermal Analysis Results Assuming Double Zirconia Thickness

As seen in Figure E.1-5, the additional zirconia mass now contains sufficient energy to raise the booster cap nodes to the melt temperature. Melting progresses through the thickness until a temperature rise above the assumed melt temperature of 1,672 K (2,550 °F) is seen indicating that the melt-through was complete. While this analysis results in melting and temperatures sufficient to ignite the booster propellant, neither occurs within the timeframe observed during testing.

Finally, it should be noted that only through-the-thickness heat transfer was modeled and conduction losses to the PCA structure were not modeled. In actual operation, these losses would reduce the energy available to heat the booster cap.

From this simplified analysis, it can be concluded that deposition of molten zirconia onto the booster cap may play a significant role in raising the temperature in addition to convective heat transfer. However, the timeframe during which heat transfer to the booster cap occurs suggests

	NASA Engineering and Safety Center Technical Assessment Report	Document #: NESC-RP- 09-00596	Version: 1.0
Title: Pyrovalve Booster Interface Temperature Measurement			Page #: 26 of 92

that this is not the primary mode of heat transfer to the booster cap. The sensitivity analysis suggests that thicker deposits of zirconia increase the propensity of melting the booster cap and accelerating heat transfer through the cap.

E.1.3 ZPP Combustion in Contact with the Booster Cap

It is estimated that up to 20 percent (22.8 mg) of the ZPP exits the NSI unburned [ref. 1]. High-speed photography obtained during NSI testing shows that a portion of the ZPP emerges from the NSI unburned as is seen in Figure E.1-6 [ref. 6].

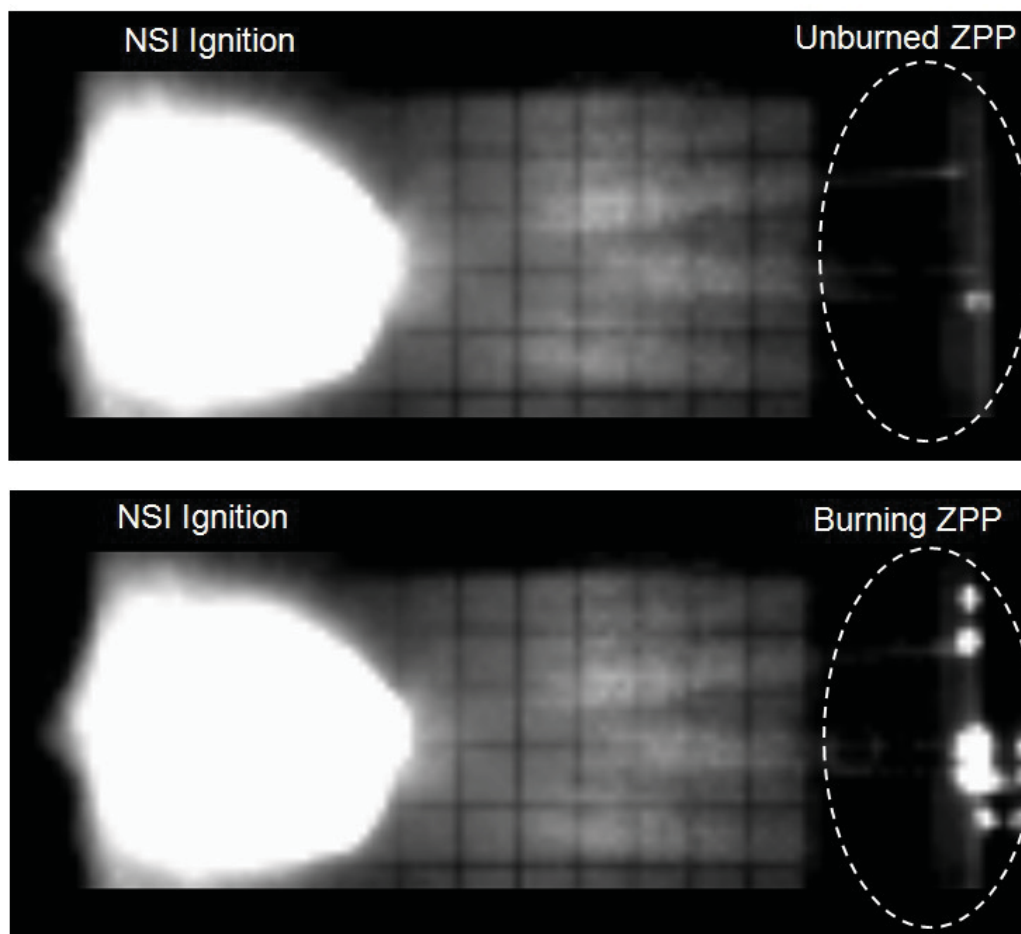



Figure E.1-6. Photographic Evidence of Late ZPP Combustion

The heat transfer associated with transport of ZPP to the top of the booster cap was investigated. ZPP has a heat of combustion (H_{zpp}) between 5,609 and 6,070 J/g and a density (ρ_{zpp}) of 3.23 g/cm³ (90 lbm/in³) [ref. 1, Section 7.4.1.2.2.1]. In the scenario examined, unburned ZPP is

	NASA Engineering and Safety Center Technical Assessment Report	Document #: NESC-RP- 09-00596	Version: 1.0
Title: Pyrovalve Booster Interface Temperature Measurement			Page #: 27 of 92

expelled from the NSI and some unknown fraction is transported to the interior-facing surface of the booster cap. The purpose of this analysis was to determine whether or not this ZPP, burning while in contact with the booster cap, could produce sufficient heat transfer to account for the booster cap temperature rise, response and observed melting. Both simplified hand calculations and a transient thermal analysis were used to investigate this possibility.

E.1.3.1 Lumped-Mass Model

In this simplified analysis, heat is distributed over the entire booster cap area exposed to the hot combustion gases and a transient analysis is performed to determine how much ZPP is required to melt the booster cap surface. The thermal model network is depicted in Figure E.1-7.

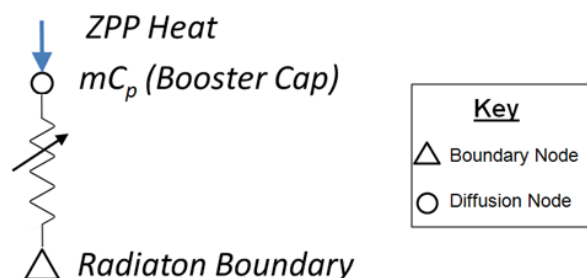


Figure E.1-7. Simplified ZPP Heating Model Network with Back-Side Radiation

A parametric analysis was performed assuming deposition of various amounts of the initial total unburned ZPP onto the booster cap surface. ZPP burning was assumed to occur over a period of 500 μ s. The results of the parametric study are presented in Table E.1-1.


	NASA Engineering and Safety Center Technical Assessment Report	Document #: NESC-RP- 09-00596	Version: 1.0
Title: Pyrovalve Booster Interface Temperature Measurement			Page #: 28 of 92

Table E.1-1. Results of Parametric Analysis Investigating the Quantity of ZPP Required to Melt the Entire Booster Cap Surface


Percentage of Unburned ZPP (%)	Percentage of Total ZPP (%)	Peak Booster Cap Temperature (F)	Melt Status
1.0	0.2	244	None
10.0	2.0	1830	None
11.0	2.2	2006	None
12.0	2.4	2182	None
13.0	2.6	2354	None
14.0	2.8	2358	None
15.0	3.0	2550	Partial
17.0	3.4	2550	Partial
19.0	3.8	2550	Partial
20.0	4.0	2621	Complete

With this model, a conservative upper limit for the amount of ZPP required to melt the booster cap was established. Note that the results are expressed as a function of percentage of unburned ZPP that is deposited onto the booster cap surface. If 20 percent of the ZPP from the NSI is unburned [ref. 1], then 20 percent of that quantity is required to fully melt the booster cap surface under the assumptions in this analysis — or only 4 percent of the initial NSI ZPP load ($0.20 \times 0.20 = 0.04$). This corresponds to a ZPP mass of approximately 4.6 mg (1.0×10^{-5} lbm).

However, photographic evidence of booster caps indicates melting is a more local phenomenon as seen in Figure E.1-8 [ref. 7].



Figure E.1-8. Phase IIB—Post-Test Images of the Booster Cover Simulators, Sapphire Windows, and Sealing Rings

	NASA Engineering and Safety Center Technical Assessment Report	Document #: NESC-RP- 09-00596	Version: 1.0
Title: Pyrovalve Booster Interface Temperature Measurement			Page #: 30 of 92

While the results presented in Table E.1-1 are suggestive of an upper bound to the required quantity of ZPP, an assessment of the temperature of local melting of metal in direct contact with the ZPP globule is desired.

E.1.3.2 Local Heating from a ZPP Globule—Transient Predictions

A refined calculation may be used to account for the physical extent of a ZPP globule by assuming the molten globule is a hemisphere as it sits upon the booster cap (Figure E.1-9).

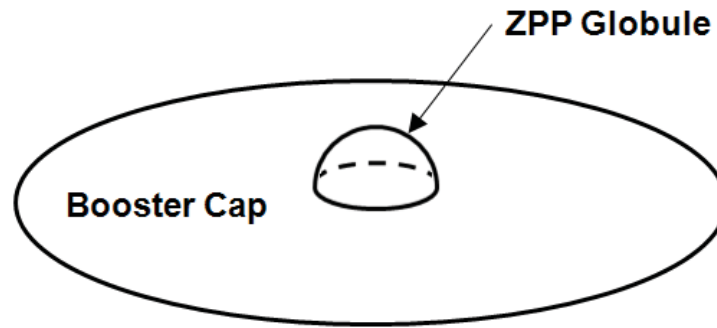


Figure E.1-9. ZPP Globule on Booster Cap

In this instance, the mass of a ZPP globule is given by:


$$m_{zpp} = \rho_{zpp} V_{zpp} = \frac{1}{2} \rho_{zpp} \left(\frac{4}{3} \pi r_{zpp}^3 \right) \quad \text{EQ. 12}$$

and the radius of the hemispherical ZPP globule is, then:

$$r_{zpp} = \sqrt[3]{\frac{1.5 m_{zpp}}{\rho_{zpp}}} \quad \text{EQ. 13}$$

The resulting globule radius is used in a simplified transient thermal analysis of the booster cap to determine if local melting will occur, assuming that all heat generated during ZPP combustion is transferred to the local booster cap surface. This analysis represents an improvement in fidelity over the simplified lumped-mass model presented in the previous section, in that heating is applied only to the region in contact with the ZPP and heating of the remaining booster cap surface is through conduction. The added benefit of the time dependency allows comparison of the transient temperature profile observed during PCA testing.

The predicted transient response to burning of a small hemispherical globule of ZPP ($m = 6.5 \times 10^{-4}$ mg) for selected booster cap nodes is shown in Figure E.1-10. In this simulation, heat generated as a result of the combustion of a small amount of ZPP conducts into a representation of the booster cap. Heat transfer is assumed to be in the radial direction

	NASA Engineering and Safety Center Technical Assessment Report	Document #: NESC-RP- 09-00596	Version: 1.0
Title: Pyrovalve Booster Interface Temperature Measurement			Page #: 31 of 92

(i.e., only a single node through-the-thickness). At this level of fidelity, it is clear that the heating is a localized effect and the temperature rises as a function of radial distance diminishes rapidly. This is suggestive of localized melting, an effect observed in booster cap testing (Figure E.1-8). Heat transfer through-the-thickness of the booster cap is investigated in the following section.

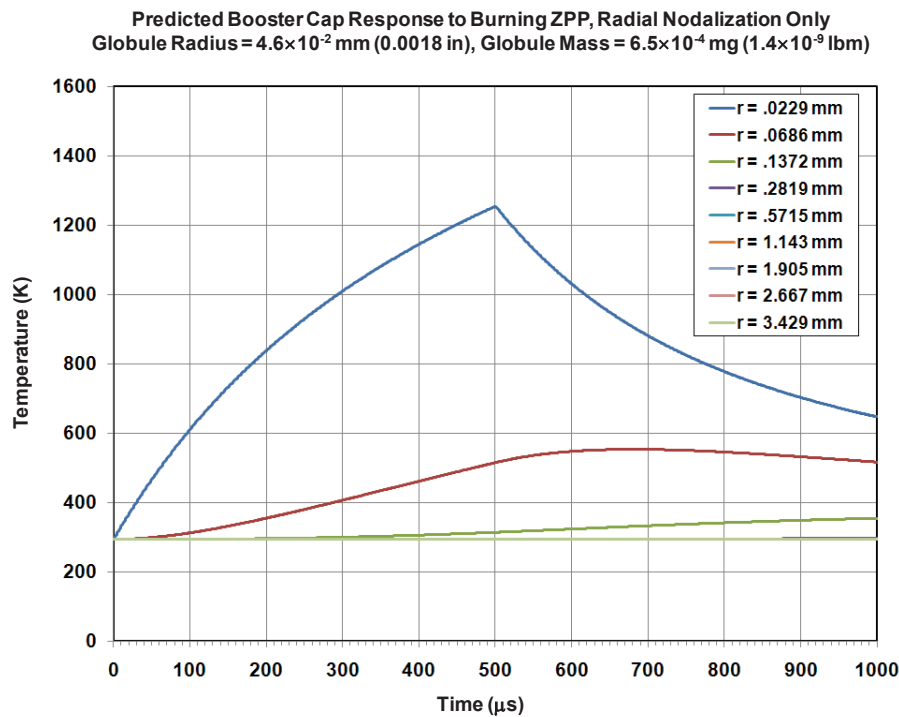



Figure E.1-10. Predicted Temperature Response of Booster Cap with Localized Globule of ZPP (Radial Nodalization Only)

E.1.3.3 Local Melting through the Booster Cap Thickness

In a previous section, an estimate of the maximum amount of ZPP required to melt the entire booster cap was given to be approximately 4.6 mg (1.0×10^{-5} lbm). An estimate of a lower bound on the amount of ZPP required to initiate local melt-through is sought. In this analytical development, heating resulting from ZPP burning is assumed to be transferred to the booster cap metal directly beneath it (i.e., a cylindrical core through-the-thickness); no radial heat transfer or back-side radiation is assumed.

The mass of a hemispherical ZPP globule was showing in Eq. 12 to be:

$$m_{zpp} = \frac{1}{2} \rho_{zpp} \left(\frac{4}{3} \pi r_{zpp}^3 \right) = \frac{2}{3} \rho_{zpp} \pi r_{zpp}^3 \quad \text{EQ. 14}$$

	NASA Engineering and Safety Center Technical Assessment Report	Document #: NESC-RP- 09-00596	Version: 1.0
Title: Pyrovalve Booster Interface Temperature Measurement			Page #: 32 of 92

The heat liberated by burning this quantity of ZPP is given by:

$$\Delta Q_{zpp} = m_{zpp} H_{zpp} = \frac{2}{3} H_{zpp} \rho_{zpp} \pi r_{zpp}^3 \quad \text{EQ. 15}$$

For simplification purposes, it is assumed that the hemispherical globule of ZPP heats only the cylindrical core of SS directly beneath it. Then, the heat required to raise the temperature of the cylindrical core to the melt temperature plus the heat required to melt the material is given by:

$$\Delta Q_{Total} = \Delta Q + \Delta Q_{Melt} \quad \text{EQ. 16}$$

Expanding yields:

$$\Delta Q_{Total} = \pi r^2 d \rho_{SS} [C_p (T_{Melt} - T_0) + H_f] \quad \text{EQ. 17}$$

Where C_p is the SS specific heat, T_{Melt} is the melting temperature, T_0 is the initial temperature, and H_f is the SS heat of fusion.

For this simplified case, the ZPP globule will have sufficient energy content to melt the metal beneath it when:


$$\Delta Q_{ZPP} \geq \Delta Q_{Total} \quad \text{EQ. 18}$$

Substituting in expressions from EQs. 15 and 17 and rearranging gives the desired result:

$$r \geq \frac{3d\rho_{SS}[C_p(T_{Melt}-T_0)+H_f]}{2H_{zpp}\rho_{zpp}} \quad \text{EQ. 19}$$

When the appropriate parameters are substituted into EQ. 19, the resulting radius is 4.6×10^{-2} mm (1.8×10^{-3} inches). This corresponds to a ZPP mass of 6.5×10^{-4} mg (1.4×10^{-3} lbm).

This result suggests that even the smallest of ZPP globules has sufficient energy to cause local melting and sets a lower bound to the ZPP required to melt through the booster cap. However, the local heating and melting assumption may not be realistic given that heat applied at one location on the booster cap can conduct both radially and through-the-thickness of the booster cap. A higher fidelity model is required.

	NASA Engineering and Safety Center Technical Assessment Report	Document #: NESC-RP- 09-00596	Version: 1.0
Title: Pyrovalve Booster Interface Temperature Measurement			Page #: 33 of 92

E.1.3.4 Two-Dimensional Axisymmetric Model

A two-dimensional axisymmetric thermal model was developed to investigate the effect of burning ZPP on a lumped-mass representation of the booster cap including localized melting effects with model fidelity in both the radial and through-the-thickness directions. Phase change for the SS was incorporated into the model with the following assumptions:

- Transient analysis was performed assuming transport of the unburned ZPP to the booster cap surface in the form of a hemispherical globule;
- ZPP combustion with constant heat generation over a period of 500 μ s;
- Heat transfer to the booster cap was assumed to be perfect; all heat generated was used to raise the booster cap temperature and melt the material, if applicable;
- No transfer from the booster cap to the PCA structure was assumed; and
- Radiation off the back-side is to a 293 K (68 °F) environment.

A schematic representation of a booster cap finite difference thermal model is shown in Figure E.1-11.

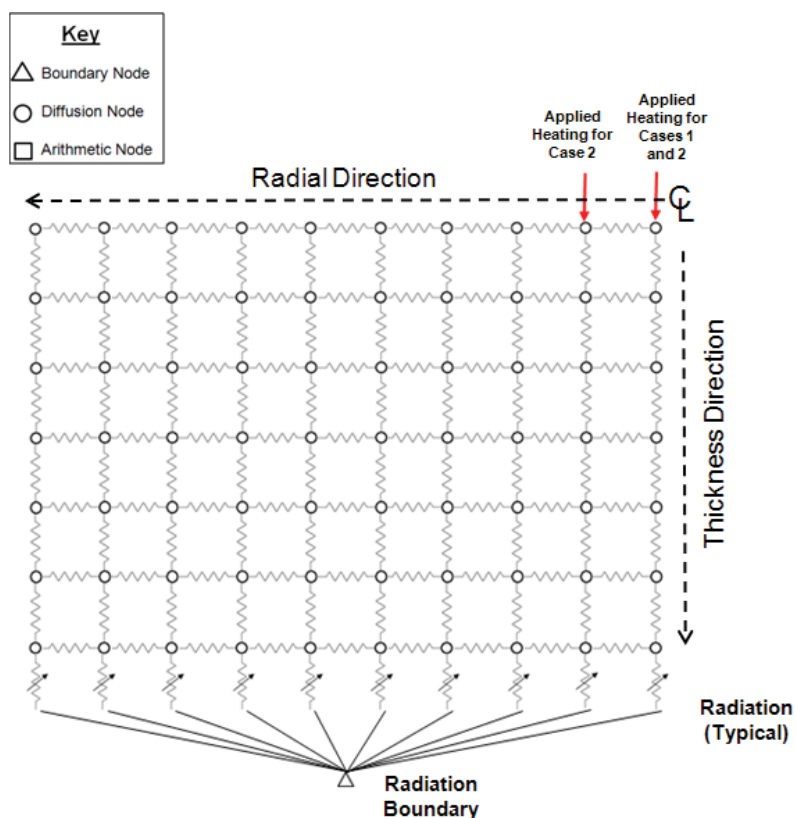



Figure E.1-11. Burning ZPP Thermal Network Model

	NASA Engineering and Safety Center Technical Assessment Report	Document #: NESC-RP- 09-00596	Version: 1.0
Title: Pyrovalve Booster Interface Temperature Measurement			Page #: 34 of 92

Heating was calculated and applied for the case where $r = 4.6 \times 10^{-2}$ mm (1.8×10^{-3} inches), a value corresponding to the radius determined by the simplified analysis in the previous section, dubbed Case 1. The results of the transient analysis are presented in Figure E.1-12.

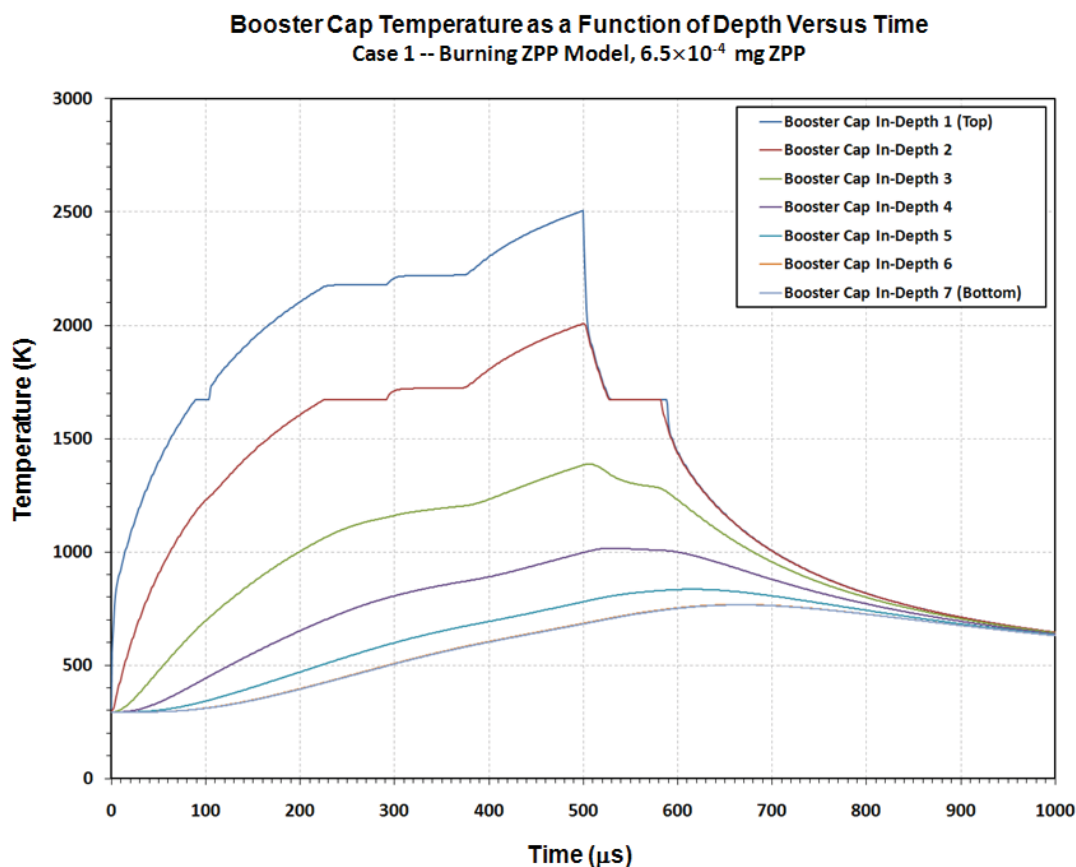



Figure E.1-12. Two-Dimensional Axisymmetric Thermal Model Results for a 4.6×10^{-2} mm (1.8×10^{-3} inches) Radius Hemispherical ZPP Globule Showing Incomplete Melt-Through

As shown in Figure E.1-12, there is sufficient energy to raise the temperature and melt nodes on the upper booster cap surface. However, due to radial conduction effects plus differentiation of nodal temperatures through-the-thickness, there is insufficient energy to melt completely through the cap. Predicted temperatures on the bottom of the cap reach a maximum of approximately 755 K (900 °F), far short of the assumed melt temperature of 1,672 K (2,550 °F).

To determine the amount of ZPP required to melt through the entire booster cap depth, the radius was raised to twice the previous value $r = 0.091$ mm (3.6×10^{-3} inches), dubbed Case 2. Since the volume of the associated hemisphere of ZPP changes with r^3 , the ZPP mass for the larger radius

	NASA Engineering and Safety Center Technical Assessment Report	Document #: NESC-RP- 09-00596	Version: 1.0
Title: Pyrovalve Booster Interface Temperature Measurement			Page #: 35 of 92

globule is 8 times that in the previous case; hence, 8 times as much energy is liberated by this larger globule. However, the surface area over which the heat is applied increases as r^2 .

The math model was rerun producing unrealistically high temperatures on the booster cap surface—temperatures far in excess of the melting point and well above the expected ZPP temperature. This is due to the chosen modeling technique wherein ZPP burning is considered to be an applied heating rate rather than a combustion temperature with a specified conductance to the booster cap. However, from a heat transfer through-the-thickness perspective, the increased heating provides sufficient energy to melt completely through the booster cap. Temperatures along the bottom of the booster cap surface as a function of time and radial distance are shown in Figure E.1-13.

While not a full fidelity analysis, the result suggests that the smallest amounts of ZPP burning in contact with the booster cap contain sufficient energy to produce the observed melting of the SS cover. It is also observed in Figure E.1-13 that melt-through is a highly localized effect. Given the mitigated temperature response as radial distance increases, the assumption of negligible heat transfer from the booster cap to the PCA structure is validated.

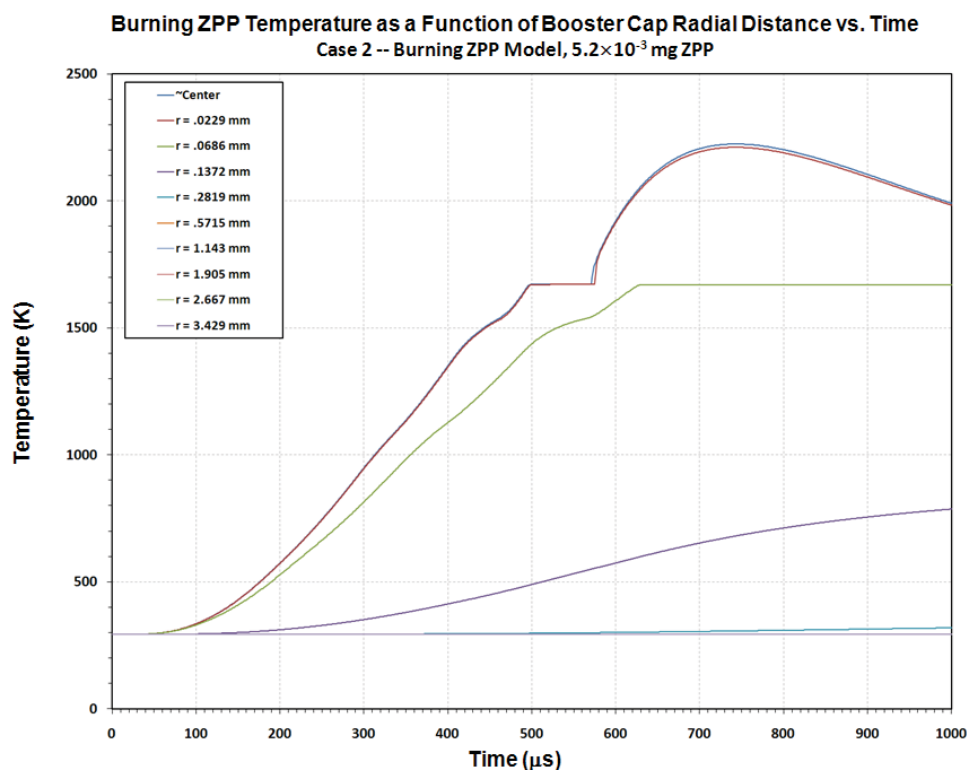



Figure E.1-13. Two-Dimensional Axisymmetric Complete Melt-Through Thermal Model Results for the Booster Cap Bottom

	NASA Engineering and Safety Center Technical Assessment Report	Document #: NESC-RP- 09-00596	Version: 1.0
Title: Pyrovalve Booster Interface Temperature Measurement			Page #: 36 of 92

The results of this refined analysis suggest that complete melt-through of the booster cap can be accomplished with as little as 5.2×10^{-3} mg (1.14×10^{-8} lbm) of ZPP forming a hemispherical globule with $r = 0.091$ mm (3.6×10^{-3} inches).

E.1.4 Conclusions


Three heat transfer mechanisms and their effect on booster cap thermal response were investigated as part of this study. From the analysis, the following conclusions were drawn:

- Convective heat transfer, by itself, may not account for the temperature rise and melting during booster cap testing. Further computational and/or empirical quantification of gas temperatures and heat transfer coefficients are needed to draw a definitive conclusion as to whether convection alone is sufficient.
- Zirconia deposition and the subsequent phase change from liquid to solid state may assist in booster cap heating and subsequent melting but do not produce booster cap temperatures in agreement with the booster cap transient temperature response observed during testing. Larger quantities of zirconia deposition increase the propensity to melt and accelerate the temperature rise of the booster cap bottom.
- Unburned ZPP deposition can liberate sufficient energy to locally melt through the booster cap as indicated by detailed thermal analysis of a hemispherical globule of ZPP with a radius of 3.6×10^{-3} in and a mass of 5.2×10^{-3} mg (1.14×10^{-8} lbm). Deposition of as little as 20 percent of the unburned ZPP (~ 4.6 mg, or 1×10^{-5} lbm) can liberate sufficient energy to melt the entire booster cap. Subsequent two-dimensional axisymmetric thermal analysis shows that local melt-through can be accomplished with considerably less ZPP. From this, it is concluded that $\ll 4.6$ mg ZPP burning in contact with the booster cap is sufficient to produce the observed response.

While heat transferred by convection and the phase change of liquid zirconia deposited on the booster cover simulator, the unburned ZPP results are a compelling indication that this mechanism could be a viable alternative mechanism. There would presumably be a lot of variation in the quantity, size and impingement locations of unburned ZPP that could explain inconsistent performance of the NSIs.

Acknowledgements

Mr. John Sharp of MSFC and the NASA Engineering and Safety Center (NESC) Passive Thermal Technical Discipline Team are acknowledged for their thorough peer review of the thermal analysis. NESC Resident Engineer, Ms. Courtney Flugstad, is acknowledged for her initial lumped-mass heating calculations for ZPP burning. NESC Resident Engineer, Mr. Brian Anderson, is acknowledged for his investigation of compression heating.

	NASA Engineering and Safety Center Technical Assessment Report	Document #: NESC-RP- 09-00596	Version: 1.0
Title: Pyrovalve Booster Interface Temperature Measurement			Page #: 37 of 92

Appendix F. Phase I Statistical Analysis and Results


The statistical approach to Phase I was designed to answer the statement of problem:

Given a limited number of test articles, what differences can be seen between the original AI Y-PCA design and the SS V-PCA one in a number of responses? Is there a difference in these responses given a dual simultaneous firing of a pair of NSI over a single-NSI firing?

The Phase I test was designed using some design of experiments (DOE) methods. The statement of problem was clearly developed. The size of the test was governed by resource considerations rather than a quantitative statement regarding a confidence level on a difference the team desired to be able to find, but the subject matter experts had reason to believe this test would be sufficient to show clear and useful differences. They were correct in this assessment, as will be seen.

Due to the availability of parts, the runs were not completely randomized. This may have had an effect on the data, though it is not quantified or likely even quantifiable. The results, however, are clear enough that the qualitative and at least the rough quantitative conclusions and resulting recommendations are correct and useful.

In addition to the direct response data analysis (generally using analysis of variance (ANOVA) techniques), some information and data surrounding conduct of the test, such as Trigger voltage, were mined for useful observations and anomalies.

	NASA Engineering and Safety Center Technical Assessment Report	Document #: NESC-RP- 09-00596	Version: 1.0
Title: Pyrovalve Booster Interface Temperature Measurement			Page #: 38 of 92


F.1 Analysis and Results

A summary of Phase I test analysis and results is shown in Table F-1.

Table F-1. Summary Table of Response Means and 95 Percent Confidence Intervals on the Means

Response	SS Mean	± 95 percent	AI Mean	± 95 percent	Notes
Time of Maximum Temperature	776	120	959	120	
Peak Temperature	2,290 °F	431	1,391 °F	431	Ignored Run 9
Temperature at 800 μs	2,247 °F	440	1,162 °F	440	Ignored Run 9
Time of Port A Pressure Rise Start	144 μs	5	137 μs	5	Ignored Run 9; included duals
Port A Calculated Peak Pressure	10,729 psi	289	7,796 psi	1,292	Ignored Run 9; included duals; weighted analysis
Port A Pressure at 800 μs	4,768 psi	406	3,420 psi	363	
Time of Port B Pressure Rise Start	~295 μs		~295 μs		Difference not significant
Port B Calculated Peak Pressure	4,779 psi	313	1,895 psi	283	Included Duals
Port B Time to Peak Pressure	~830 μs		~1,400 μs		Runs 9 and 9B may be outliers
Port B Pressure at 800 μs	4,588 psi	300	1,637 psi	269	

The Data. This narrative will refer to the Run Number to signify individual trials. The order in which its trials were run is different from the Run Number. Run 9 showed some unusual characteristics, including being the only AI run to burn through the diaphragm simulating the booster charge, and was rerun as Run 9B. Run 9B ended up as a misfire and was not rerun again. It is possible that no run after Run 3 is valid, but the conclusions presented below do not depend heavily on these later runs.

	NASA Engineering and Safety Center Technical Assessment Report		Document #:	Version:
			NESC-RP-09-00596	1.0
Title: Pyrovalve Booster Interface Temperature Measurement			Page #: 39 of 92	


Run Number	Order Trials Run	Material	Number of NSIs	TIME OF PRESS A START	PRESS A CALC PEAK	TIME OF PRESS A PEAK	TIME OF PRESS B START	PRESS B PEAK	TIME OF PRESS B PEAK	DIA-PHRAGM MAX TEMP	TIME OF MAX TEMP	800us PRESS A	800us PRESS B	800us TEMP DIA
2	1	SS	Single	140	10926	156	255	4570	824	2823	835	4638	4527	2836
6	2	SS	Dual	152	10419	168	151	9735	168			9252	9196	
7	3	SS	Single	147	10781	166	324	4996	787	1967	821	4933	4979	1957
14	4	SS	Single	144	10436	159	314	4441	870	1885	726	4690	4232	1842
15	5	SS	Single	147	11085	169	259	4805	845	2485	721	4811	4614	2352
4	6	Al	Single	143	6881	157	286	1650	1241	1308	1053	2938	1580	1133
8	7	Al	Single	138	8199	154	297	1860	1480	1412	913	3337	1307	1264
3	8	Al	Single	130	8001	156	319	2269	1440	1691	1064	3857	1716	1404
9	9	Al	Single	155	6560	160	292	1848	1130	2902	804	3077	1762	2894
1	10	Al	Dual	149	6456	164	149	6244	163	719	10210	4863	4857	
9B	11	Al	Single	137	9445	154	307	2149	1445	1154	2875	3892	1820	846

All PCAs had the same channel area, though the volume was likely different between the Al and SS blocks due to the design differences.

Dual Firings. Both dual firings resulted in peak temperatures below the temperature required for booster charge ignition and times to these maxima. Pressures in these were high. This was a clear indication that dual, simultaneous firing of redundant NSIs *could* result in a chain of events resulting in lower reliability instead of the higher reliability intended.

Parameters Involved in NSI Firing. No important conclusions were drawn from the measurements discussed in this section, but the reader should be aware of the observations. Traces for Runs 1 and 8 were different from the others.

Firing Voltage. No important conclusions were drawn from this measurement, but the reader should be aware of the observations. An exponentially weighted moving average (EWMA) (Roberts, 1959) was used in Figure F-1 to smooth the data for visual analysis.

	NASA Engineering and Safety Center Technical Assessment Report	Document #: NESC-RP- 09-00596	Version: 1.0
Title: Pyrovalve Booster Interface Temperature Measurement			Page #: 40 of 92

Two of the runs, Run 1 (dark grey) and 8 (dark blue), exhibited unusual firing voltage signatures over time compared to the other runs. Run 2 was the AI dual firing. Run 8 was another AI run that seemed to have no other distinguishing responses or features. The apparent differences showed up as a noise event at just over 700 μ s. Discussion was held on these anomalies, but as the firing voltage appeared only to be an issue for the extremely short interval needed for actually firing the NSIs and no anomalies were seen during that time frame for these trials, it was not explored further.

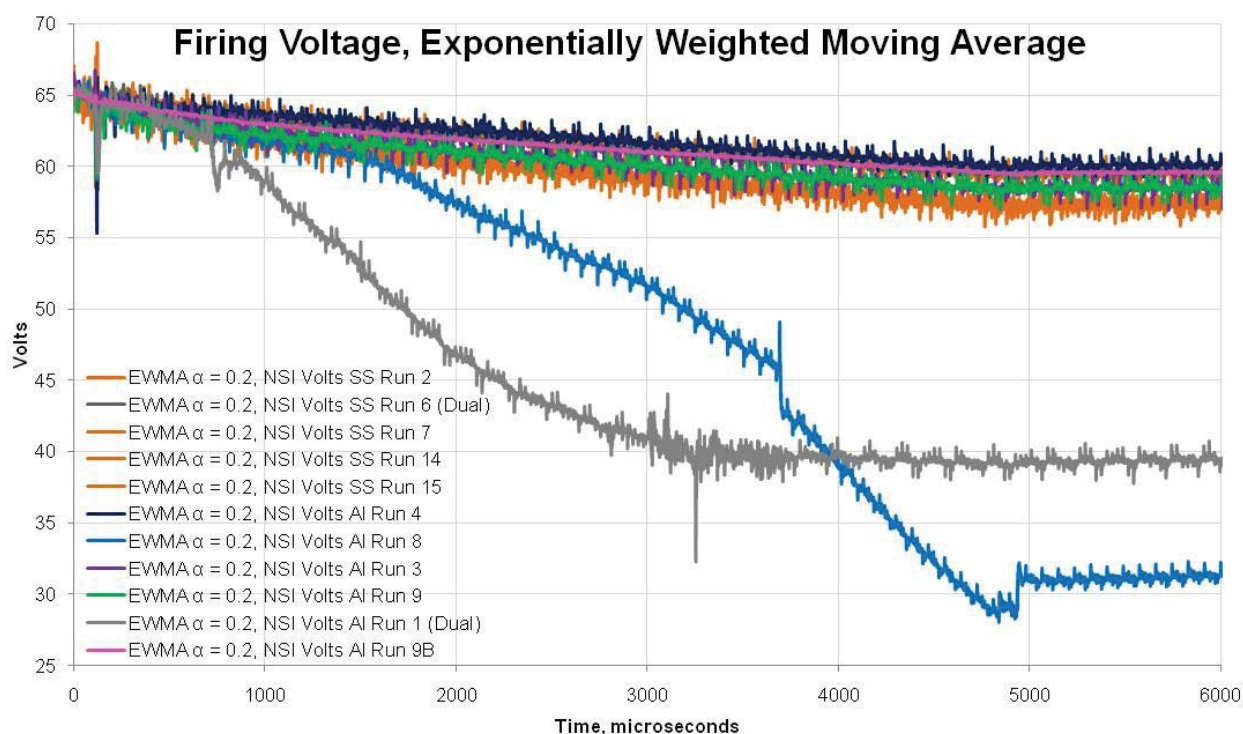


Figure F-1. Phase I Firing Voltages, Smoothed Data, All Runs, Long (6 ms) Time Scale, showing Range of Voltages Measured

	NASA Engineering and Safety Center Technical Assessment Report	Document #: NESC-RP- 09-00596	Version: 1.0
Title: Pyrovalve Booster Interface Temperature Measurement			Page #: 41 of 92

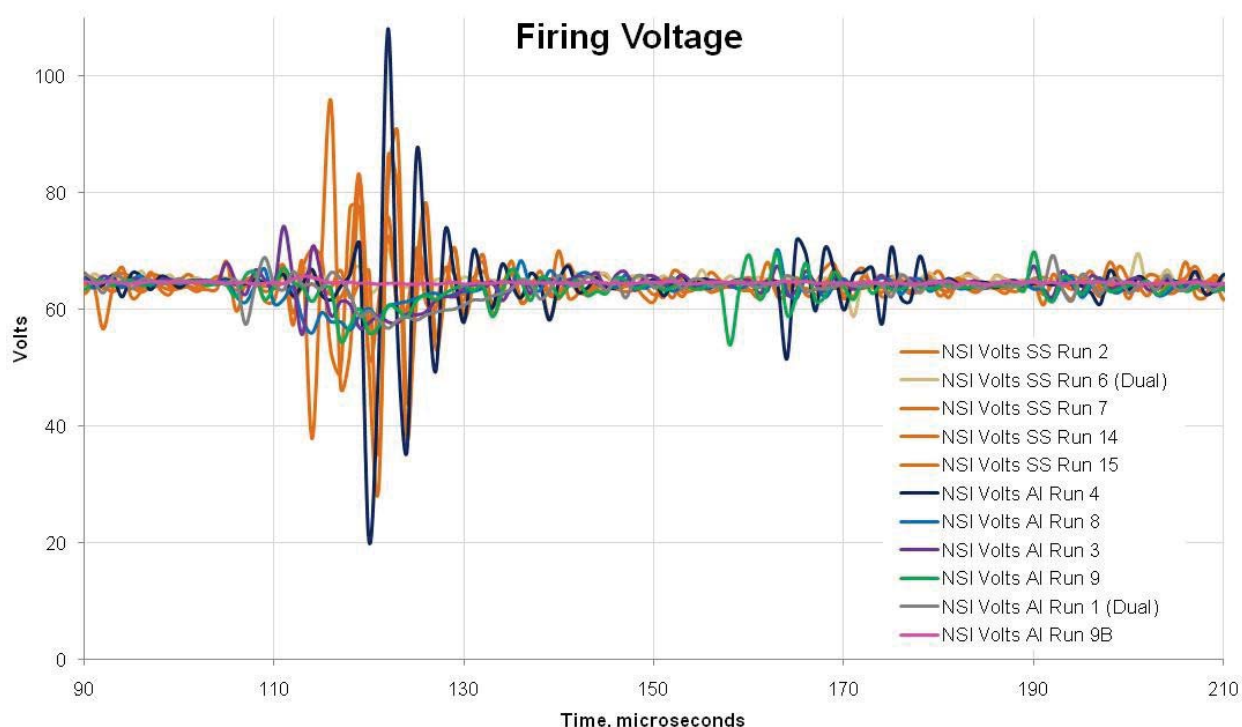


Figure F-2. Firing Voltage, Smoothed Data, All Runs, Time Scale Showing Detail of NSI Firing Event, Showing Range of Voltages Measured

Using a small time scale, visual analysis of this data showed a number of differences between trials. Again, the SS runs (run first) appeared to show different features than the AI runs. This may have been due to some change in the firing circuit or some difference in the blocks themselves, but it was decided that this was only of minor interest.

Run 9B (dark pink), which held considerable interest for analysis, gave an unusual firing voltage trace including comparatively low noise features during the 90–150 μ s time interval.

All the SS runs showed a tight and slightly lower firing voltage than the AI runs, which showed some variability. Again, no important differences were seen during the actual time when the voltage was required for NSI firing, so this was not extensively explored. Again, this information is provided in the interest of completeness.

Firing Current. It is in this trace that Runs 1 and 8 appear to have experienced shorts or some similar disturbance. Again, Run 1 is the dark grey trace and Run 8 is the medium blue one. Both show their differences after the NSIs actually fire. The event at 5,000 μ s is discontinuance of energy to the NSI.



NASA Engineering and Safety Center Technical Assessment Report

Document #:
**NESC-RP-
09-00596**

Version:
1.0

Title:

Pyrovalve Booster Interface Temperature Measurement

Page #:

42 of 92

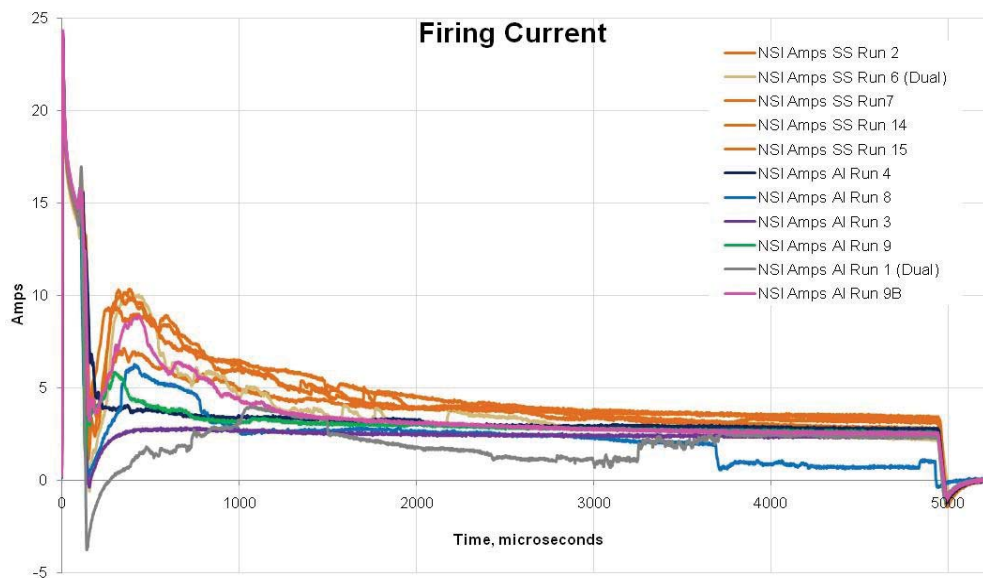


Figure F-3. Firing Current, All Runs, Long (5 ms) Time Scale, Showing Range of Amperages Measured

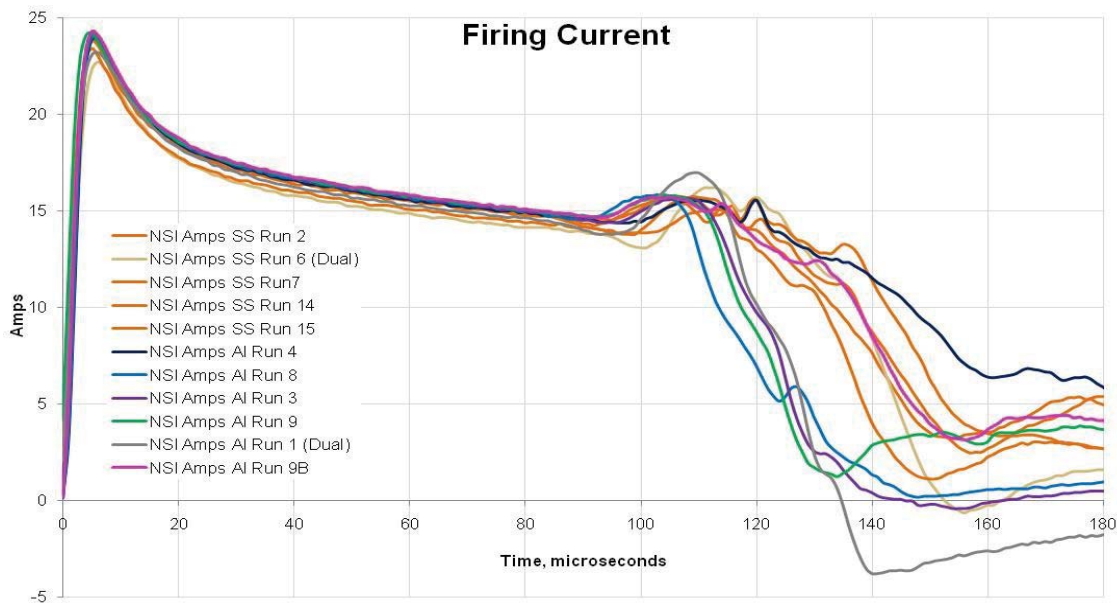



Figure F-4. Firing Current, All Runs, Time Scale Including NSI Initiation through Firing Event, Showing Range of Amperages Measured

	NASA Engineering and Safety Center Technical Assessment Report	Document #: NESC-RP- 09-00596	Version: 1.0
Title: Pyrovalve Booster Interface Temperature Measurement			Page #: 43 of 92

Temperature. The IR setup, again, did not register temperatures below 572 °F.

Temperature traces indicated differences between runs. Most of the SS trials showed a higher peak temperature than the AI trials.

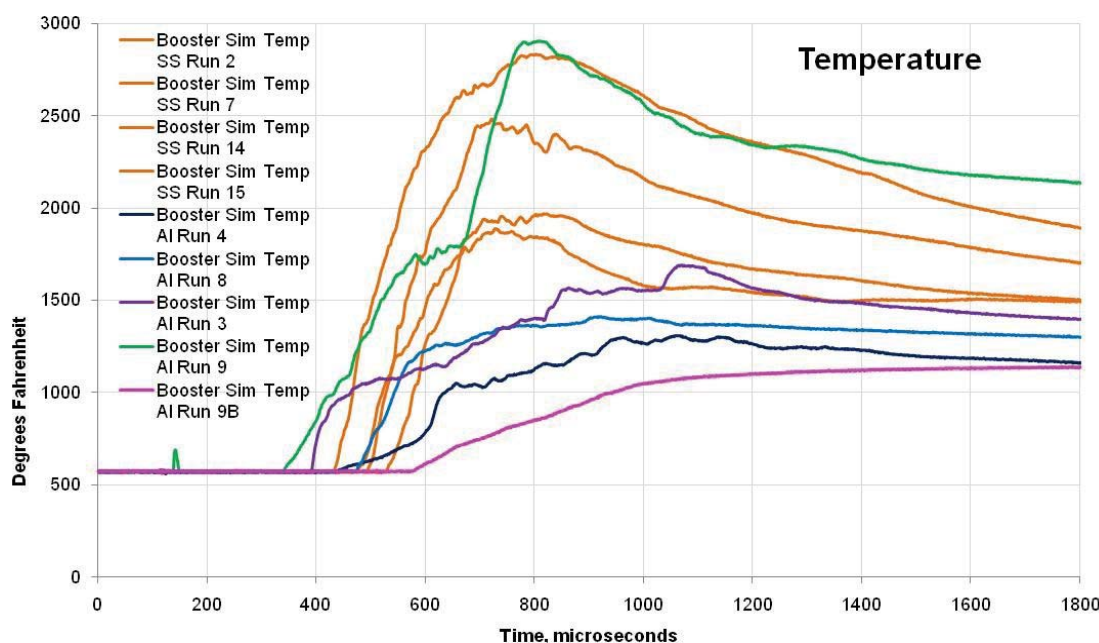



Figure F-5. Temperature Readings, Single Firings Only, Over Time Scale Including NSI Initiation, NSI Firing, Temperature Registration on IR Instrument and an Approximate Millisecond after Temperature Rise

Run 9B's initiator clearly fired, but the temperature climbed only slowly and never reached a high value. This could have resulted in a misfire in actual use. Remember that this was not a dual firing. It is possible that a redundant NSI would have resulted in a successful booster firing. It is also possible that the firing circuit was to blame and a second NSI would have experienced a failure due to a common cause.

If it is assumed that the possible misfire was due to a discrete event that could occur in actual use conditions, it cannot be assumed conclusively that the event cannot happen in SS PCAs. There are too few trials to be able to conclude this. However, if one assumes that the 9B run is part of a continuum of responses that AI Y-PCAs could give, which is reasonable given this graph (Run 9B looks qualitatively like a low-response cousin to Runs 3, 4 and 8), it seems reasonable to believe that the SS design will be less likely to produce this type of outcome.

Peak Temperature. If Run 9, the only AI run having diaphragm burn-through, is included, the team cannot show, using the data, that there is a difference between AI and SS designs. Removing Run 9 allows a conclusion that SS results in a higher peak temperature than AI at

	NASA Engineering and Safety Center Technical Assessment Report	Document #: NESC-RP- 09-00596	Version: 1.0
Title: Pyrovalve Booster Interface Temperature Measurement			Page #: 44 of 92

greater than 95 percent confidence. (From this point on, it will be assumed that confidence is greater than 95 percent unless otherwise indicated and the confidence level will not be generally stated explicitly.) Run 9B was left in this dataset for analysis. Its removal results in little difference in conclusions.

Design-Expert® Software
Factor Coding: Actual
Diaphragm Peak Temperature

● Design Points

X1 = A: Design

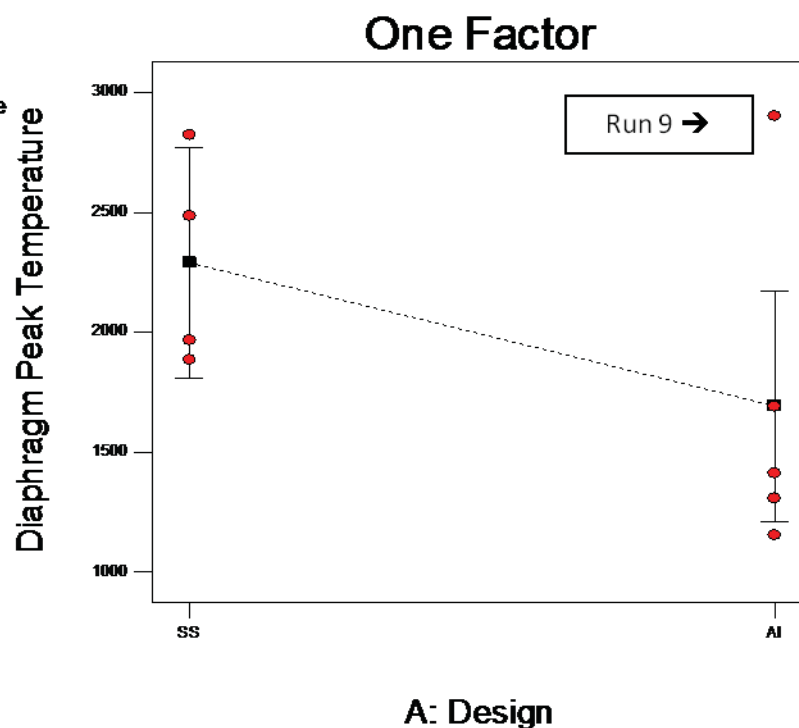



Figure F-6. Diaphragm Peak Temperature, Data Including Run 9

	NASA Engineering and Safety Center Technical Assessment Report	Document #: NESC-RP- 09-00596	Version: 1.0
Title: Pyrovalve Booster Interface Temperature Measurement			Page #: 45 of 92

Design-Expert® Software
Factor Coding: Actual
DIAPHRAGM MAX TEMP

● Design Points

X1 = A: Design

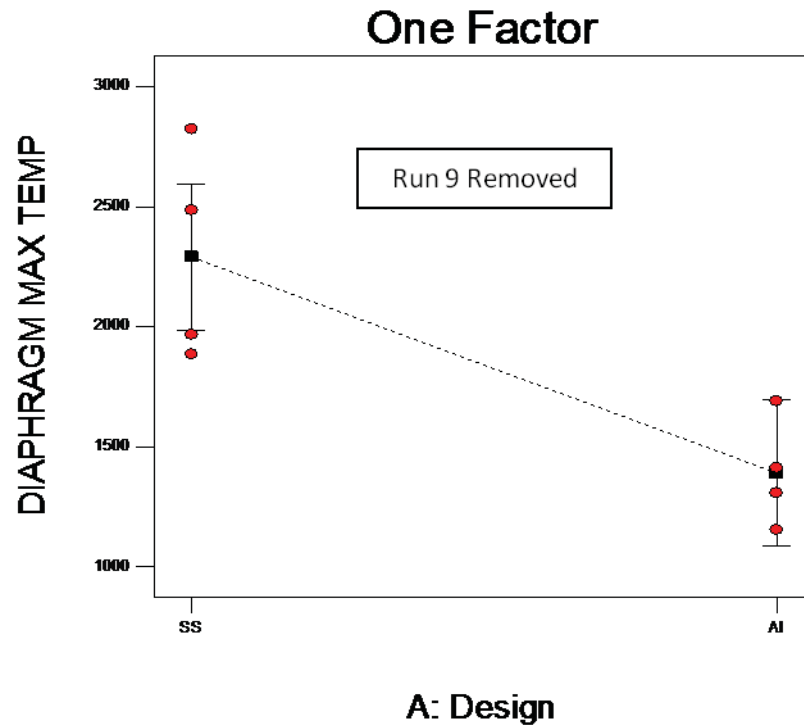



Figure F-7. Diaphragm Peak Temperature, Data Not Including Run 9

Time to Peak Temperature. Quantitative analysis shows clearly that time of maximum temperature is lower for SS than for AI PCAs.

	NASA Engineering and Safety Center Technical Assessment Report	Document #: NESC-RP- 09-00596	Version: 1.0
Title: Pyrovalve Booster Interface Temperature Measurement			Page #: 46 of 92

Design-Expert® Software
Factor Coding: Actual
S Time of Max Temp

● Design Points

X1 = A: Design

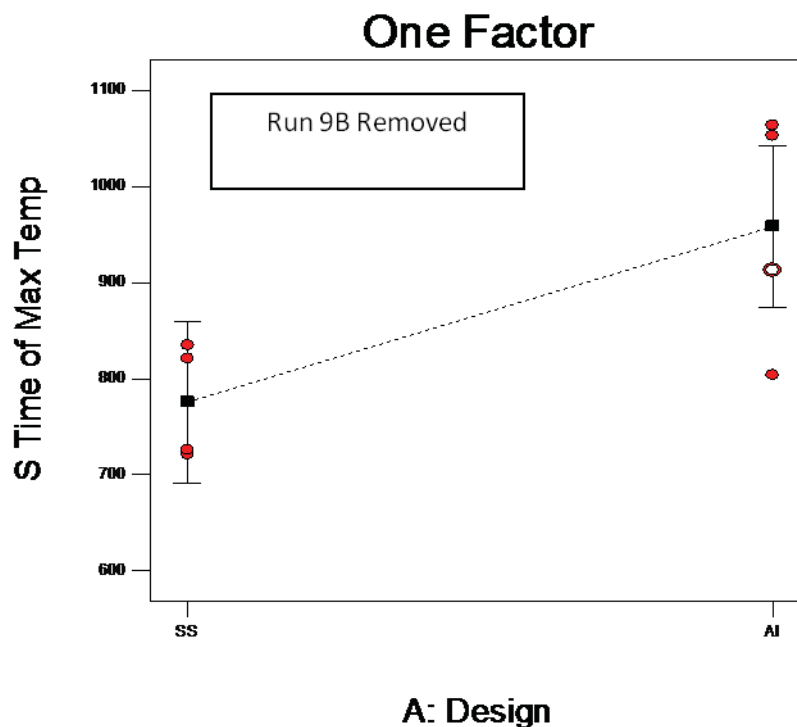


Figure F-8. Time of Maximum Temperature from Time NSI fired, Run 9B Not Included

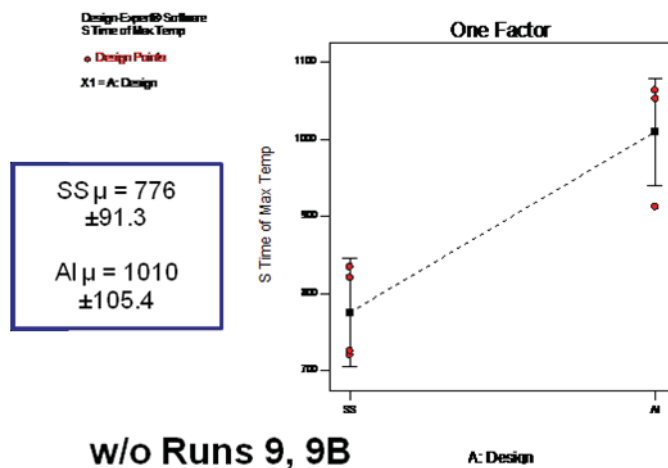



Figure F-9. Time of Maximum Temperature from Time NSI Fired, Runs 9 and 9B Not Included

	NASA Engineering and Safety Center Technical Assessment Report	Document #: NESC-RP- 09-00596	Version: 1.0
Title: Pyrovalve Booster Interface Temperature Measurement			Page #: 47 of 92

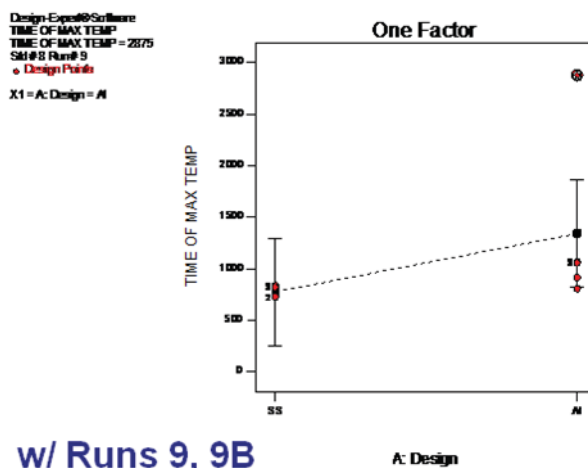



Figure F-10. Time of Maximum Temperature from Time NSI Fired, Runs 9 and 9B Included

If Run 9B is not included in analysis, it can be concluded with greater than 95 percent confidence that SS gives shorter Time than AI. Adding 9B back in will increase the difference, as it has a long Time to Max Temperature. However, because 9B increases spread tremendously, it has the paradoxical effect of decreasing confidence in the hypothesis. Removing *both* 9 and 9B increases confidence in this statement. Note that the analysis without Runs 9 and 9B makes Run 4, the first AI trial run, look like a potential wild point.

Diaphragm Temperature at 800 μ s. Again, Run 9 affected results; including Run 9 resulted in a finding of no significant difference, while leaving it out resulted in rejecting the hypothesis that there was no difference between SS and AI PCA designs.

	<h1 style="text-align: center;">NASA Engineering and Safety Center Technical Assessment Report</h1>	Document #: NESC-RP-09-00596	Version: 1.0
Title: <h2 style="text-align: center;">Pyrovalve Booster Interface Temperature Measurement</h2>			Page #: 48 of 92

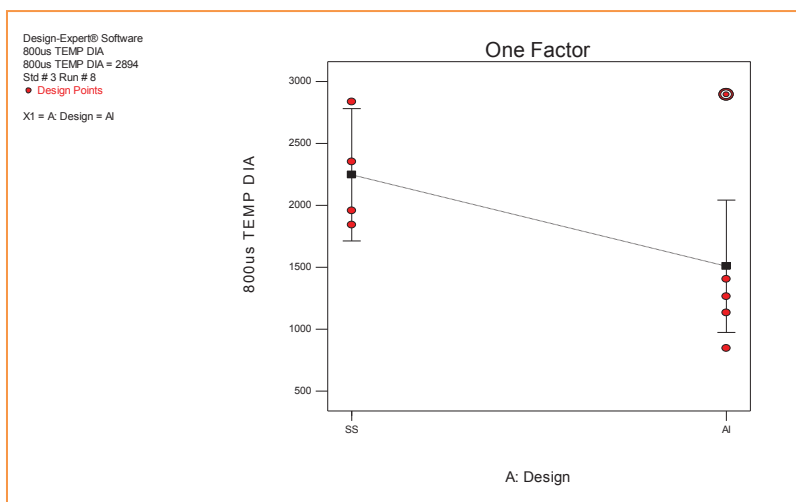


Figure F-11. Diaphragm Temperature at 800 μ s, Run 9 Included

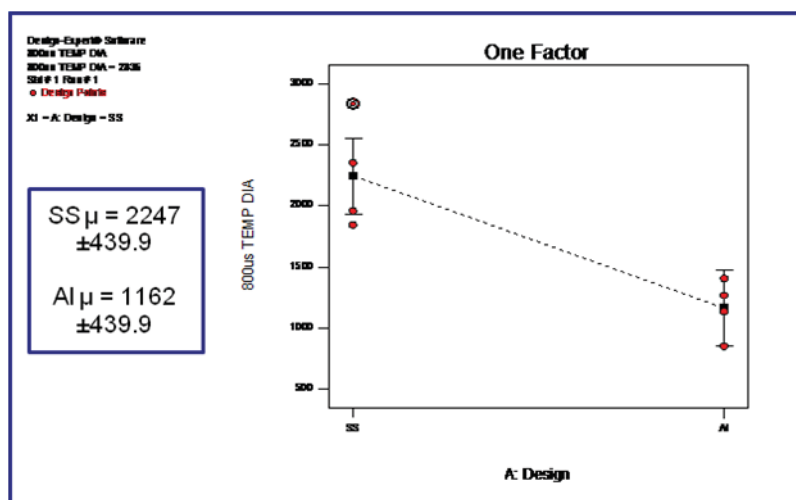



Figure F-12. Diaphragm Temperature at 800 μ s, Not Including Run 9

Pressure. Port A Measured Pressure. In visual analysis of the traces, pressure reached a peak close in time for both designs. A small blip occurred just before pressure rise to the peak pressure. Stainless PCAs resulted in higher pressures after peak than for the AI design. Ringing oscillations were seen and showed a reasonably distinct signature. Oscillations damped out by 800 μ s.

	NASA Engineering and Safety Center Technical Assessment Report	Document #: NESC-RP- 09-00596	Version: 1.0
Title: Pyrovalve Booster Interface Temperature Measurement			Page #: 49 of 92

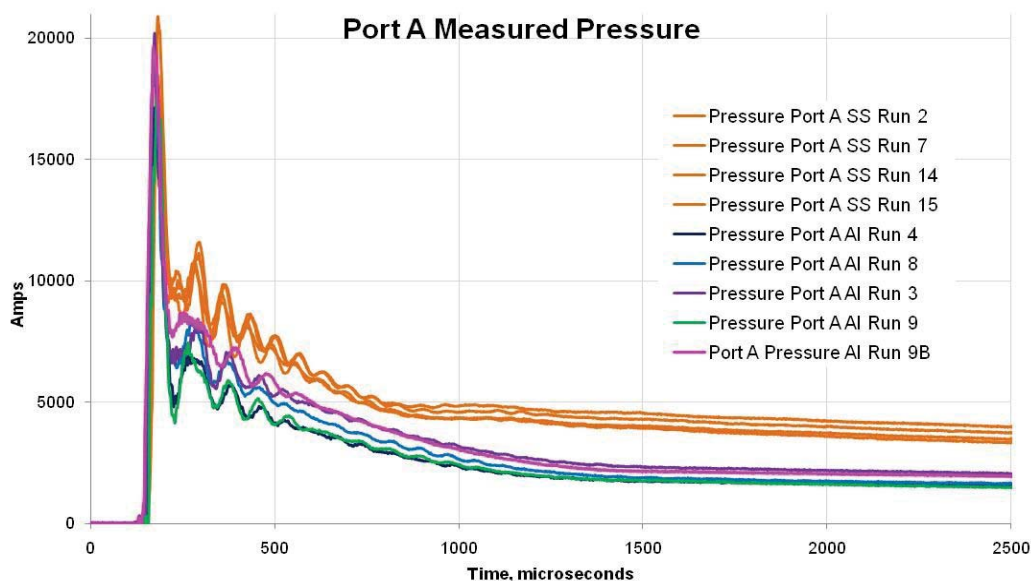



Figure F-13. Traces of Port A Pressures

Time of Pressure Rise Start, Port A. There may have been a difference between SS and AI designs, but it was small and borderline statistically significant. Not including Run 9 and including dual/single firing as a factor improved resolution and resulted in a statistically significant difference seen between AI and SS. It is not obvious that the 6.6 μ s difference seen between AI and SS is significant in engineering terms. This parameter does not have much practical significance and is probably influenced by minor differences in how the grease is packed into the pressure transducer sense ports.

	<h1 style="text-align: center;">NASA Engineering and Safety Center Technical Assessment Report</h1>	Document #: NESC-RP-09-00596	Version: 1.0
Title: <h2 style="text-align: center;">Pyrovalve Booster Interface Temperature Measurement</h2>			Page #: 50 of 92

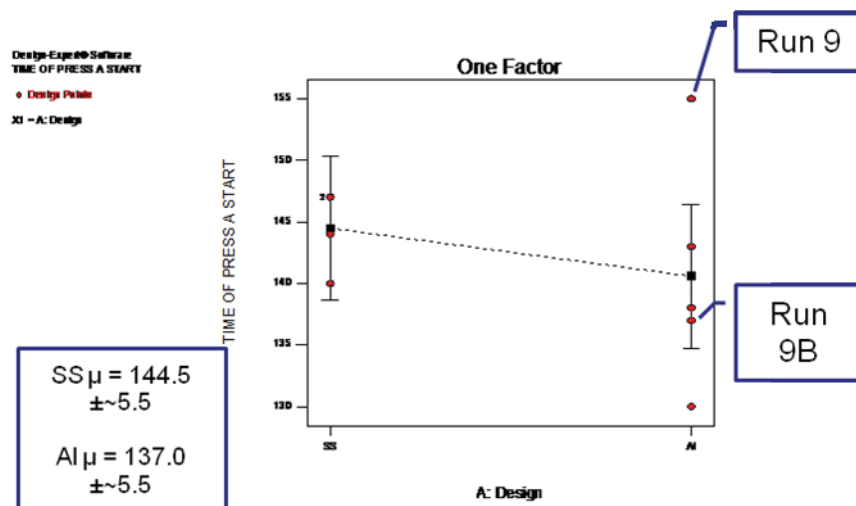


Figure F-14. Time of Rise in Pressure, All Runs

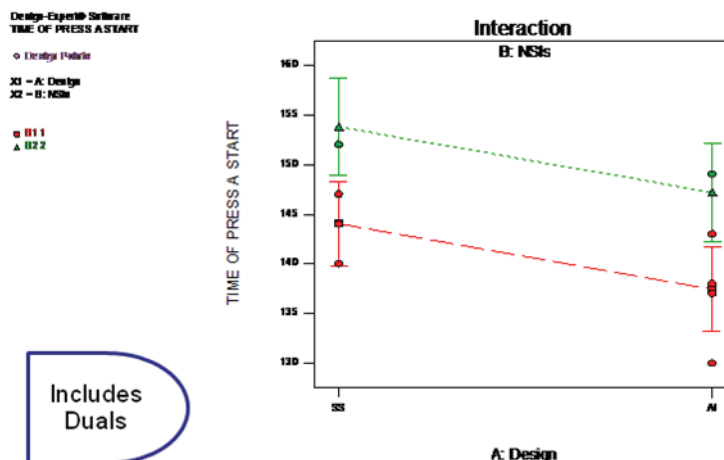



Figure F-15. Analysis Showing Difference between Dual and Single Firings and SS and AI Firings If Particular Data Are Included (See Text)

Port A Extrapolated Peak Pressure. A team member (W. Sipes) developed a method to calculate an approximate peak pressure for each test that eliminated response issues in the data. The method is described elsewhere in this report. This data showed a significant difference between SS and AI ($p = 0.003$, or confidence at 99.7 percent). Graphical results are shown in the Figure F-16.

	<h1 style="text-align: center;">NASA Engineering and Safety Center Technical Assessment Report</h1>	Document #: NESC-RP-09-00596	Version: 1.0
Title: <h2 style="text-align: center;">Pyrovalve Booster Interface Temperature Measurement</h2>			Page #: 51 of 92

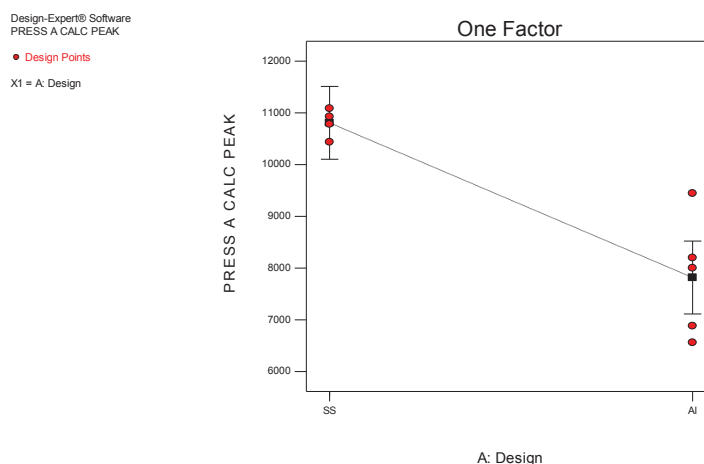


Figure F-16. Peak Pressure in A

However, there was a potential issue with variability growth toward end of testing. The difference in variability between AI and SS is shown in the following graphs. Figure F-17 shows the difference in variability.

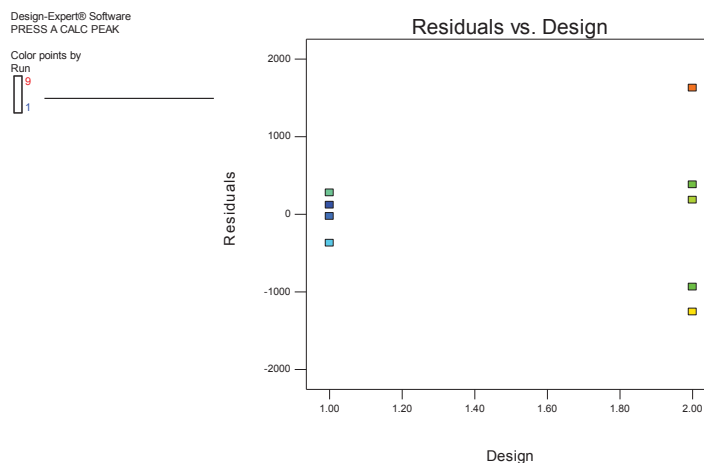


Figure F-17. Residuals (Actual Data Value—Predicted Value) Compared between AI Y-PCA (Left-Hand Points) and SS V-PCA (Right) for Peak Pressure in A


	NASA Engineering and Safety Center Technical Assessment Report	Document #: NESC-RP- 09-00596	Version: 1.0
Title: Pyrovalve Booster Interface Temperature Measurement			Page #: 52 of 92

Figure F-18 shows the increase in variability as testing continues. Cook's distance <http://data.princeton.edu/wws509/notes/c2s9.html> is a measure of how far a (standardized) datum is away from expectation given a model.

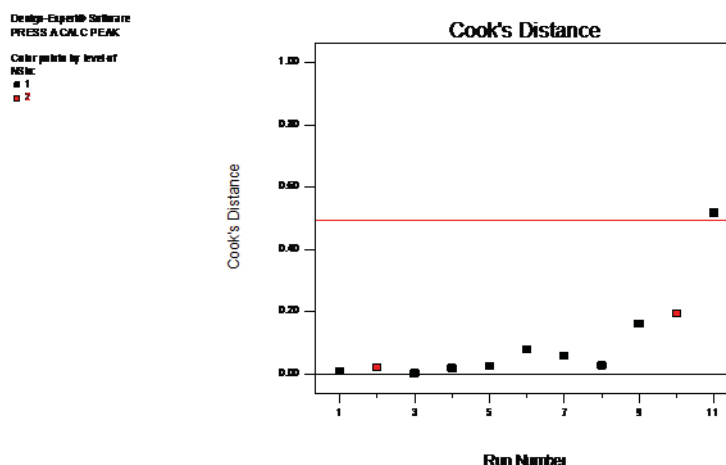


Figure F-18. Analysis of Residuals; Bottom Axis Is Order of Trials Run; Suggestion Is that Variability Increased as Testing Progressed; Issue Would Have Been Able To Be Separated from Other Conclusions Had Order of Tests Run Been Randomized

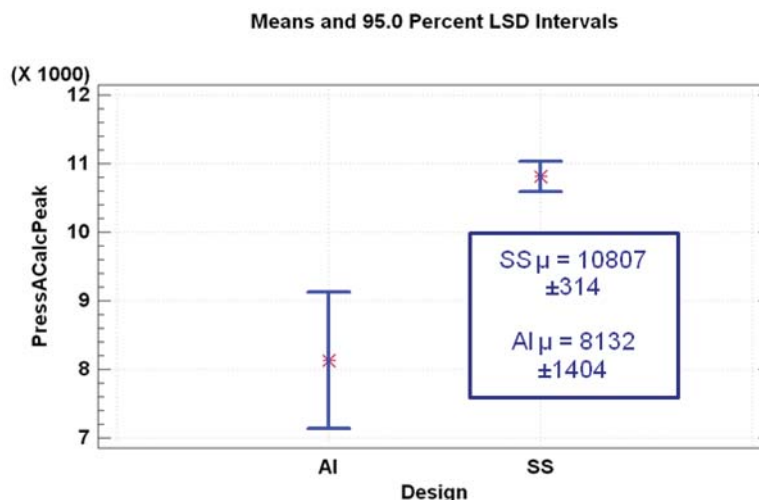



Figure F-19. Peak Pressure in A: Comparison Using Weighted Least Squares

	NASA Engineering and Safety Center Technical Assessment Report	Document #: NESC-RP- 09-00596	Version: 1.0
Title: Pyrovalve Booster Interface Temperature Measurement			Page #: 53 of 92

Port A Pressure at 800 μ s. The difference in variability appears also to occur at long times. The following analysis uses simple regression, as the difference in variabilities between AI and SS is lower at this time scale. If weighted least squares had been used, the difference in means (and the means estimates) would have been the same, but the confidences on the means would have been different: larger for AI, smaller for SS.

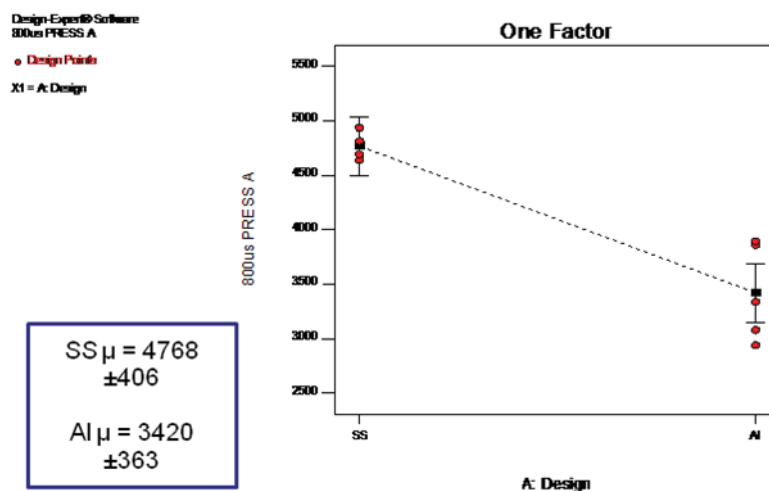


Figure F-20. Pressure in Port a at 800 μ s

Port B Measured Pressure. Measured pressures in single NSI firings for the SS design were easily seen to be higher than for AI PCAs. The traces for each were highly characteristic and clearly showed that the SS design allowed much higher flow rates across the top of the booster charge and into the opposite NSI cavity.



Title:

Pyrovalve Booster Interface Temperature Measurement

Page #:

54 of 92

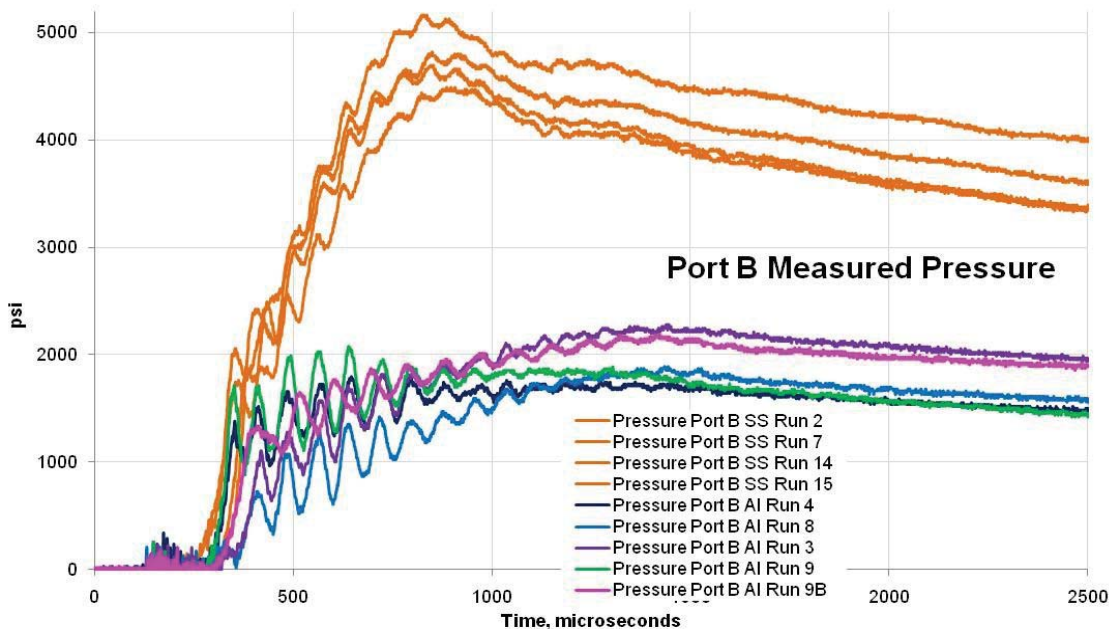



Figure F-21. Pressure Traces for Non-Fired Port

Time of Start of Pressure Rise, Port B. The difference between SS and AI for the time at which pressure began to rise in the non-fired port was not significantly different statistically. Note that this does not mean that there is no difference, only that the difference could not be discerned with this data given its size and variability.

	NASA Engineering and Safety Center Technical Assessment Report	Document #: NESC-RP- 09-00596	Version: 1.0
Title: Pyrovalve Booster Interface Temperature Measurement			Page #: 55 of 92

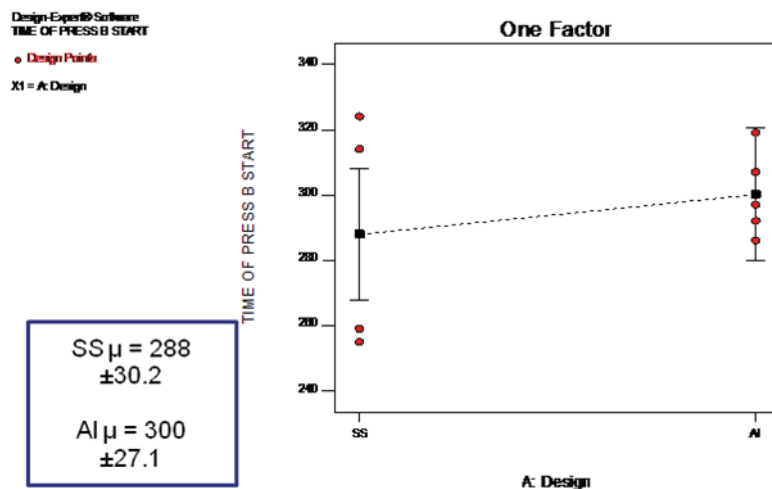


Figure F-22. Time of Start of Pressure Rise

Port B Pressure at 800 μs. Again, as is abundantly clear in the pressure traces, AI pressure in the non-fired port is considerably lower than in the SS non-fired port at late time slices.

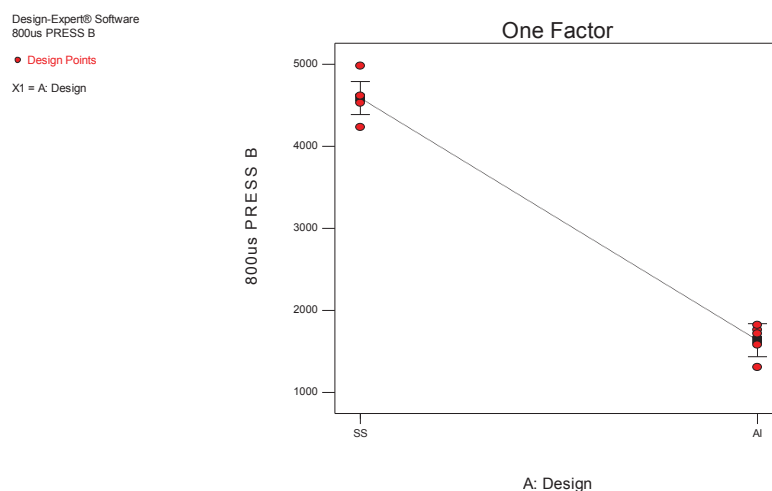



Figure F-23. Port B Pressure at 800 μs

Difference between Port A and Port B Pressure. It takes some time for pressure to equilibrate between the fired and non-fired ports. A couple of features are interesting in the following trace

	NASA Engineering and Safety Center Technical Assessment Report	Document #: NESC-RP- 09-00596	Version: 1.0
Title: Pyrovalve Booster Interface Temperature Measurement			Page #: 56 of 92

of this value. For SS NSIs, the difference is larger than for Al during the time from just after the initial peak to about 500 μ s. It then decreases quickly, and for a short time, the *Pressure* in *A* appears to be lower than that in the non-fired port for a few tens of a microsecond. Al PCAs may ring for a bit longer than the SS and the ports take more time to equilibrate than for SS. It is also possible that there are two families of Al firings in this data: Runs 9 and 4 have similar traces, while the others overlap each other at a parallel, higher value as compared to Runs 9 and 4.

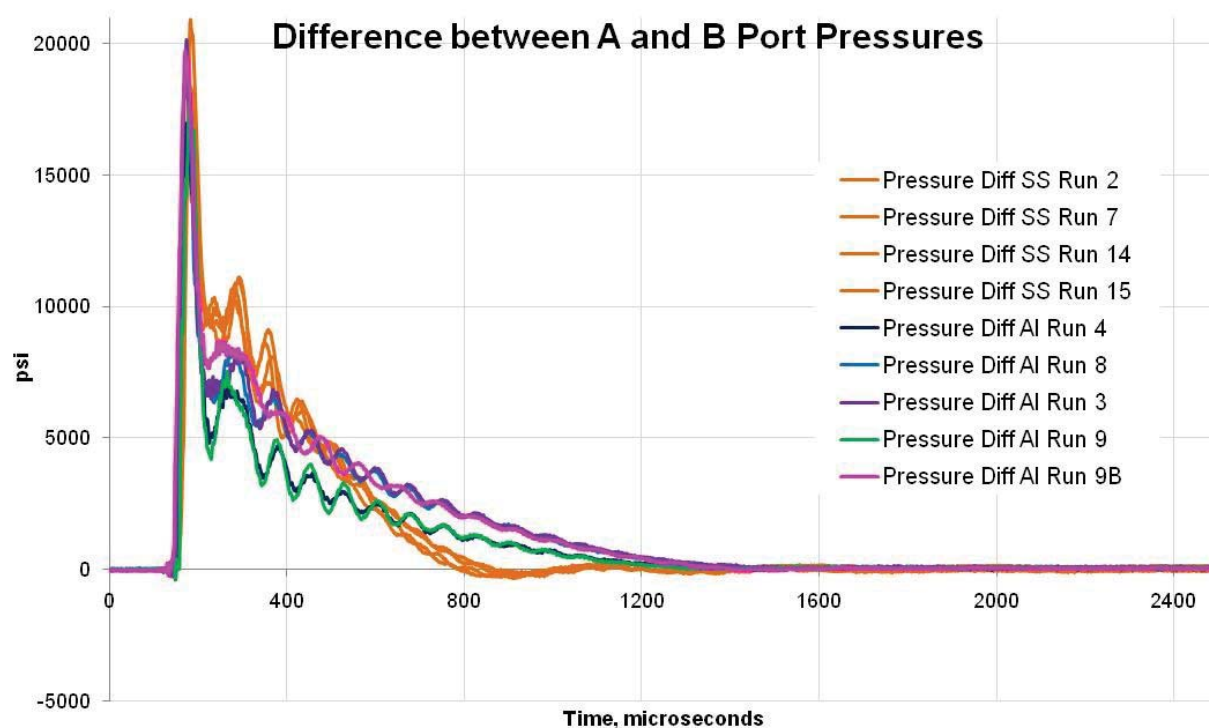



Figure F-24. Trace Showing Difference in Pressure between Ports A and B Over Time

	NASA Engineering and Safety Center Technical Assessment Report	Document #: NESC-RP-09-00596	Version: 1.0
Title: Pyrovalve Booster Interface Temperature Measurement			Page #: 57 of 92

Appendix G. Phase IIB Statistical Analysis and Results

Phase IIB was designed to evaluate the relationship between firing skew and the cross-sectional area of the flow passages and various responses relating to factors involved with firing a booster charge. It was assumed that the following model would apply.

$$Y = \beta_0 + \beta_1 \text{ Skew} + \beta_2 \text{ Area} + \beta_{12} \text{ Skew} \times \text{Area} + \beta_{11} \text{ Skew}^2 + \beta_{22} \text{ Area}^2$$

where the β 's are linear regression parameters fit using the data.

G.1 Analysis and Results


The analysis results were clear: within the tested range of the two inputs studied, no-fires due to insufficient temperature at the booster interface are entirely possible at low skews, even in designs having enlarged channels. A low-temperature response occurred in this test at conditions of high skew and channel area (Run 3). Because of this, it cannot be ruled out that a no-fire at more than 500 μs could occur, but the team believes it much more likely that the response is due to installation of two booster simulator diaphragms in error. In fact, the inner of the two diaphragms was burnt through in that trial. Temperatures increase with increasing skew but are fairly insensitive to channel area. Channel area affects pressure and increases variability of the time it takes to attain peak temperature.

The data analyzed is shown in Figure G-1. It was developed from the raw traces and other sources by team members.

Test Run No.	Test Run Order	Test Date - Time	PCA No.	Times PCA Used	Channel Dia-meter, in.	Channel Area, sq. in.	Actual Timing Skew, μs	Press A Calc Peak	Press B Calc Peak	Press before B Rise	A Press at B Press Peak	Press Δ at B Press Peak	Press A, 1600 μs	Time of Press A Peak	Time of Press B Peak	Overall Max Temp	Diaphragm Temp, 1600 μs	Time to 1000 F	Time of Max Temp	Diaphragm Hole Pct
1	1	10/21/2010 13:58	3	1	0.060	0.0028	6	10437	9781		10427	1602	8825	225	235					0.00
3	2	10/26/2010 9:21	9	1	0.125	0.0123	481	6835	12430	4135	4152	-3806	7958	217	698	634			6980	
4	3	10/26/2010 11:07	5	1	0.060	0.0028	486	11389	15076	2532	6321	-2781	9102	224	713	2913	2379	212	1132	0.46
5	4	10/26/2010 15:25	6	1	0.060	0.0028	485	10780	15371	5661	5609	-2800	8409	220	710	3078	2538	215	1161	0.35
7	5	11/4/2010 12:51	4	1	0.060	0.0028	5	9715	10719		9714	1000	8714	223	229	1723	870	213	217	0.00
8	6	11/4/2010 14:09	1	1	0.088	0.0061	0	10010	10477		10010	1469	8541	240	240	2095	1106	208	246	0.00
10	7	11/5/2010 12:38	10	1	0.125	0.0123	243	7500	11546	3528	3528	-4180	7708	219	458	2501	1903	216	648	0.34
11	8	11/5/2010 13:27	7	1	0.060	0.0028	235	10670	13344	2494	8229	-1162	9391	228	460	2275	1911	531	825	0.26
12	9	11/15/2010 13:58	9	2	0.125	0.0123	5	9208	9785		9204	1253	7951	215	221	1957	1160	209	216	0.00
13	10	11/16/2010 13:20	1	2	0.088	0.0061	237	9017	14220	3208	5521	-2568	8089	219	459	1733	1723	716	1208	0.36
14	11	11/16/2010 13:56	10	2	0.125	0.0123	484	7208	10389	3528	3736	-2899	6635	219	706	3630	3157	204	774	0.50
9	12	11/19/2010 13:16	2	1	0.088	0.0061	242	8493	13094	3140	5258	-2173	7431	222	461	2517	1191	511	965	0.32
15	13	11/24/2010 13:55	9	3	0.125	0.0123	5	9161	9077		9148	1648	7500	222	237	699	634		3700	0.00
16	14	11/30/2010 10:46	8	1	0.088	0.0061	484	8435	14027	4074	3900	-4337	8237	222	717	3312	2352	478	803	0.40
17	15	11/30/2010 14:33	2	2	0.088	0.0061	236	8828	12826	3052	5158	-2602	7760	220	468	2315	2007	553	770	0.25
6A	16	12/3/2010 10:30	2	3	0.088	0.0061	250	9440	12212	5765	5540	-2255	7795	212	461	1896	1890	251	1578	0.19
2B	17	12/8/2010 8:53	8	2	0.088	0.0061	236	8618	13734	3018	4962	-3452	8414	222	466	1837	1773	579	2555	0.26

Figure G-1. Data

Channel Area was used as the input factor for these analyses rather than Channel Diameter. Actual Skew was used in place of the intended value.

	NASA Engineering and Safety Center Technical Assessment Report	Document #: NESC-RP- 09-00596	Version: 1.0
Title: Pyrovalve Booster Interface Temperature Measurement			Page #: 58 of 92

The models created below are not primarily physics-based and are not intended to be. The exact shapes of the response surfaces created, particularly in low-skew conditions, cannot be, nor are intended to be, strictly representative of the physics. They provide a useful predictive picture of what is happening. If greater fidelity is required, the analyses and response surfaces point the way to where follow-on tests will be most informative.


Temperature. Two clear misfires, Runs 1 and 3, were observed: Run 1 did not result in temperatures above the infrared (IR) measurement threshold of 574 °F and Run 3 barely exceeded the threshold and took a considerable amount of time to do so. These were excluded from analysis in most cases. Run 15, another apparent misfire, was also often excluded, as shown in the figures below. It may be more appropriate to perform an analysis where these points are censored. Details will be discussed in each case below.

Overall Maximum Temperature was influenced by Runs 1 and 3. These misfires clearly include a different heat transfer mode than most of the other runs. These were removed from the data for analysis. A censored analysis was not performed: because of the way the data were censored, there would be no effect on the analysis conclusions.

Run 15 also showed a low Peak Max Temperature of 699 °F. This run also is probably dominated by an undesirable heat transfer mode. Analysis including this data point suggests it may be since it shows as a possible wild point using Cook's D test, but not any other diagnostic measures used. Analysis with Run 15 included results in the following model:

$$\begin{aligned} \text{Overall Maximum Temperature} &= \\ &+1485. \\ &+3.359 \quad * \text{Actual Skew} \end{aligned}$$

Given Run 15 is not unusual since *Overall Max Temperature* increases predictably with increasing *Skew*, *Channel Area* does not have a discernable effect.

	NASA Engineering and Safety Center Technical Assessment Report	Document #: NESC-RP- 09-00596	Version: 1.0
Title: Pyrovalve Booster Interface Temperature Measurement			Page #: 59 of 92

Design-Expert® Software

Factor Coding: Actual

Overall Max Temp

● Design points above predicted value

○ Design points below predicted value

X1 = A: Channel Area

X2 = B: Actual Skew

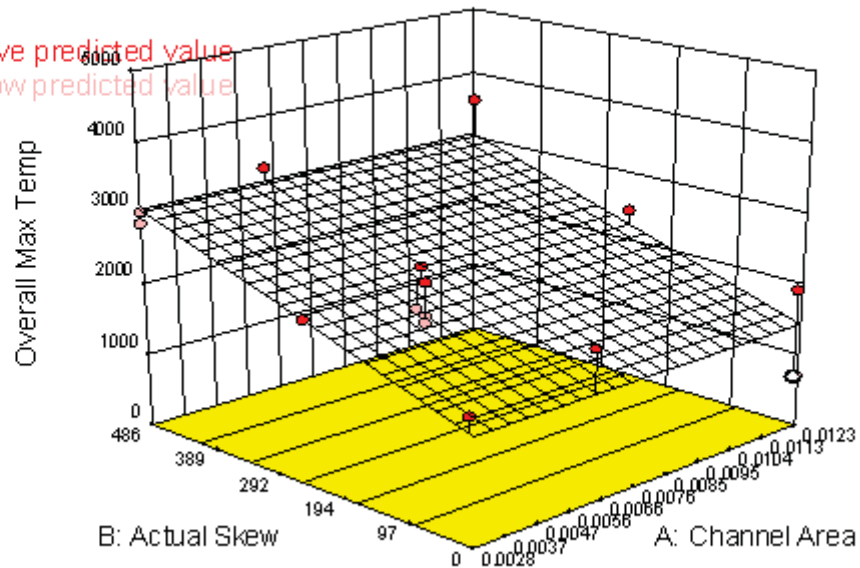



Figure G-2. Maximum Temperature, Prediction Response Surface Given Various Actual Skew and Channel Area, Data Including Run 15 (Hollow Point Marker)

Analysis without Run 15 shows a weak ($p = 0.08$) and slight effect of *Channel Area*. It also suggests an increasing rate of increase in *Max Temperature* with *Skew*.

$$\begin{aligned}
 \text{Overall Maximum Temperature} &= \\
 &+1629. \\
 &+42670 && * \text{Channel Area} \\
 &-0.6889 && * \text{Actual Skew} \\
 &+0.007156 && * \text{Actual Skew}^2
 \end{aligned}$$

	NASA Engineering and Safety Center Technical Assessment Report	Document #: NESC-RP- 09-00596	Version: 1.0
Title: Pyrovalve Booster Interface Temperature Measurement			Page #: 60 of 92

Design-Expert® Software

Factor Coding: Actual

Overall Max Temp

● Design points above predicted value

○ Design points below predicted value

X1 = A: Channel Area

X2 = B: Actual Skew

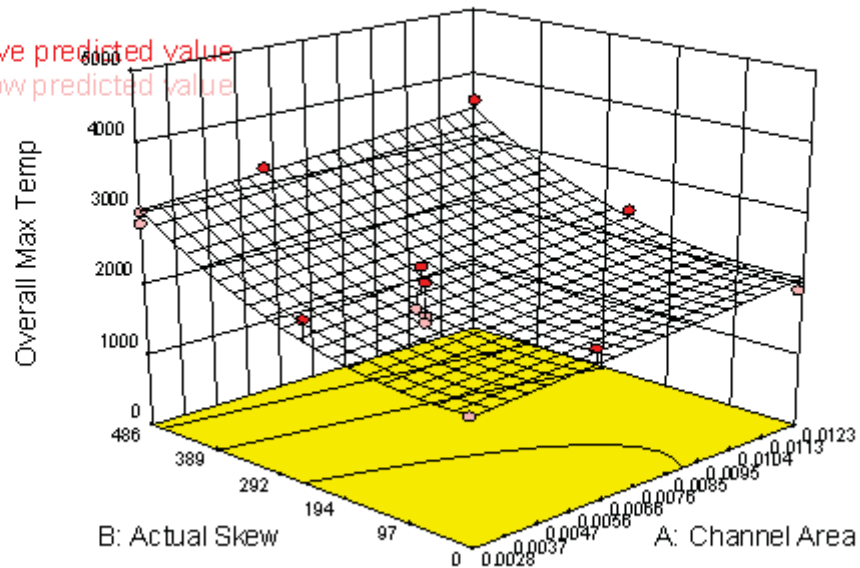


Figure G-3. Maximum Temperature, Response Surface Created Ignoring Run 15

Analysis of Diaphragm Temperature at 1,600 μ s did not include Runs 1 and 3. An analysis using censored data would not change the analysis results. Run 15 did not flag as an outlier in tests of residuals.

$$\begin{aligned} \text{Diaphragm Temperature at 1,600 } \mu\text{s} &= \\ &+936.8 \\ &+3.452 \quad * \text{ Actual Skew} \end{aligned}$$

	NASA Engineering and Safety Center Technical Assessment Report	Document #: NESC-RP- 09-00596	Version: 1.0
Title: Pyrovalve Booster Interface Temperature Measurement			Page #: 61 of 92

Design-Expert® Software

Factor Coding: Actual

1600us Temp Dia

● Design points above predicted value

○ Design points below predicted value

X1 = A: Channel Area

X2 = B: Actual Skew

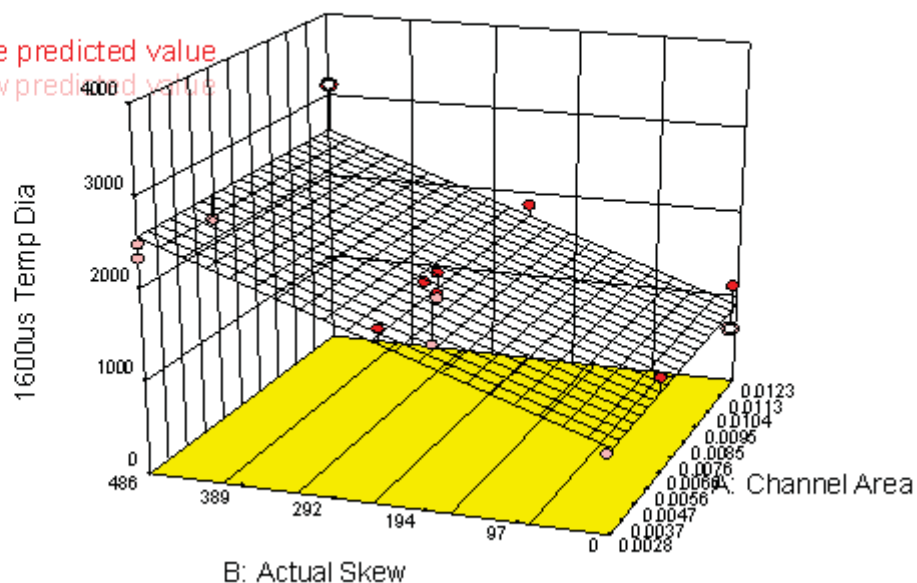



Figure G-4. Diaphragm Temperature at 1,600 μ s

Run 14 flags a possible unusual point using a Cook's D statistic, but it has substantive effect on predictions and none on conclusions. It was a replicate run of Run 3, but it had the correct number of diaphragms installed (1).

Time of Maximum Temperature was difficult to interpret. Run 1 resulted in no data as its temperature never ventured above the detection threshold of the IR unit. Values for Run 3 and Run 15, the other two runs that never achieved 1,000 °F, were also quite high.

The data could not be modeled as-is using ordinary least-squares regression assuming normally distributed residuals, even if Runs 1 and 3 are left off. However, if Run 15 is also ignored—the assumption then being that only the trials reaching at least 1,100 °F are modeled—a useful relationship can be modeled.

A log transformation of the response was applied to account for an increasing variability with increasing response value. It also has the beneficial effect of making negative values impossible, which is useful for constructing predictions and uncertainty bounds on them. This model fit the data reasonably well; Run 2 was somewhat high compared to expectation, but it did not flag as a clear outlier. The model:

	NASA Engineering and Safety Center Technical Assessment Report	Document #: NESC-RP- 09-00596	Version: 1.0
Title: Pyrovalve Booster Interface Temperature Measurement			Page #: 62 of 92

$$\begin{aligned}
 \text{Log}_{10}(\text{Time of Max Temp}) &= \\
 &+2.340 \\
 &+4.492\text{E-}003 && * \text{ Actual Skew} \\
 &-6.548\text{E-}006 && * \text{ Actual Skew}^2
 \end{aligned}$$

The graph of this response surface is in Figure G-5:

Design-Expert® Software
Factor Coding: Actual
Original Scale
Time of Max Temp

- Design points above predicted value
- Design points below predicted value

X1 = A: Channel Area
X2 = B: Actual Skew

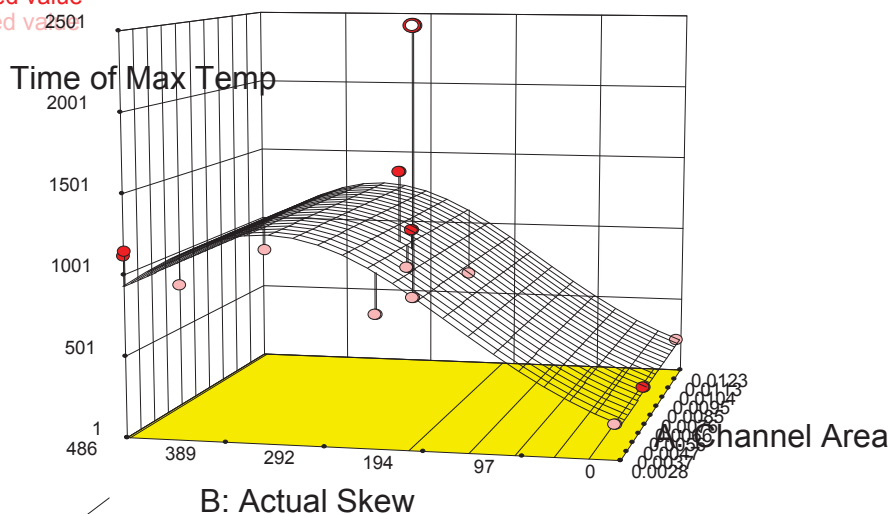



Figure G-5. Time of Maximum Temperature, Model Formed Using Data for which Maximum Temperatures Reached at Least 1,100 °F. Run 2 Is Signified by a Hollow-Center Marker.

Removing Run 2 provides a better fit all around, but the model and predictions change little. It is apparent from the data that at low skew, maximum temperature is reached quickly compared to higher-skew trials, or near 200 μs at 0 skew. It increases to a median value just under 1,000 μs at or before 235 μs skew and appears to plateau. Variability appears to increase with increasing skew. Again, this assumes peak temperature achieves 1,100 °F. Channel area was not shown to have significant effect on this response.

If only the data for trials run at medium and high factor settings are examined, excluding Run 3 for skew, a significant linear regression model could not be fit. That is, neither skew nor area

	NASA Engineering and Safety Center Technical Assessment Report	Document #: NESC-RP- 09-00596	Version: 1.0
Title: Pyrovalve Booster Interface Temperature Measurement			Page #: 63 of 92

had a discernable effect on *Time to Peak Temperature* when *Skew* was above about 235 μs . The data can thus be described as randomly distributed. A reasonable fit to a normal distribution was made when $\log_{10}(\text{Time to Peak Temperature})$ was modeled. The expected mean was 1,040 μs , with 95 percent confidence limits on that mean estimate of 800, 1360. This model will be used in predictions.

Time to 1,000 °F excludes Runs 1, 3 and 15 because the temperature never reached that level. A model suggested by the data resulted in the following response surface, shown in Figure G-6.

Design-Expert® Software

Factor Coding: Actual

Time to 1000F

● Design points above predicted value

○ Design points below predicted value

X1 = A: Channel Area

X2 = B: Actual Skew

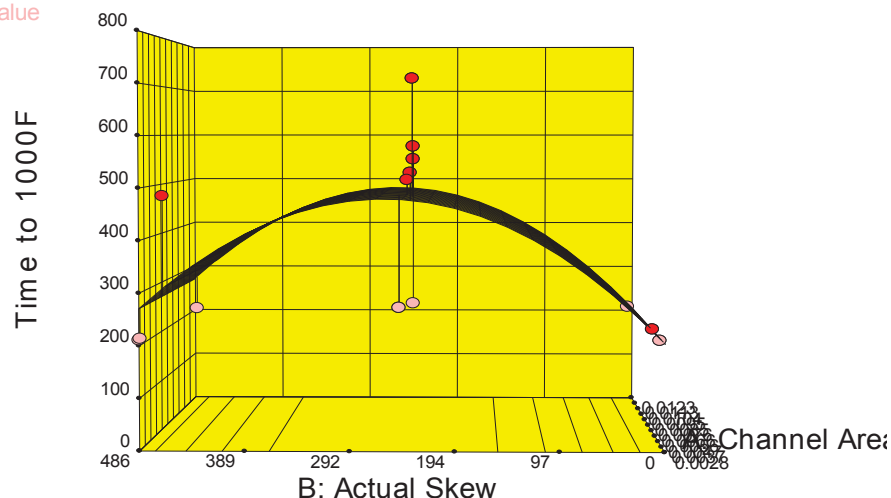



Figure G-6. Time to 1,000 °F

The surface was not satisfactory to the assessment team. It is possible that there are two processes: one that drives a quick, 200 μs jump to 1,000 °F; another that results in a more leisurely pace of 500–600 μs . It is also quite possible that above 0 skew, time to 1,000 °F is distributed randomly

Calculated Peak Pressure in the A and B Channels. This was the highest pressure recorded in the A (first-fired) and B (second-fired) channel. Simultaneous firings result in no first-second ordering, but two pressure readings were taken. Some estimation was used due to noise and overshoot in the data.

	NASA Engineering and Safety Center Technical Assessment Report	Document #: NESC-RP- 09-00596	Version: 1.0
Title: Pyrovalve Booster Interface Temperature Measurement			Page #: 64 of 92


This data was relatively straightforward to analyze and fit two linear response surfaces. Run 14 showed as a possible wild point in the Peak B response. There is evidence that this run's window leaked slightly, which jibes with the Peak B analysis results. Removing the point does not change the overall conclusions. The point was left in the model.

The prediction model fit for **Peak A** is shown below.

$$\begin{aligned}
 \text{Press A Calc Peak} &= \\
 &+10380 \\
 &-102700 && * \text{Channel Area} \\
 &+9.152 && * \text{Actual Skew} \\
 &-2933 && * \text{Channel Area} * \text{Actual Skew} \\
 &-183500 && * \text{Channel Area}^2 \\
 &+148100 && * \text{Channel Area}^2 * \text{Actual Skew}
 \end{aligned}$$

Fit to assumptions was good although the goodness-of-fit of the model was only fair. Removing Run 14 did not change this and extensive diagnostics and model-fitting were not performed to find the source of the issue. Again, the overall conclusions due to this data are clear, and it is expected that a better model fit would only result in more accurate point predictions without real value to the aims of this test.

A 3-dimensional view of the fit including the data points is shown in Figure G-7. Run 14 is highlighted by an open marker.

	NASA Engineering and Safety Center Technical Assessment Report	Document #: NESC-RP- 09-00596	Version: 1.0
Title: Pyrovalve Booster Interface Temperature Measurement			Page #: 65 of 92

Design-Expert® Software

Factor Coding: Actual

Press A Calc Peak

● Design points above predicted value

○ Design points below predicted value

X1 = A: Channel Area

X2 = B: Actual Skew

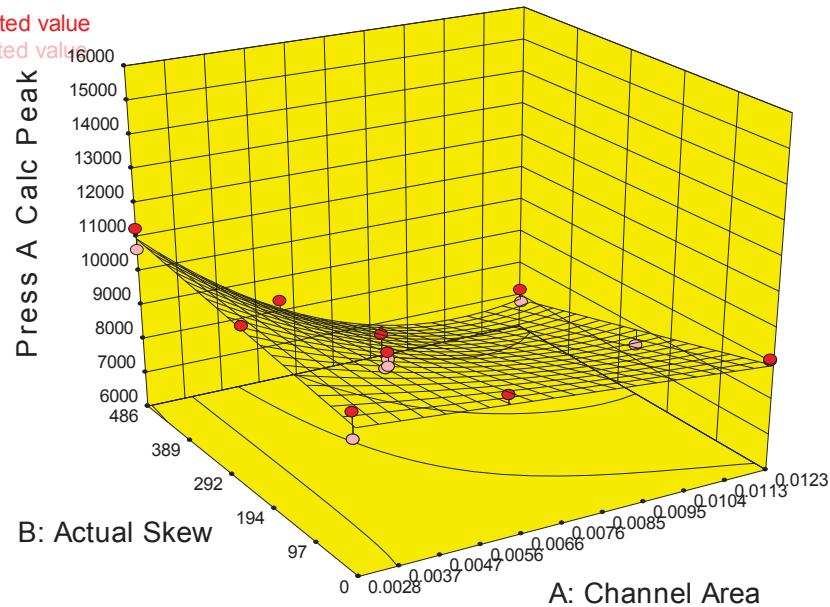



Figure G-7. Peak Pressure in First-Fired Chamber / Port A

Highest *Peak A Pressure* occurred at the most-commonly designed low *Channel Area* and higher *Skew* times. Note that *Channel Area* produced only a ~1,000-lb drop from the minimum to maximum tested *Area on Peak A Pressure* at low skew. Similarly, at low channel areas, *Peak A Pressure* increased only about 1,000 lbs from 0–500 μ s skew. Both look linear at these settings. However, with large *Channel Area* and *Skew*, *Peak A Pressure* falls off noticeably. There is a clear curvature in the response to *Channel Area*.

Peak B data was fit to a model that was in some ways similar.

$$\begin{aligned}
 \text{Press A Calc Peak} &= \\
 &+10510 \\
 &-83450 \quad * \text{Channel Area} \\
 &+21.60 \quad * \text{Actual Skew} \\
 &-649.6 \quad * \text{Channel Area} * \text{Actual Skew} \\
 &-0.01976 \quad * \text{Actual Skew}^2
 \end{aligned}$$

	NASA Engineering and Safety Center Technical Assessment Report	Document #: NESC-RP- 09-00596	Version: 1.0
Title: Pyrovalve Booster Interface Temperature Measurement			Page #: 66 of 92

The response surface described is shown in Figure G-8.

Design-Expert® Software

Factor Coding: Actual

Press B Calc Peak

- Design points above predicted value
- Design points below predicted value

X1 = A: Channel Area

X2 = B: Actual Skew

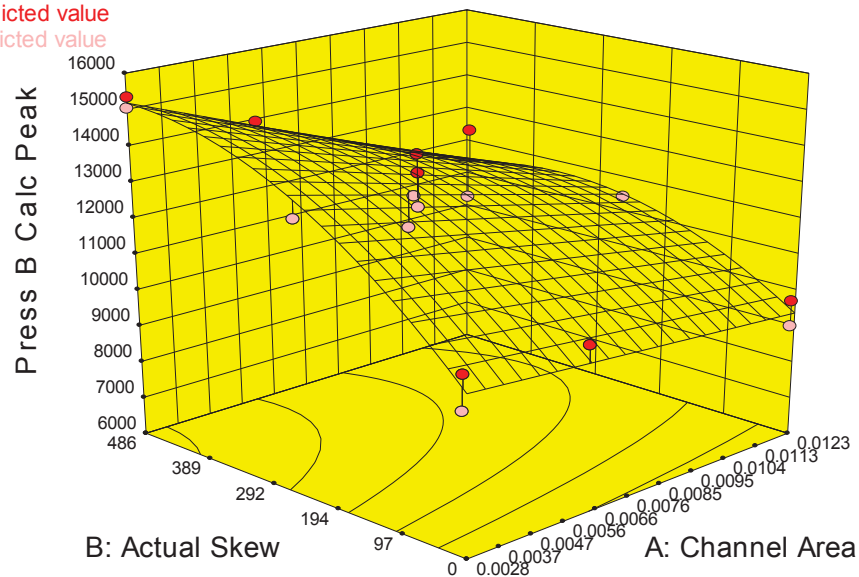



Figure G-8. Peak Pressure in Second-Fired Chamber / Port B

Again, at no skew, *Channel Area* had little effect on *Peak B Pressure*. *Peak B Pressure* rises from here with higher skew. The model appears to show a peak around 300 μ s skew, but it seems possible that given the physics, *Peak B Pressure* levels off at a pressure that is a function, which decreases with increasing *Channel Area*. In either case, the *Peak B Pressure* peak value is highest at low *Channel Area*.

Figure G-9 shows the relationship between the two response surface models. The lower surface is *Peak A Pressure* and the upper is *Peak B Pressure*.

	NASA Engineering and Safety Center Technical Assessment Report	Document #: NESC-RP- 09-00596	Version: 1.0
Title: Pyrovalve Booster Interface Temperature Measurement			Page #: 67 of 92

Design-Expert® Software

Factor Coding: Actual

Press B Calc Peak

● Design points above predicted value

○ Design points below predicted value

Press A Calc Peak = 7208

Press B Calc Peak = 10389

Std # 17 Run # 11

X1 = A: Channel Area = 0.0123

X2 = B: Actual Skew = 484

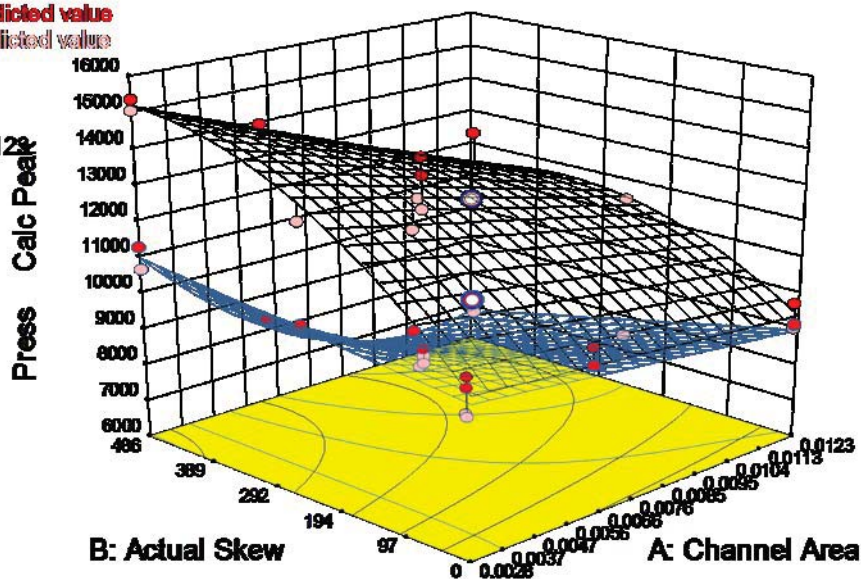


Figure G-9. Overlain Plots of Peak A (blue / lower) and B (black / upper) Pressures. Point Markers with Hollow Centers Are Run 14

As expected, the modeled surfaces meet at the 0-skew point. The *Peak Pressure* after *B* fires builds predictably above the Peak A, again an expected result. Larger channel area can only decrease *Peak Pressure* given any *Skew*. Given the current default 0.060-inch-diameter channel design, *Peak Pressure* after the first NSI fires is stable and predictable, and pressure builds considerably on *B*'s firing.

Pressures at Key Times. Analysis of *Pressure in Channel A at Time of Channel B Pressure Peak* data results in a fairly complex surface. It was modeled as follows.

	NASA Engineering and Safety Center Technical Assessment Report	Document #: NESC-RP- 09-00596	Version: 1.0
Title: Pyrovalve Booster Interface Temperature Measurement			Page #: 68 of 92

$$\begin{aligned}
& \text{A Press at B Press Peak} = \\
& +10780 \\
& -225900 \quad * \text{Channel Area} \\
& +2.332 \quad * \text{Actual Skew} \\
& -5207. \quad * \text{Channel Area} * \text{Actual Skew} \\
& +9345000 \quad * \text{Channel Area}^2 \\
& -0.01024 \quad * \text{Actual Skew}^2 \\
& +151700 \quad * \text{Channel Area}^2 * \text{Actual Skew} \\
& +5.470 \quad * \text{Channel Area} * \text{Actual Skew}^2
\end{aligned}$$

This model provides a close fit to the data, which show little variability at each factor setting combination. It appears that the linear drop of ~1,000 lbs is seen again from low to high *Channel Area* at 0 *Skew*. Increasing skews, as might be expected, produce a steeper, but still linear drop from ~10,000 lbs to ~6,000 lbs over the range 0–5,000 μs at lowest area. Again, this pressure drops markedly from these cases. It can be conjectured that the dip in the response surface just before the *high-Skew/high-Channel Area* factor combination is an artifact of the modeling process, and the true process may in fact level off at approximately 4,000 lbs in this region.

Design-Expert® Software

Factor Coding: Actual

A Press at B Press Peak

● Design points above predicted value

○ Design points below predicted value

X1 = A: Channel Area

X2 = B: Actual Skew

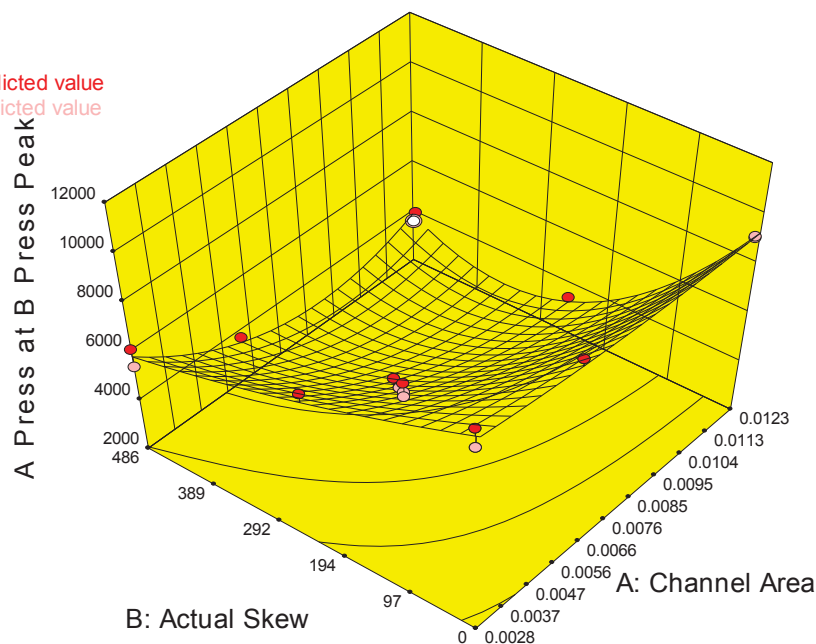



Figure G-10. Pressure in First Chamber at Time of Peak Pressure in Redundant NSI's Chamber

	NASA Engineering and Safety Center Technical Assessment Report	Document #: NESC-RP- 09-00596	Version: 1.0
Title: Pyrovalve Booster Interface Temperature Measurement			Page #: 69 of 92

The *Difference in Pressure at the Time of Peak Pressure in B* shows little if any dependence on *Channel Area* and a markedly decreasing dependence on *Skew*. A floor at approximately -11,000 lbs seems reasonable. The data suggest a slight downward bow with minimum due to *Channel Area* with minimum at $\sim 0.0070 \text{ in}^2$, but it is small. This term was arbitrarily left out of the model.

$$\begin{aligned}
\Delta \text{ Pressure at Time of B Pressure Peak} &= \\
&-90.96 \\
&-44.02 * \text{Actual Skew} \\
&+0.05412 * \text{Actual Skew}^2
\end{aligned}$$

Design-Expert® Software

Factor Coding: Actual

Diff in Press at B Peak

● Design points above predicted value

○ Design points below predicted value

X1 = A: Channel Area

X2 = B: Actual Skew

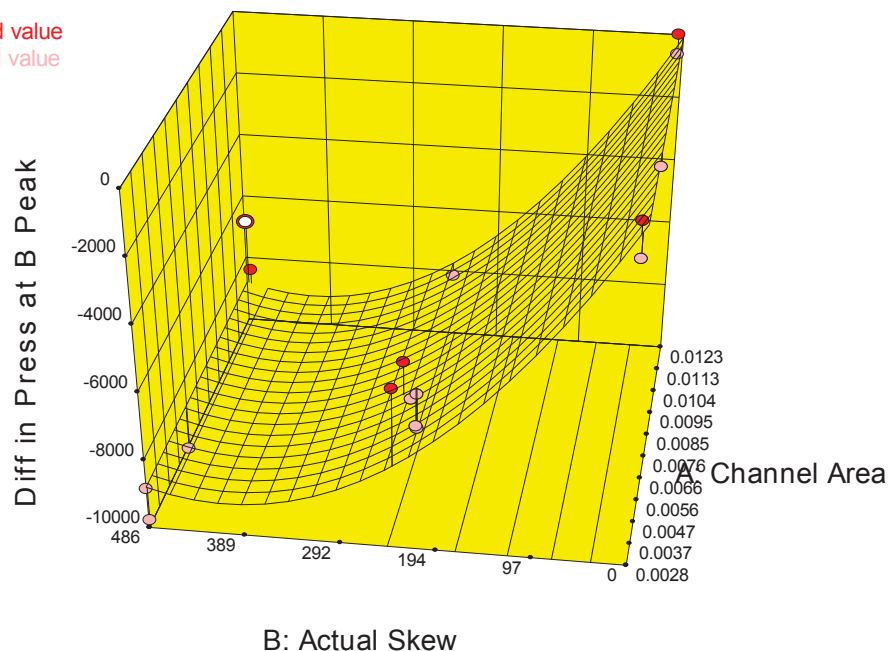



Figure G-11. Difference between Port A and Port B Pressures at Time of B Peak Pressure

Pressure in Channel A at 1,600 μs depends on *Channel Area* but not appreciably on *Skew*. Clearly the effect of *Skew* has diminished by this time and total PCA volume and/or metal area available for heat dissipation drive this.

	NASA Engineering and Safety Center Technical Assessment Report	Document #: NESC-RP- 09-00596	Version: 1.0
Title: Pyrovalve Booster Interface Temperature Measurement			Page #: 70 of 92

$$\begin{aligned}
 &\text{Pressure in Channel A at } 1600\mu\text{s} &= \\
 &+9942. \\
 &-430000 & * \text{Channel Area} \\
 &+19150000 & * \text{Channel Area}^2
 \end{aligned}$$

At the default *Channel Area*, one could expect pressures of around 8,800 lbs. It may decrease to a floor of around 7,500 lbs.

Design-Expert® Software

Factor Coding: Actual

1600us Press A

● Design points above predicted value

○ Design points below predicted value

1600us Press A = 6635

Std # 17 Run # 11

X1 = A: Channel Area = 0.0123

X2 = B: Actual Skew = 484

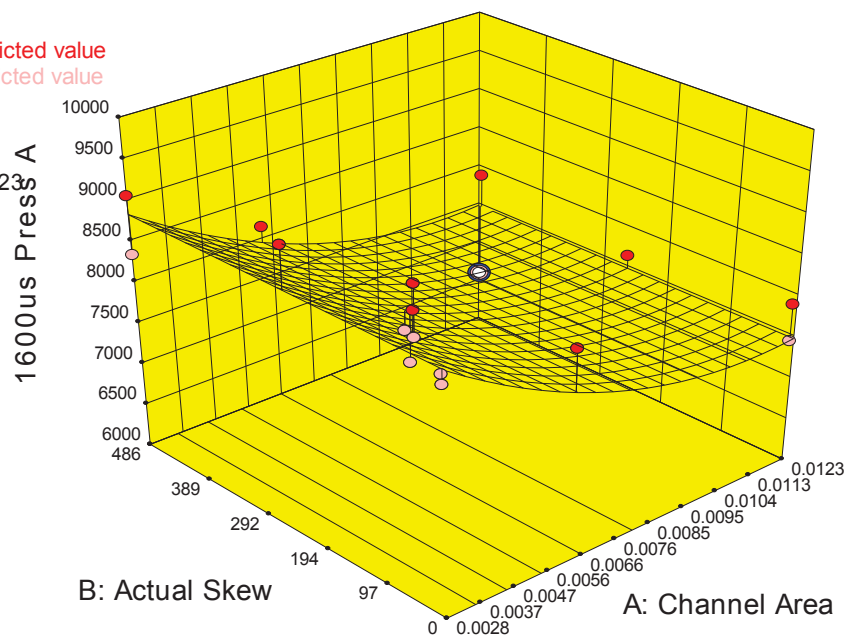



Figure G-12. Pressure in Port A at 1,600 μ s. Run 14 Is the Hollow-Center Point in the Graph.

Time of Peak Pressure A decreased slightly but fairly dependably with increasing *Channel Area*. Run 6A attained peak pressure at an unusually low time, according to this model, but the test value (212 μ s, blue-circled point in the graph) was not far off the expected value (221 μ s) in real terms due to a fairly small spread. Nevertheless, it does look unusual in the plot of the response surface.

	NASA Engineering and Safety Center Technical Assessment Report	Document #: NESC-RP- 09-00596	Version: 1.0
Title: Pyrovalve Booster Interface Temperature Measurement			Page #: 71 of 92

Design-Expert® Software

Factor Coding: Actual

Time of Press A Peak

● Design points above predicted value

○ Design points below predicted value

X1 = A: Channel Area

X2 = B: Actual Skew

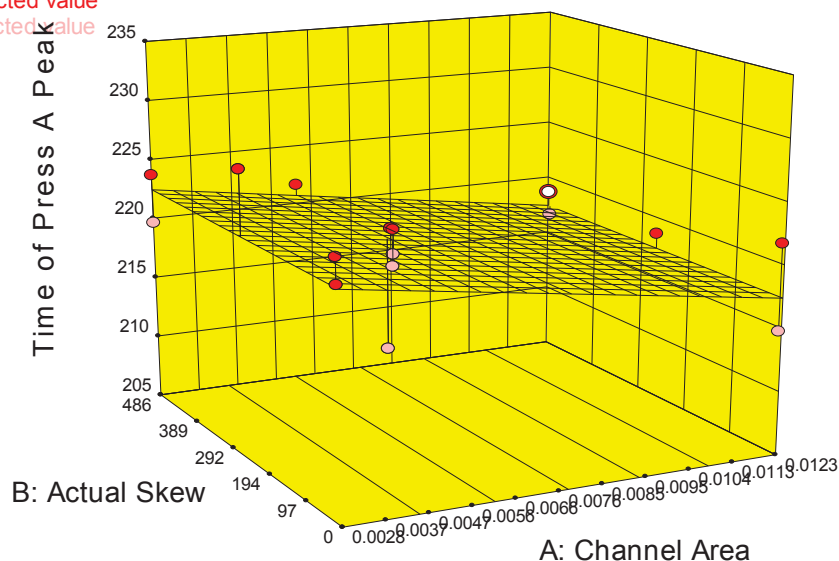



Figure G-13. Time of Peak Pressure in Port A

The model fit is as follows.

$$\begin{aligned} \text{Time of Press A Peak} = & \\ & +224.3 \\ & -528.3 * \text{Channel Area} \end{aligned}$$

No linear model was found to fit *Pressure before B Begins to Rise*. This measure is not defined for 0-skew runs. The natural logarithm of the data for the remaining domain can be fit to a normal distribution. This would suggest that the variability in the *Pressure before B Rise* data has little to do with either *Area* or *Skew* and is due to random (uncontrolled) factors, and its variability can be modeled using a lognormal distribution.

The QQ plot shown in Figure G-14 indicates the fit to the distribution. A perfect fit of the data to the distribution would have the points lying exactly along the centerline. Note that it takes a large dataset to pin down a distribution, so this information is presented as being useful, but not certain.

	NASA Engineering and Safety Center Technical Assessment Report	Document #: NESC-RP- 09-00596	Version: 1.0
Title: Pyrovalve Booster Interface Temperature Measurement			Page #: 72 of 92

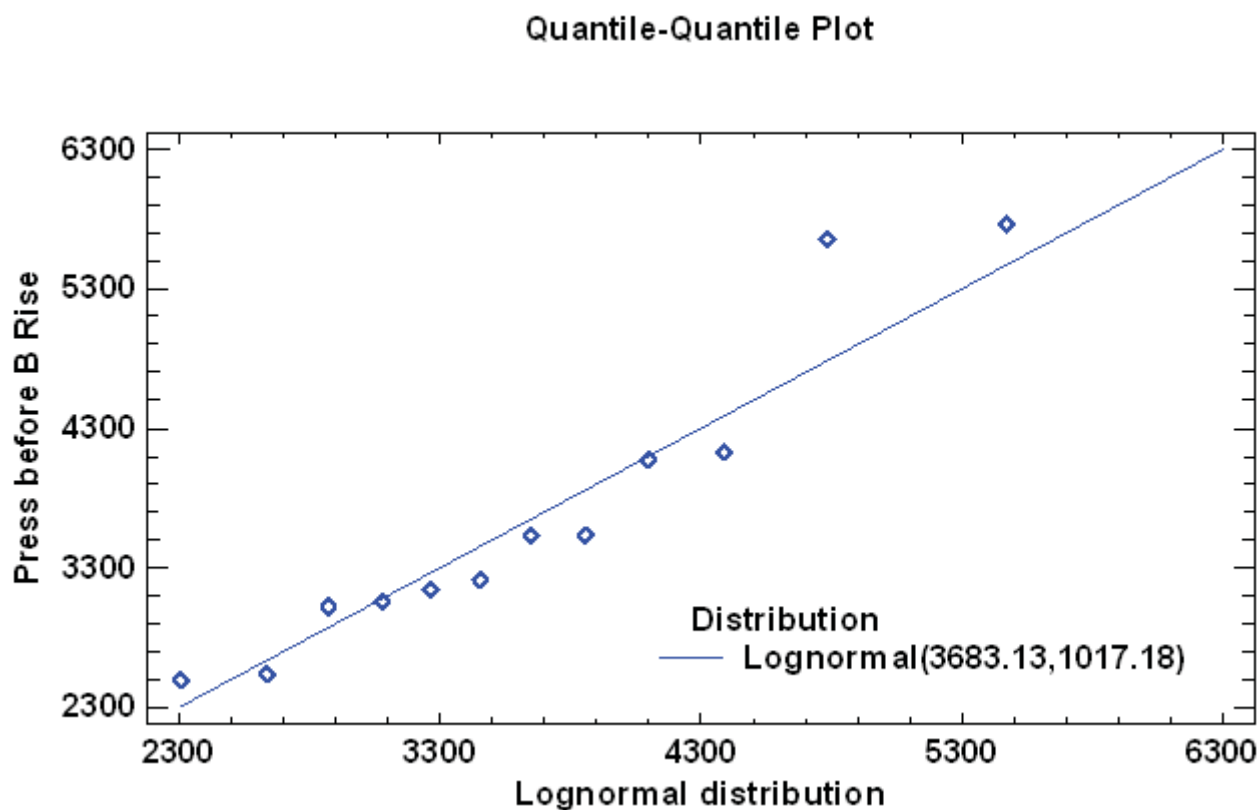


Figure G-14. Pressure before Port B's Pressure Begins to Rise, Modeled Using a Lognormal Distribution

The distribution shown in Figure G-15 is the probability density function (PDF).

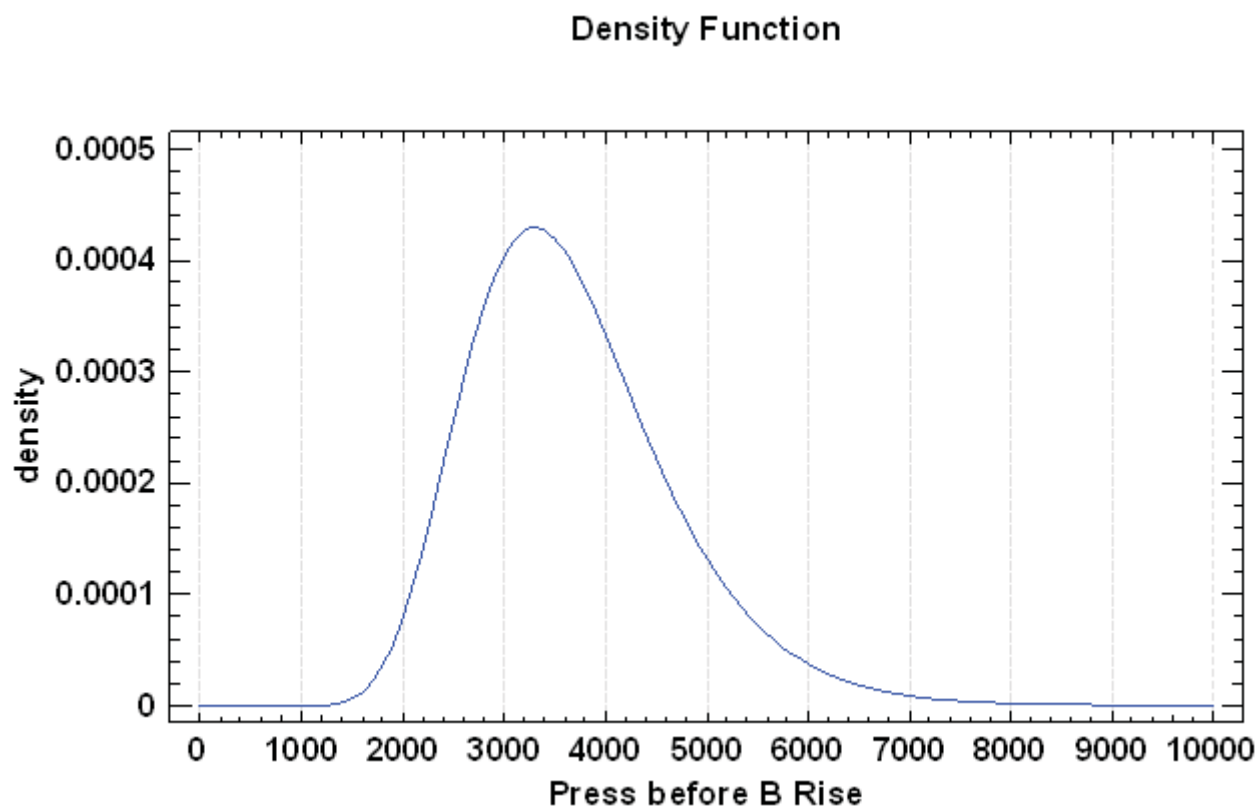



Figure G-15. Probability Density Function for Distribution Best-Fit to Data and Indicated in Figure G-14

Its parameters:

<i>Lognormal</i>
mean = 3683
standard deviation = 1017
Log scale: mean = 8.175
Log scale: std. dev. = 0.2711

	NASA Engineering and Safety Center Technical Assessment Report	Document #: NESC-RP- 09-00596	Version: 1.0
Title: Pyrovalve Booster Interface Temperature Measurement			Page #: 74 of 92

Time of Pressure B Peak is clearly due to *Skew*, which because skew is directly related to *B*'s firing time, was not a surprise. A case can be made that there is lower variability at lowest *Channel Area* than at other areas tested. *Skew* had no effect.

Size of Hole Made in Diaphragm

Responses on a percent scale are bounded at 0 percent and 100 percent. These are best handled using a transformation of the response that reflects this such as a Logit but, in practice, if responses are in the center of this range, this may not be necessary. After confirming that there is no substantial difference in conclusions reached by the more complex model and a model reached using no transformation, the untransformed response was used in analysis.

This measure's analytical results depend on how no-fires are handled. No-fires reliably resulted in 0-percent diaphragm hole. All of the 0-skew runs resulted in 0-percent puncture area. The one no-fire at the largest skew setting, Run 3, presents a problem, particularly because the team was not able to collect direct data from its replicate point, Run 14. There is a sufficient still from Run 14 that clearly shows substantial diaphragm burn-through.

There is no reason to call Run 14's response 0 percent; in fact, it may have the largest burn-through of any test. It could be treated as a point censored at 0 percent, the most correct method, but doing so would result in Run 3 driving the analysis. Censoring at a higher value would work, but was not done at the time of this report's writing.


It seems clear that Run 3 is somehow anomalous. One method is to ignore or right-censor this point. Censoring this value has little effect on results and presents a challenge, which takes time to solve, so it was decided to ignore the point. A placeholder value of 50 percent was used for Run to avoid the previously mentioned analysis time issue. Using 70 percent results in an anomalously high value, an outlier; it also suggests an effect due to Area.

It is also possible that these assumptions are entirely incorrect and that the large *Skew*/large *Area* point simply results in unpredictable burn-through.

A fit model, assuming Run 3 does not exist and Run 14 is 50 percent:

$$\begin{aligned} \text{Diaphragm Fract. Hole, Nonzero Skew} = & \\ & +0.1427 \\ & +0.0005861 \quad * \text{ Actual Skew} \end{aligned}$$

The response surface (Run 14 is the hollow marker) is shown in Figure G-16.

	NASA Engineering and Safety Center Technical Assessment Report	Document #: NESC-RP- 09-00596	Version: 1.0
Title: Pyrovalve Booster Interface Temperature Measurement			Page #: 75 of 92

Design-Expert® Software

Factor Coding: Actual

Diaphragm Fract. Hole, Nonzero Skew

● Design points above predicted value

○ Design points below predicted value

X1 = A: Channel Area

X2 = B: Actual Skew

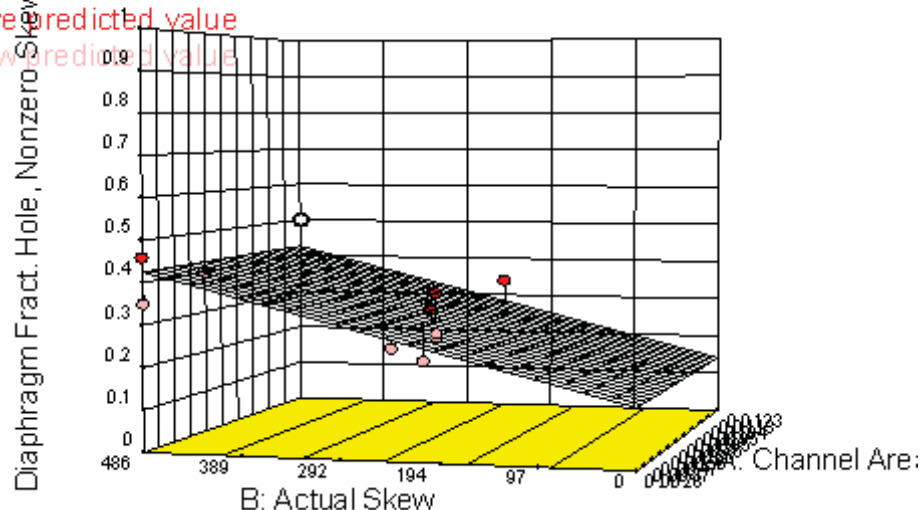



Figure G-16. Size of Hole in Booster Simulator Diaphragm

Clearly, low *Skew* could result in 0 burn-through, an undesirable result. Given Run 14 is due to a special cause or given a no-fire does not occur, it appears that larger *Skew* results in larger fraction of the diaphragm burning.

Phase IIB Confirmation Run. A confirmation run is a test trial withheld from the dataset, which had been used to construct predictive models. The models are created without this run, but it is then used to check the reasonableness of the model predictions by comparing the results of the withheld test to the predictive models. One useful way to evaluate this comparison is through the use of prediction intervals (Montgomery, Peck and Vining, 2001: Introduction to Linear Regression Analysis, 3rd Ed., Wiley Interscience, New York, NY). Prediction intervals are test result ranges within which one would expect a future observation to lie with some specified probability, given a model formed from data that has already been observed. This is, of course, exactly what is desired here.

A single confirmation run at factor settings Nominal Skew = 500 μ s, NSI flow channel cross-sectional area = 4 times the nominal (Channel Diameter = 0.120 inches) was performed. This point was chosen because of the issues with Run 3, inadvertently run with two booster simulator diaphragms instead of one, and Run 14, having indications of a pressure leak. The results were as follows:

	NASA Engineering and Safety Center Technical Assessment Report	Document #: NESC-RP-09-00596	Version: 1.0
Title: Pyrovalve Booster Interface Temperature Measurement			Page #: 76 of 92

SS, Dual NSI	Channel Diameter (Area)	Actual Timing Skew, μ s	Press A Calc Peak	Time Of Press A Peak	Overall Max Temp	Time Of Max Temp	Press Before B Rise	Press B Calc Peak	Time Of Press B Peak	1600 μ s Press in A	1600 μ s Temp
Run 3A	0.120 4 times nom)	488	8243	214	>3630 (above limit of IR)	299	4140	10,114	700	7773	2958
All times are measured from start of firing signal.											

Note that the maximum temperature reported is at the upper limit of the pyrometer. The pyrometer sensor was saturated for some period of time, so the actual maximum temperature is higher than the value reported, but it cannot be used.

To evaluate reasonableness, 95-percent prediction intervals (PI) on the models created as earlier described were compared to the values above. The summary is shown in Table G-1.

Table G-1. Confirmation Run 3A Compared to Model Predictions and Prediction Intervals

Confirmation Report


Two-sided

Confidence = 95%

	Name	Level	Low Level	High Level	Run 3A
	Channel Area	0.0123	0.0028	0.0123	0.0123
	Actual Skew	488	0	486	488 μ s

Response	Prediction	Std Dev	SE (n=1)	95% PI lower	95% PI upper	Run 3A
Overall Max Temp	3522	269.0	331.3	2783.7	4260.0	>3,630
1600us Temp Dia	2622	286.1	313.0	1945.3	3297.8	2,958
Time of Max Temp	1040			416	2607	299
Press A Calc Peak	6876	380.1	459.5	5864.9	7887.8	8,243
Time of Press A Peak	217.8	3.39	3.68	209.9	225.7	214
Press Before B Rise	not analyzed					4,140
Press B Calc Peak	11417	712.8	863.5	9535.4	13298.2	10,114
Time of Press B Peak	not analyzed					700
1600us Press A	7550	438.8	480.7	6519.4	8581.4	7,773

For most measures where a model was constructed, Run 3A falls within the 95-percent PI upper and lower bounds. This gives confirmation that these models are useful for prediction of future test runs. Note that prediction intervals are not intended to predict the range within *all* future test


	NASA Engineering and Safety Center Technical Assessment Report	Document #: NESC-RP- 09-00596	Version: 1.0
Title: Pyrovalve Booster Interface Temperature Measurement			Page #: 77 of 92

runs can be expected to lie. That construct is known as a tolerance interval and is understood and calculated quite differently. Tolerance intervals are normally considerably wider than prediction intervals. Maximum temperature was not evaluated, as its true value exceeded the upper limit of the IR unit's capability.

For the case of *Peak Pressure in Channel A* and *Time of Maximum Temperature*, Run 3A's measured value is outside the 95-percent PI. By chance, one might expect one out of every 20 observations (1–0.95, or 5 percent) to be outside these limits. However, given six (not including *Max Temperature*) independent measurements to be compared at one time, there will be a greater than 5-percent chance that any one of these measurements will be exceeded. The chance that there will be at least one exceedance in six of these intervals simply due to chance can be calculated using the Bonferroni correction (Montgomery, Design and Analysis of Experiments, 6th ed., Wiley, 2004), which comes out to more than 26 percent. Clearly, it is quite possible to experience at least one exceedance of these limits in six chances to do so without needing to resort to any explanation regarding special causes.

To reduce the chance that a single exceedance of these six prediction limits would be observed due to Run 3A to 5 percent, the confidence level to 99.17 percent would need to change. Doing so increases the upper limit on the prediction limit (now a two-sided upper 99.17-percent prediction limit) to 8713, bounding 3A's value. The *Time of Max Temperature* two-sided lower 99.17-percent prediction limit is 271 μ s, again bounding 3A's observation; 3A appears to be bounded by the models created, meaning that this confirmation run does not invalidate these models.

It is possible that the model predicting *Peak Pressure in A* does not well represent high skew/large area. Run 3A's Peak Pressure in A compared to the predicted model is pictured in Figure G-17. The point included in that corner is Run 3; the model was constructed without Run 14. It is possible that the response surface model is not adequate in that corner of the input domain and Run 3A is reasonable. This would imply that *Peak Pressure* levels off more sharply at long *Skew* and large *Channel Area* than modeled, perhaps near 8,000 psi.

	NASA Engineering and Safety Center Technical Assessment Report	Document #: NESC-RP- 09-00596	Version: 1.0
Title: Pyrovalve Booster Interface Temperature Measurement			Page #: 78 of 92

Design-Expert® Software

Factor Coding: Actual

Press A Calc Peak

● Design points above predicted value

○ Design points below predicted value

Press A Calc Peak = 7208

Std # 17 Run # 11

X1 = A: Channel Area = 0.0123

X2 = B: Actual Skew = 484

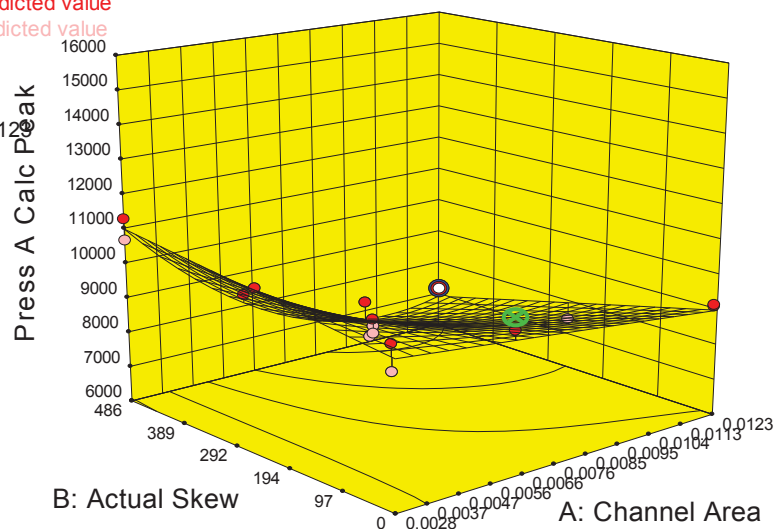



Figure G-17. Response Surface Model, Peak Pressure in Channel A. The Green “X” Marks Run 3A’s Value (8243 psi). Run 3A Was Not Considered when this Model Was Built.

The confirmation run appears to underline the robustness of this test planning using DOE, the test performance, and the models created. It does not appear to indicate that most of the models inadequately predict their respective responses. It does not appear to call into question the findings, observations and NESC recommendations of this team.

Analysis Excluding Runs 3 and 15. An analysis of the data was performed without either of the data points collected at 500 μs and 0.0123 in^2 . It was expected that, since the test matrix was constructed using DOE methods, and most of the data and analyses were reasonably straightforward and well-behaved, this would have minimal effect on conclusions.

In fact, this was the case. The temperature cases’ response surfaces were barely affected by removal of Run 15; Run 3 had already been removed before analysis. Run 14 was no longer flagged as a possible outlier in the 1,600 μs temperature analysis. *Time of Maximum Temperature* was more clearly more variable at higher *Channel Area*.

Peak pressure predictions were affected somewhat. The surfaces, now not tempered by the high *Skew/ high Channel Area* points, were slightly less complex. Given the values measured at this high/ high point, however, it seemed clear that the surface was extrapolating in that corner of the

	NASA Engineering and Safety Center Technical Assessment Report	Document #: NESC-RP- 09-00596	Version: 1.0
Title: Pyrovalve Booster Interface Temperature Measurement			Page #: 79 of 92

response surface, whereas predictions at that corner still matched the actual, but missing, temperature measurements. The models and surfaces describing *Pressure* at 1,600 μ s and *Time of Peak Pressure* in A looked similar whether or not the high/high data was included. The size of the hole in the diaphragm was also little affected by presence or absence of these points.

Optimization and Summary

A summary of effects of factors and runs that appear to give the individual model problems is shown in Figure G-18.

		Significant Effect of Factor	
	Response	Channel Area	Actual Skew
Temp.	Overall Maximum Temperature		
	Diaphragm Temperature at 1600 μ s		
	Time of Maximum Temperature		
	Time to 1000F		
Pressure	Peak Pressure in A (Calculated)		
	Peak Pressure in B (Calculated)		
	Pressure in A at B Peak Pressure		
	Δ Pressure at Time of Peak B		
	Pressure in A at 1600 μ s		
	Time of Peak Pressure in A		
	Pressure before B Pressure Rise		
	Time of Peak Pressure in B		
Hole	Size of Hole Made in Diaphragm		

Figure G-18. Summary of Significant Effects. A Green Box Indicates a Statistically Significant Effect of the Factor on the Response.

An optimization routine was run. This optimization analysis was not meant to determine absolute optimum values for input factor settings in this case. Instead, it was meant to roughly determine what input factor settings would produce desirable results and look for issues.

Team subject matter experts were polled for their estimation of importance of the responses to whether the booster would fire or not. There was general, though not unanimous, agreement. Individual responses will not be supplied, but Table G-2 shows a summary of the combined responses.


	NASA Engineering and Safety Center Technical Assessment Report	Document #: NESC-RP- 09-00596	Version: 1.0
Title: Pyrovalve Booster Interface Temperature Measurement			Page #: 80 of 92

Table G-2. Subject Matter Expert Responses to Booster Fire

Name	Goal	Lower Limit	Upper Limit	Importance
1600 μ s Temp @ Diaphragm	maximize	1000	6000	5
Overall Max Temp	maximize	1000	5000	4
Diaphragm Fract. Hole, Nonzero Skew	maximize	0	0.5	3
A Press at B Press Peak	minimize	3528	10427	1
Diff in Press at B Peak	maximize	-10127	646	1
Time of Press A Peak	minimize	200	250	1

A possible graph of the desirability of the total of responses weighted by team opinion over the range of the input factors *Skew* and *Area* is shown in Figure G-19.

Design-Expert® Software
Factor Coding: Actual
Desirability
X1 = A: Channel Area
X2 = B: Actual Skew

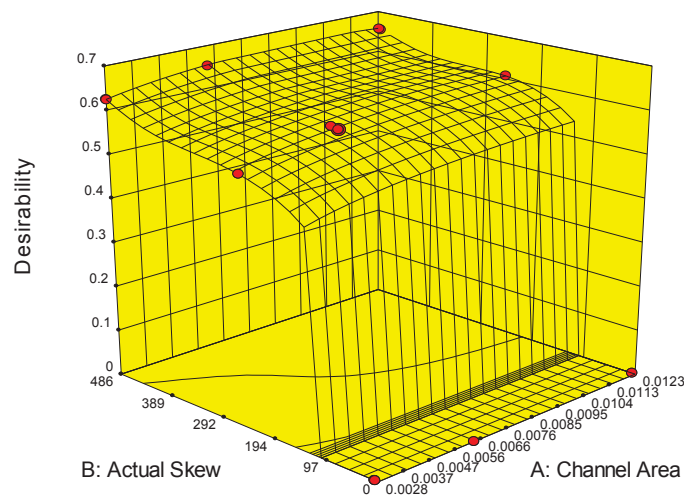



Figure G-19. Desirability Function Suggested by Expert Ratings of Relative Importance of Responses Combined with Response Surface Models in this Analysis


	NASA Engineering and Safety Center Technical Assessment Report	Document #: NESC-RP- 09-00596	Version: 1.0
Title: Pyrovalve Booster Interface Temperature Measurement			Page #: 81 of 92

The region was cut off at 100 μ s skew to reflect the clear issue of no-fires. This cutoff point is arbitrary, and characterization of the probability of no-fires given a skew value is left to future testing. The most desirable region of this space is with higher skew. Temperatures under 1,000 °F were weighted as unacceptable, but greater temperatures were given a high and only gradually increasing weight, resulting in a flat desirability over much of the region.

The analysis of Phase II data clearly shows:

- Low skew times can result in no-fires.
- Maximum temperatures are clearly affected by skew, with longer skews associated with higher temperatures.
- The time at which these temperatures are reached is lengthened with larger channels.
- Designs using larger channel areas should be reconsidered, particularly if the sole aim of their design is to prevent no-fires.

In addition, a no-fire at 500 μ s skew indicates a possibility that skews greater than 500 μ s may be necessary and/or that channel areas should not be increased much beyond 0.0028 inches. However, it seems most likely that this event actually was due to an incorrectly assembled test article.

	NASA Engineering and Safety Center Technical Assessment Report	Document #: NESC-RP- 09-00596	Version: 1.0
Title: Pyrovalve Booster Interface Temperature Measurement			Page #: 82 of 92

Appendix H. Numerical Simulations of Single and Simultaneous Dual Firing Initiators in the SS V-PCA Design

The objective of the numerical simulation (computer modeling) is to provide a detailed fluid dynamic analysis of the single and dual, simultaneous NSI firings in the SS V-PCA design. This work did not include the AI Y-PCA design.

Some simplifications have been made to allow for a quicker and more efficient preliminary investigation. Specifically, the heat transfer to the solid walls was neglected and an inviscid gas was assumed. All combustion of the ZPP was assumed to take place in the NSI. That is, continuing combustion of any ejected large particles was neglected. In addition, the calculations reported here were conducted on a 2-D planar configuration. For the dual, simultaneous firing simulation, the difference in firing times of the NSIs (skew) was chosen to be 0 μ s.


H.1 CRUNCH CFD[®] Numerical Framework

The numerical simulations were performed using the CRUNCH CFD[®] multi-physics numerical code [2]-[4] that has been developed by Craftech[®] and is commercially-licensed. This code is a three-dimensional, unstructured finite-volume solver for viscous, generalized fluid simulations that allow hybrid element grids (i.e., tetrahedral, prismatic, pyramid, and hexahedral cells). Some of its key capabilities are: (i) accurate transient shock wave propagation in high-pressure gas, (ii) strongly coupled conjugate heat transfer capability to model temperature rise in solid material, and (iii) multi-phase capability to model solid propellant particulates as well as molten metal that has eroded from the PCA casing.

H.2 Numerical Results for 2-D Planar Configuration

For this work, inviscid flow was assumed and combustion of the propellant charges was not modeled directly. Instead, a zone of high pressure and temperature was initialized in the region of the charges (top of the NSI cavities) as shown in Figure H-1(a), Figure H-2(a), Figure H-3(a), and Figure H-4(a). The pressure and temperature levels (82.7 MPa and 2,850 K) were derived from an analytical solution of a closed-bomb problem for the complete burn of a typical NSI charge. The flow-field is initially quiescent and atmospheric conditions are assumed in the areas of the PCA outside of the high-pressure zones. In addition, a trace amount of 20 μ m diameter ZrO₂ particles were uniformly distributed in the high pressure/temperature zones to track the particulate location since heat transfer from the particulate phase is expected to be a major factor in the gas burning through the booster cap.

The pressure contours for the single and simultaneous dual firings at 50 μ s, 100 μ s, and 150 μ s area are shown in Figure H-1 and Figure H-2. It is clear from these figures that the pressure rise in the booster cap region for the dual, simultaneous firing case reaches and sustains a much higher peak level than the single firing case due to interaction between the flows from each flame channel. In contrast, the pressure in the single firing case gets relief from the unused flow


	NASA Engineering and Safety Center Technical Assessment Report	Document #: NESC-RP- 09-00596	Version: 1.0
Title: Pyrovalve Booster Interface Temperature Measurement			Page #: 83 of 92

channel, which is at a low ambient pressure. However, the high pressure in the booster cap region for the dual firing case effectively creates a stagnation zone and reverses the flow back into the flow channels. This effect is more evident when looking at the Mach number contours in Figure H-5 and Figure H-6. The single firing case shows a high Mach number in the booster cap cavity (Figure H-5) while the corresponding Mach number for the dual simultaneous firing case is very low (Mach number colors are blue in the booster cavity). The stagnation zone in the dual, simultaneous firing case will significantly reduce the convective heat transfer to the booster cap from the gas-phase despite the large values of temperatures that arise from compression of the gas (see Figure H-4(c) and (d)). Conversely, the convective heat transfer is enhanced for the single firing case due to the high temperature and Mach number values in the booster cavity (Figure H-3(c) and Figure H-5 (c)). The effect of the stagnation zone created by the dual, simultaneous firing on the particulate motion is described below.

The concentration contours of the ZrO_2 particles are shown in Figure H-7 and Figure H-8. The complex shock structure that forms in the flame channels (see Figure H-1 and Figure H-2) causes the particles to enter into the flame channel at an angle and slide along the inside wall. As discussed previously, the pressure in the booster cap region for the single firing case is allowed to relieve into the unused channel, whereas a stagnation zone is formed in the simultaneous, dual firing case eventually leading to backward flow. The effect of this difference on the particle-phase can be seen in the concentration contours at $150\ \mu\text{s}$ in Figure H-7(d) and Figure H-8(d). For the single firing case, the particles are able to travel unimpeded into the booster cavity and a high amount of particles impact and collect on the booster cap. Conversely, the backward flow in the simultaneous, dual firing case impedes the forward progress of the particle phase and only trace amounts of particles are able to reach the booster cap potentially resulting in much reduced heat transfer and a less reliable burn through. Thus, the simulations presented here provide a credible mechanism to explain the failure mode in dual, simultaneous firings of the NSI initiators.

H.3 Concluding Remarks

The simulations performed on a 2-D planar configuration of the SS design indicate that the failure mode for simultaneous dual NSI firings may be caused by flow interactions between the flame channels. The shock waves from each initiator interact in the booster cap region resulting in a high pressure that prevents the gas and particulate velocity from rising in the booster cavity and in fact preventing the bulk of the particulate phase from impacting the booster cap. This reduces the heat transfer to the booster cap both because the particles do not reach the booster cap, and the heat transfer coefficient is reduced due to lack of convective effects. The current study will be continued to provide estimates of the heat transfer to the booster cap as well as the walls of the flow channels. In addition, 3-D simulations will be performed to further investigate the failure mode and ensure that the proposed theory suggested by the 2-D simulation continue to hold for the complete 3-D configuration.

	NASA Engineering and Safety Center Technical Assessment Report	Document #: NESC-RP- 09-00596	Version: 1.0
Title: Pyrovalve Booster Interface Temperature Measurement			Page #: 84 of 92

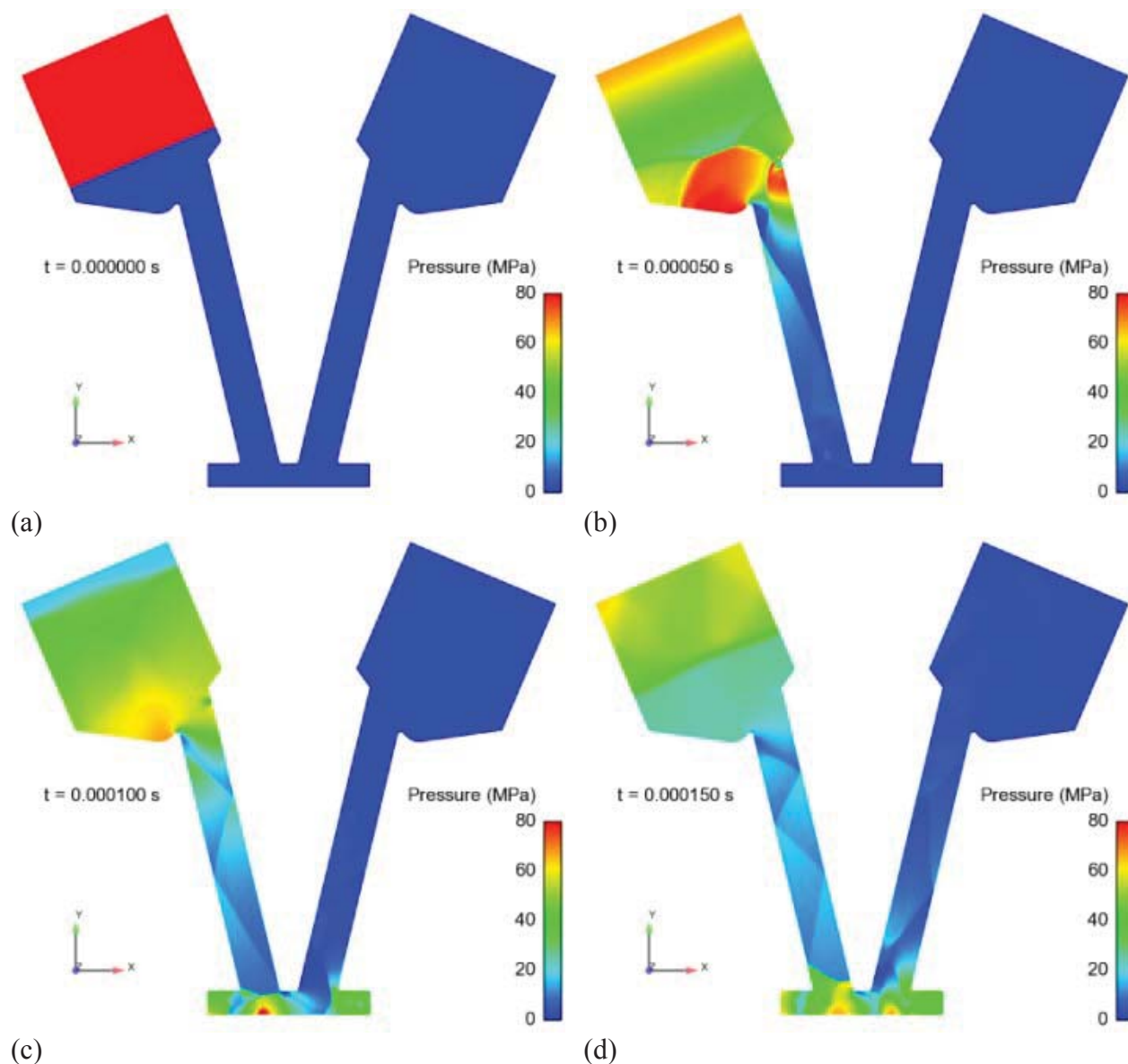



Figure H-1. Pressure Distribution for Single Initiator Firing at 0, 50, 100, and 150 μ s

	NASA Engineering and Safety Center Technical Assessment Report	Document #: NESC-RP- 09-00596	Version: 1.0
Title: Pyrovalve Booster Interface Temperature Measurement			Page #: 85 of 92

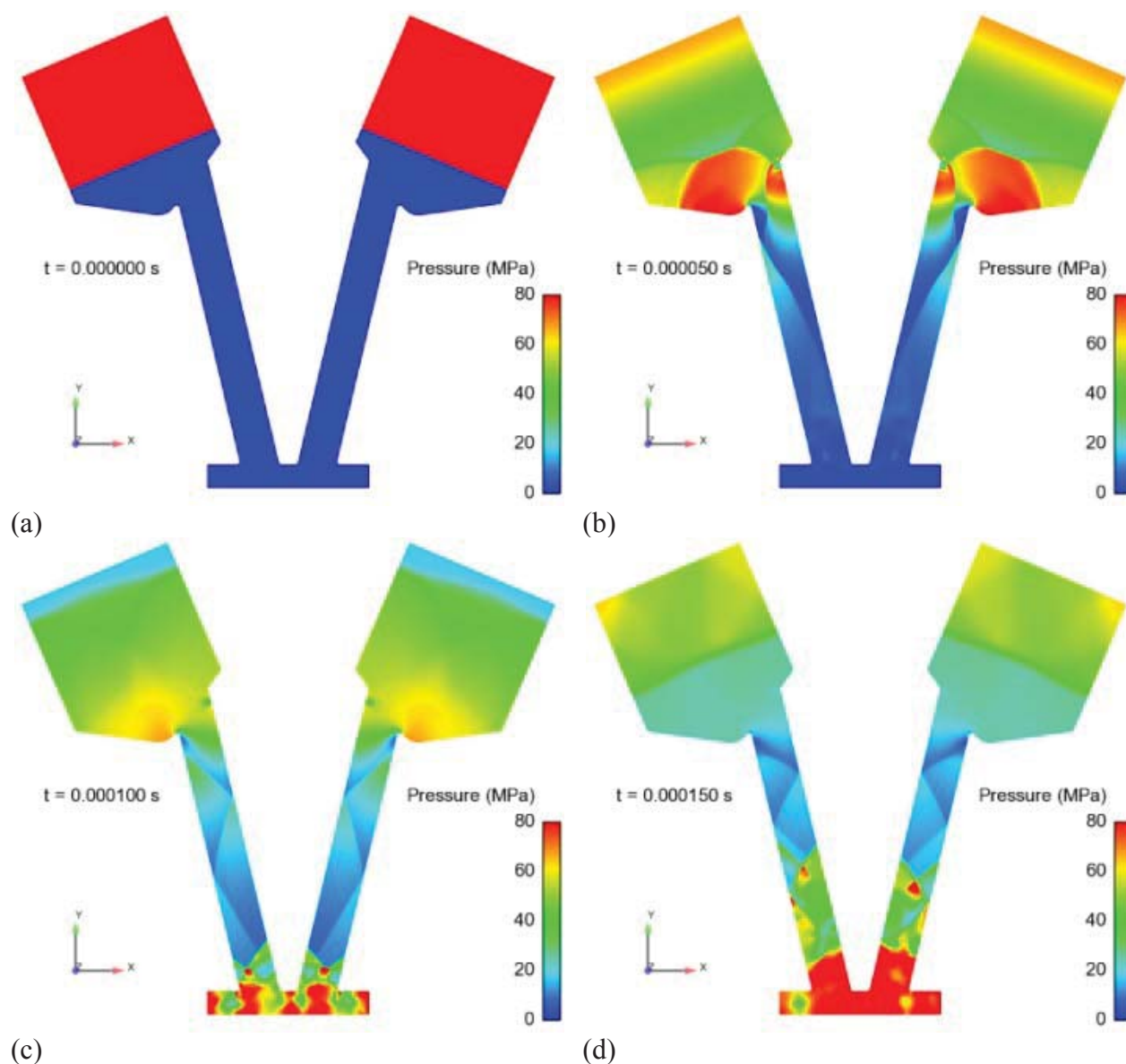



Figure H-2. Pressure Distribution for Simultaneous Dual Firings at 0, 50, 100, and 150 μs

	NASA Engineering and Safety Center Technical Assessment Report	Document #: NESC-RP- 09-00596	Version: 1.0
Title: Pyrovalve Booster Interface Temperature Measurement			Page #: 86 of 92

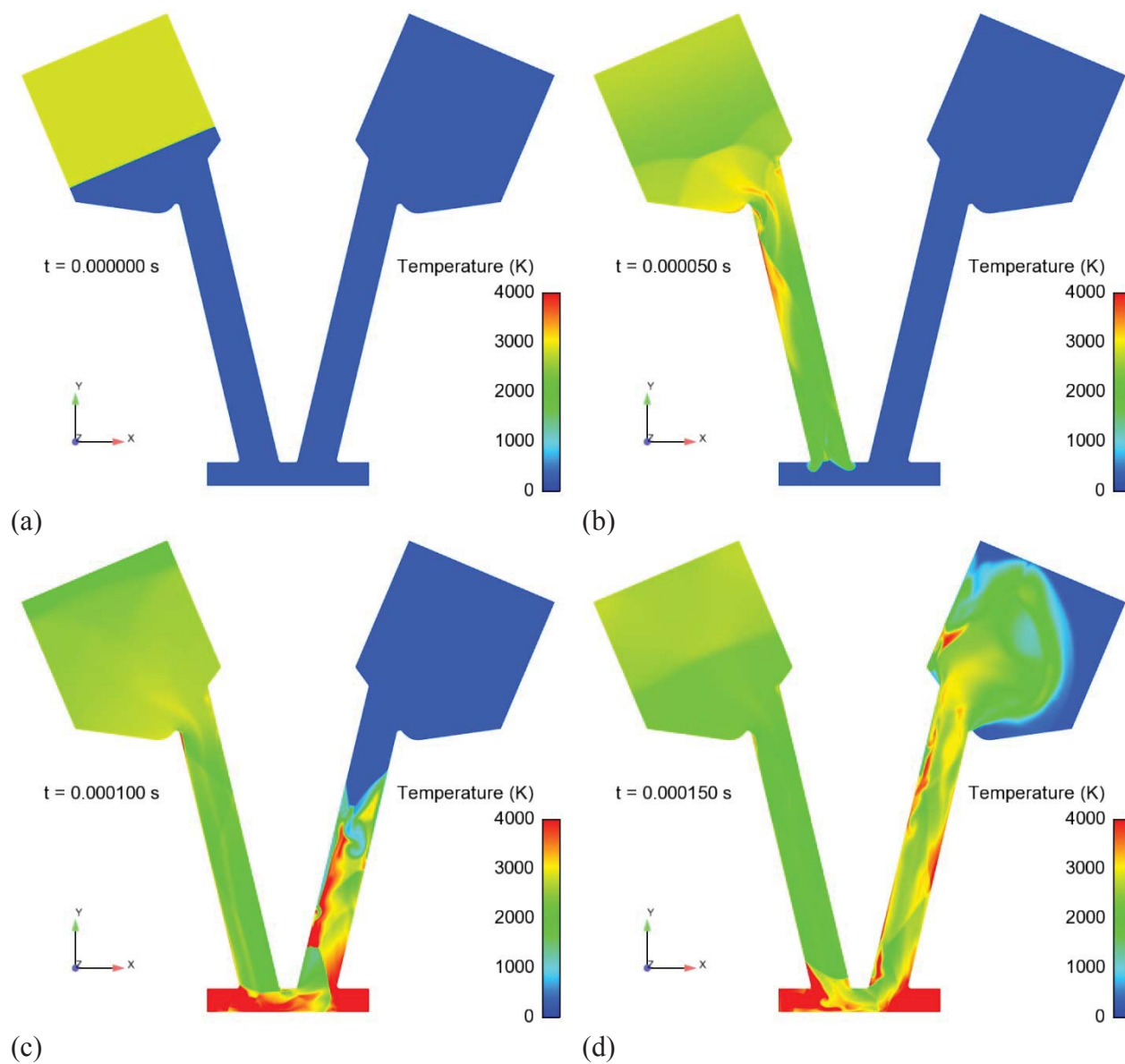



Figure H-3. Temperature Distribution for Single Initiator Firing at 0, 50, 100, and 150 μ s

	NASA Engineering and Safety Center Technical Assessment Report	Document #: NESC-RP- 09-00596	Version: 1.0
Title: Pyrovalve Booster Interface Temperature Measurement			Page #: 87 of 92

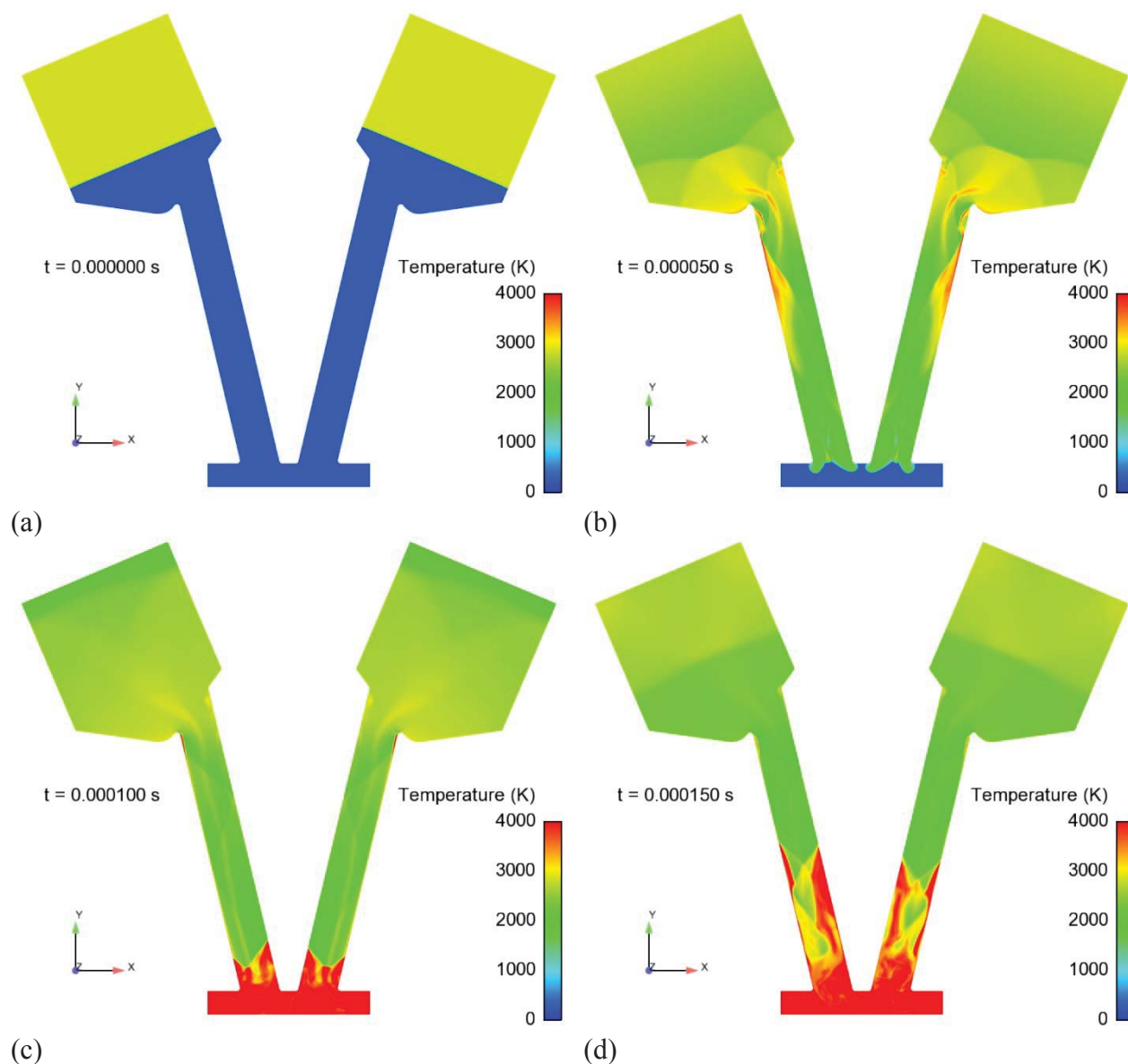


Figure H-4. Temperature Distribution for Simultaneous Dual Firings at 0, 50, 100, and 150 μ s



NASA Engineering and Safety Center Technical Assessment Report

Document #:
**NESC-RP-
09-00596**

Version:
1.0

Title:

Pyrovalve Booster Interface Temperature Measurement

Page #:

88 of 92

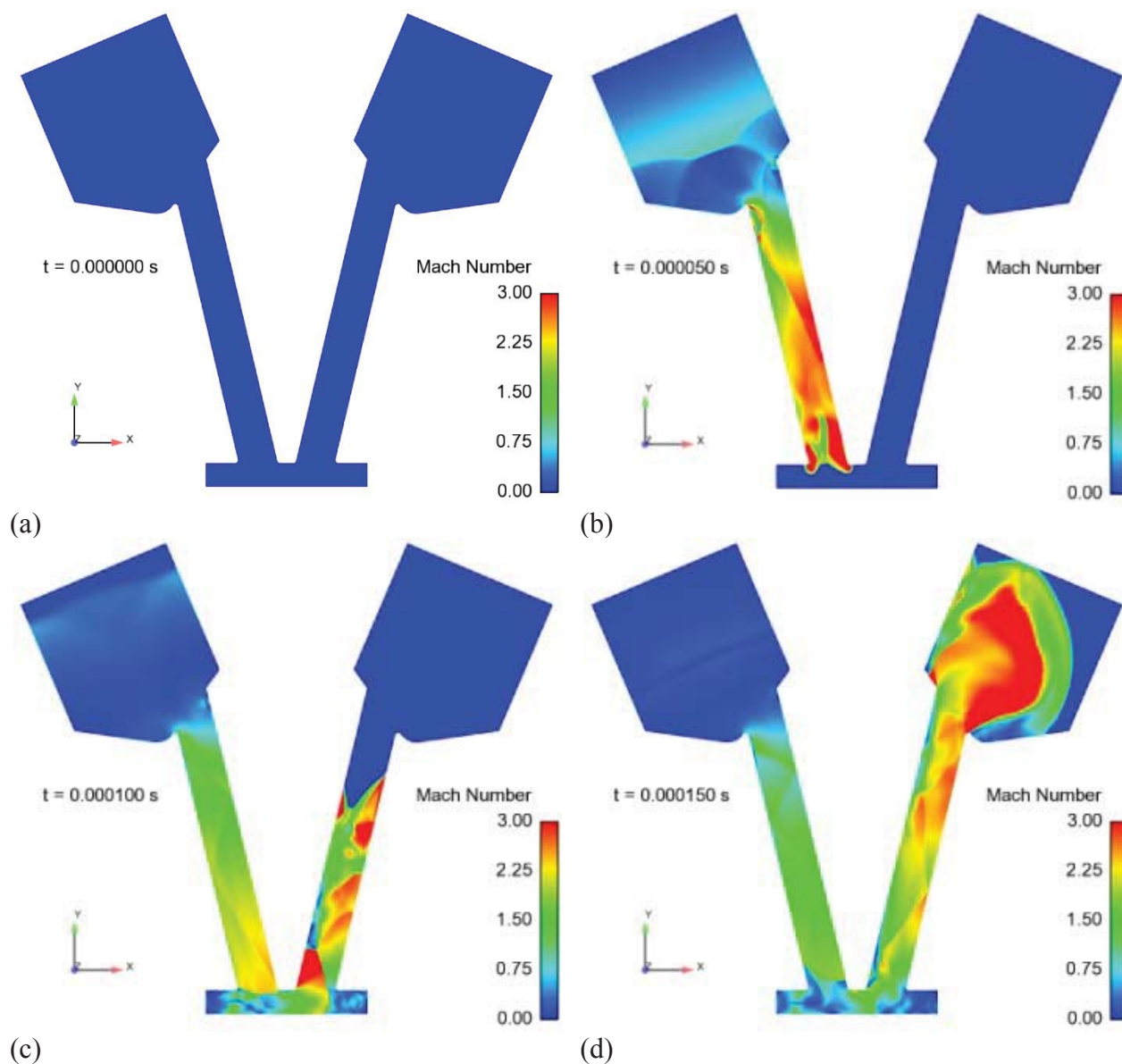


Figure H-5. Mach Number Distribution for Single Firing at 0, 50, 100, and 150 μ s



NASA Engineering and Safety Center Technical Assessment Report

Document #:
**NESC-RP-
09-00596**

Version:
1.0

Title:

Pyrovalve Booster Interface Temperature Measurement

Page #:

89 of 92

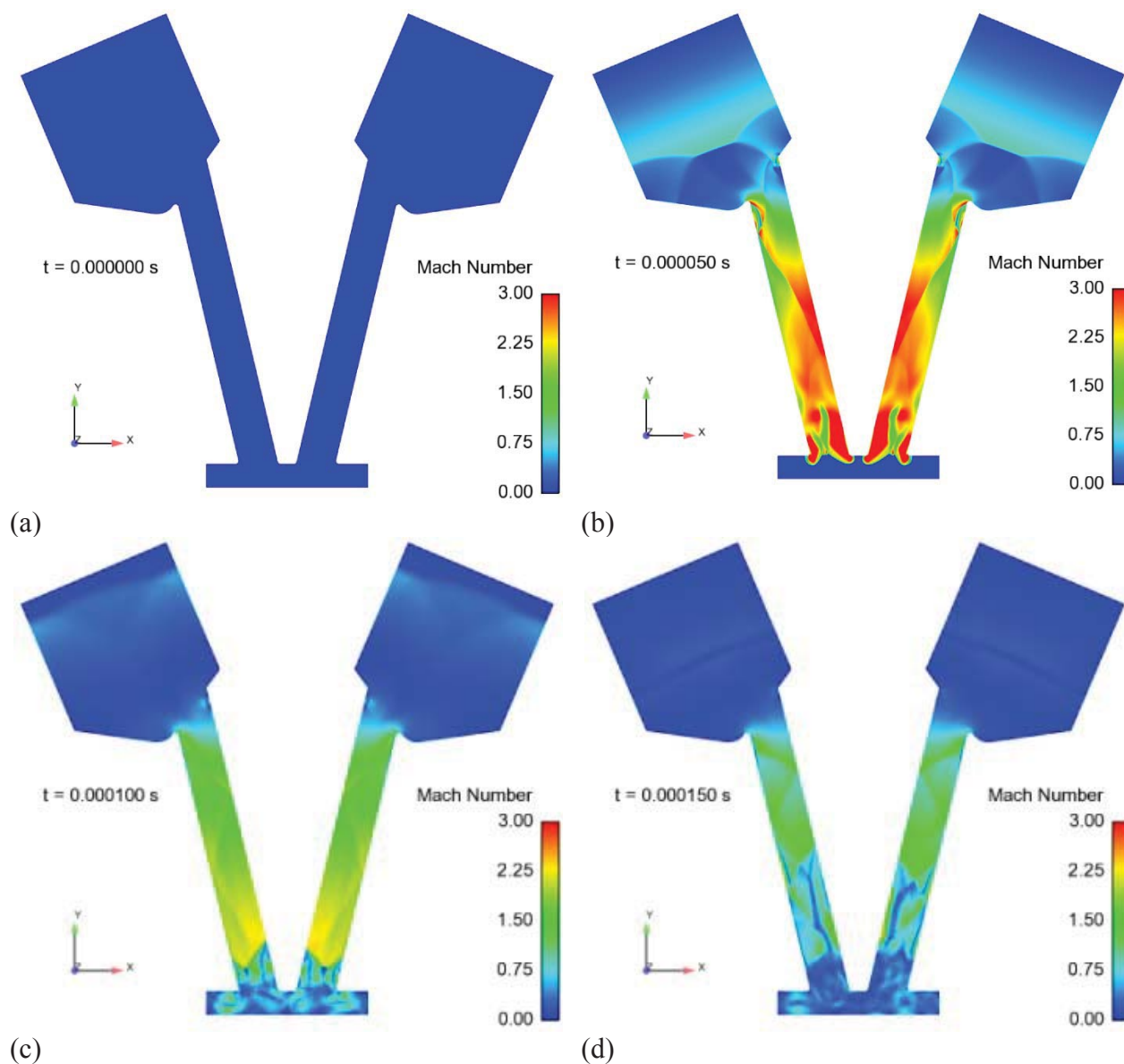



Figure H-6. Mach Number Distribution Simultaneous Dual Firing at 0, 50, 100, and 150 μ s

	NASA Engineering and Safety Center Technical Assessment Report	Document #: NESC-RP- 09-00596	Version: 1.0
Title: Pyrovalve Booster Interface Temperature Measurement			Page #: 90 of 92

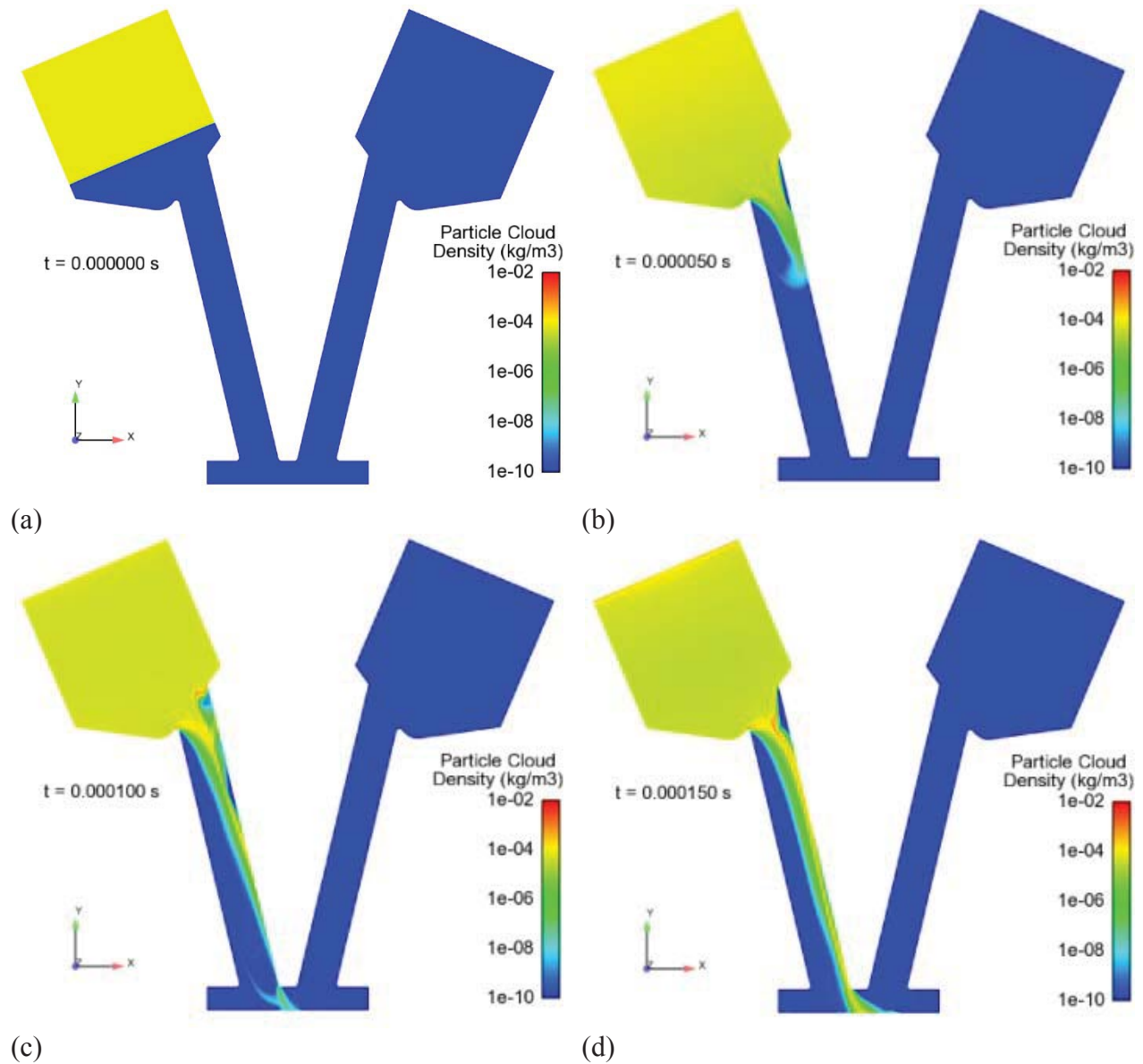



Figure H-7. Particulate Distribution for Single Firing at 0, 50, 100, and 150 μ s

	NASA Engineering and Safety Center Technical Assessment Report	Document #: NESC-RP- 09-00596	Version: 1.0
Title: Pyrovalve Booster Interface Temperature Measurement			Page #: 91 of 92

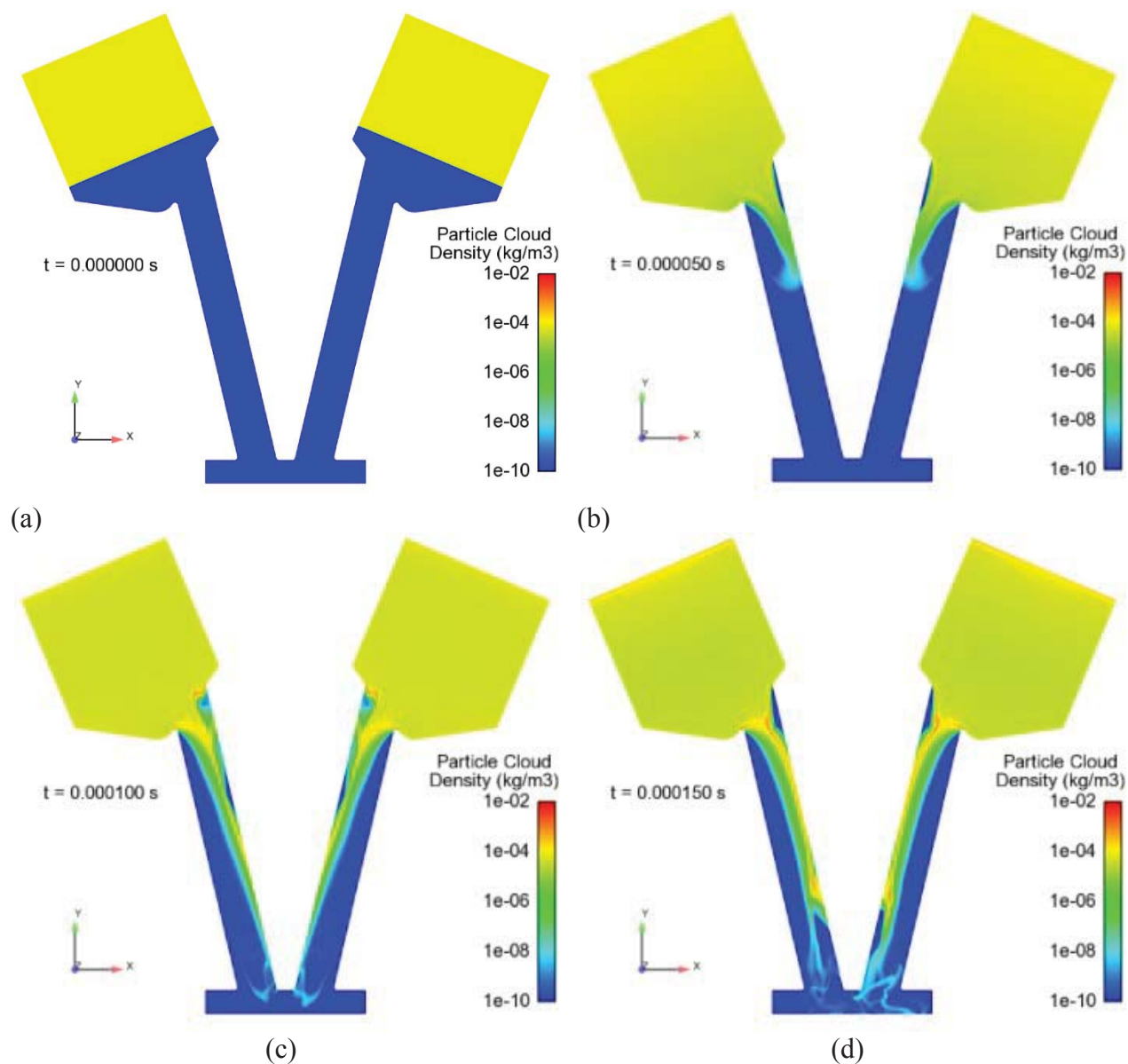


Figure H-8. Particulate Distribution for Simultaneous Dual Firing at 0, 50, 100, and 150 μ s

	NASA Engineering and Safety Center Technical Assessment Report	Document #: NESC-RP- 09-00596	Version: 1.0
Title: Pyrovalve Booster Interface Temperature Measurement			Page #: 92 of 92

H.4 References

- [1] Zenz, Z.D., Schummer, S.W., Pender, A., and Mizukami, M., “Stainless Steel Primer Chamber Assemblies for Dual Initiated Pyrovalves,” Presented at the 6th Modeling and Simulation, 4th Liquid Propulsion, 3rd Spacecraft Propulsion Joint Subcommittee Meeting, Orlando, FL, 8–12 December 2008.
- [2] Hosangadi, A., Lee, R.A., York, B.J., Sinha, N. and Dash, S.M., “Upwind Unstructured Scheme for Three-Dimensional Combusting Flows,” *Journal of Propulsion and Power*, Vol. 12, No. 3, pp. 494-503, May–June 1996.
- [3] Hosangadi, A., Lee, R.A., Cavallo, P.A., Sinha, N., and York, B.J., “Hybrid, Viscous, Unstructured Mesh Solver for Propulsive Applications,” AIAA-98-3153, AIAA 34th Joint Propulsion Meeting and Exhibit, Cleveland, OH, July 13–15, 1998.
- [4] Sachdev, J.S., Ahuja, V., Hosangadi, A., and Allgood, D.C., “Analysis of Flame Deflector Spray Nozzles in Rocket Engine Test Stands,” AIAA-2010-6972, AIAA 46th Joint Propulsion Meeting and Exhibit, Nashville, TN, July 25–28, 2010.

Additional References

1. Hagopian, Michael and Dibbern, Andreas, Conax Pyrotechnic Valve Failures Investigation, NASA/TM-20008-215548 (NESC-RP-08-111/06-009-E), October 30, 2008.
2. Lee, H.S., Estimating Heat Losses in Pyrotechnic Devices, AIAA-2005-3837, July 2005.
3. <http://www.americanelements.com/zrox.html>.
4. Sharafat, S., Kobayashi, A., Ogden, V., and Ghoniem, N., Development of Composite Thermal Barrier Coatings with Anisotropic Microstructure, *Vacuum* 59 (2000), pp. 185-193, Pergamon.
5. CAD file: Alum 1125-279-04.stp.
6. Computer File: NSI-29_No_Filter_V1_0.avi.
7. MCDUGLE_PHOTO Model(1).pdf.

REPORT DOCUMENTATION PAGE					Form Approved OMB No. 0704-0188	
<p>The public reporting burden for this collection of information is estimated to average 1 hour per response, including the time for reviewing instructions, searching existing data sources, gathering and maintaining the data needed, and completing and reviewing the collection of information. Send comments regarding this burden estimate or any other aspect of this collection of information, including suggestions for reducing this burden, to Department of Defense, Washington Headquarters Services, Directorate for Information Operations and Reports (0704-0188), 1215 Jefferson Davis Highway, Suite 1204, Arlington, VA 22202-4302. Respondents should be aware that notwithstanding any other provision of law, no person shall be subject to any penalty for failing to comply with a collection of information if it does not display a currently valid OMB control number.</p> <p>PLEASE DO NOT RETURN YOUR FORM TO THE ABOVE ADDRESS.</p>						
1. REPORT DATE (DD-MM-YYYY)		2. REPORT TYPE		3. DATES COVERED (From - To)		
01- 10 - 2011		Technical Memorandum		November 2009 - July 2011		
4. TITLE AND SUBTITLE Comparison of the Booster Interface Temperature in Stainless Steel (SS) V-Channel versus the Aluminum (Al) Y-Channel Primer Chamber Assemblies (PCAs) <i>Appendices</i>				5a. CONTRACT NUMBER		
				5b. GRANT NUMBER		
				5c. PROGRAM ELEMENT NUMBER		
6. AUTHOR(S) Garcia, Roberto; Saulsberry, Regor L.				5d. PROJECT NUMBER		
				5e. TASK NUMBER		
				5f. WORK UNIT NUMBER 869021.05.07.01.10		
7. PERFORMING ORGANIZATION NAME(S) AND ADDRESS(ES) NASA Langley Research Center Hampton, VA 23681-2199				8. PERFORMING ORGANIZATION REPORT NUMBER L-20082 NESC-RP-09-00596		
9. SPONSORING/MONITORING AGENCY NAME(S) AND ADDRESS(ES) National Aeronautics and Space Administration Washington, DC 20546-0001				10. SPONSOR/MONITOR'S ACRONYM(S) NASA		
				11. SPONSOR/MONITOR'S REPORT NUMBER(S) NASA/TM-2011-217182/Volume II		
12. DISTRIBUTION/AVAILABILITY STATEMENT Unclassified - Unlimited Subject Category 20 Spacecraft Propulsion and Power Availability: NASA CASI (443) 757-5802						
13. SUPPLEMENTARY NOTES						
14. ABSTRACT NASA's Technical Fellow for Propulsion, requested a technical assessment of the performance improvement achieved by the introduction of the stainless steel (SS) V-channel compared to the aluminum (Al) Y-channel Primer Chamber Assembly (PCA) design. The SS V-channel PCA was developed for NASA's Mars Science Laboratory (MSL) Project. The principle focus of the assessment was to measure the transient temperature at the booster interface with both designs. This document contains the Appendices to the Volume I main report.						
15. SUBJECT TERMS Primer Chamber Assembly; NASA Engineering and Safety Center; Pyrovalve Booster; Dual Pyrovalve Initiator Circuit						
16. SECURITY CLASSIFICATION OF:			17. LIMITATION OF ABSTRACT	18. NUMBER OF PAGES	19a. NAME OF RESPONSIBLE PERSON	
a. REPORT	b. ABSTRACT	c. THIS PAGE			STI Help Desk (email: help@sti.nasa.gov)	
U	U	U	UU	97	19b. TELEPHONE NUMBER (Include area code) (443) 757-5802	